

ANALYSIS AND MODELLING OF MATRIX CONVERTER AS A FREQUENCY CHANGER

*A Dissertation submitted in partial fulfilment of the requirements for the award
of degree*

of

MASTER OF ENGINEERING

in

Power Electronics and Drives

Submitted by

Sidharth Pandit

801543005

Under the guidance of

Ms Suman Bhullar

Assistant Professor

EIED, Thapar University

Patiala

Dr. Santosh Sonar

Assistant Professor

EIED, Thapar University

Patiala



Electrical and Instrumentation Engineering Department

Thapar University, Patiala

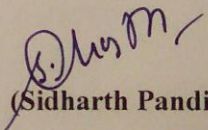
2017

DECLARATION

I hereby declare that the work which I have presented in dissertation entitled, "*Analysis and Modelling of Matrix Converter as a Frequency Changer*", in partial fulfilment of the requirements for the award of degree of Master in Engineering in Power Electronics and Drives, submitted to Electrical & Instrumentation Engineering Department of Thapar Institute of Engineering & Technology University, Patiala is an authentic record of my own work carried under the supervision of Dr. Santosh Sonar. It refers to other researcher's work which is duly listed in the reference section. The matter contained in this dissertation has not been submitted, neither in part nor in full to any other degree to any other university or institute except as reported in text and references.

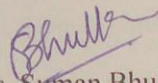
Place: Patiala

Date: 17th July 2017

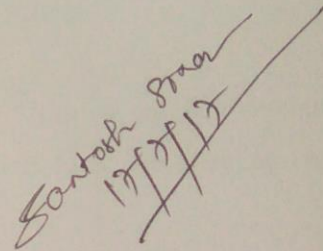

(Sidharth Pandit)
Roll No: 801543005

CERTIFICATE

Certified that the dissertation entitled, "Analysis and Modelling of the Matrix Converter as a frequency changer", which is being submitted by Sidharth Pandit in partial fulfilment of the requirements for the award of the Master of Engineering in Power Electronics and Drives, to Thapar University, Patiala, is a bonafide record of the candidates own work carried out by him under my supervision and guidance. The matter contained in this dissertation has not been submitted, neither in part nor in full to any other university or institute for the award of any degree.



Ms. Suman Bhullar
Assistant Professor
EIED, Thapar University
Patiala



Dr. Santosh Sonar
Assistant Professor
EIED, Thapar University
Patiala

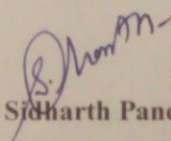
ACKNOWLEDGEMENT

I feel honoured in expressing my profound sense of gratitude and indebtedness to **Dr. Santosh Sonar**, Assistant Professor, EIED, Thapar University, Patiala and Ms. Suman Bhullar, Assistant Professor, EIED, Thapar University, Patiala for their guidance, meticulous effort, constructive criticism, inspiring encouragement, unflinching support and invaluable co-operation which helps me to enrich my knowledge and reproduce it in the present form.

I also like to extend my gratefulness to **Dr. Ravinder Agarwal**, Professor and Head, Electrical and Instrumentation Engineering Department, Thapar University, Patiala for his perpetual encouragement, generous help, and inspiring guidance. I am thankful for kind coordination during my Master of Engineering to **Ms. Manbir Kaur**, PG coordinator, Associate Professor, Electrical and Instrumentation Engineering Department, Thapar University, Patiala

I am also very thankful to the entire faculty and staff members of Electrical and Instrumentation Engineering Department for their direct-indirect help, co-operation, love, and affection, which made my stay at Thapar University memorable.

I wish to thank to mates for their time-to-time suggestions and cooperation without which I would not able to complete my work.


Sidharth Pandit
801543005

Dedicated to

My

DAD

ABSTRACT

From the last few years, there is a continuous increase in the use of electronics converters like AC to AC converters AC to DC or DC to AC converters. So, there is a requirement of devices with generates fewer harmonics, minimum switching losses and generate the high quality desired waveforms in input and output. It stimulates the researchers to innovate new ideas to minimize these effects. In this thesis, the main focus is to design and Implementation of Matrix Converter (MC) for frequency changing applications. In this thesis, space vector based PWM mechanism is used to design a mathematical model of single phase and three phase Matrix Converter. There is no DC link between rectifier and inverter stage which add up some efficient properties like compact design, bi-directional current flow capabilities. Along with that it has demerits like maximum output input voltage ratio is low and these systems are not commercially available and require more research on this converter to make it available commercially. This thesis work analyses some novel achievements reported in recent literature. For the supply application of the MC, a comparative analysis has been done and implemented on different MC models. MC control strategies have been implemented for SPMC and TPMC. Simulation work is done in MATLAB Simulink environment and comparison with mathematical results is presented.

Keywords: MC- Matrix Converter, SPMC- Single Phase Matrix Converter, TPMC Three Phase Matrix Converter, SVPWM, Rectifier, Inverter.

TABLE OF CONTENT

	Page Number
Abstract	vi
List of Figures	ix
List of Tables	xii
Nomenclature	xiii
List of Abbreviations	xiv
Organisation of Thesis	xv
Chapter 1	1-8
Introduction	1-8
1.1 Background	1
1.2 Modulation	3
1.3 Literature survey	5
Chapter 2	9-19
Fundamentals of the Matrix Converter(MC)	9-19
2.1 Matrix Converter	9
2.1.1 Single Phase Matrix Converter (SPMC)	9
2.1.2 Three Phase Matrix Converter (TPMC)	12
2.2 Bi-directional Switch Realization	13
2.3 Commutation Strategy	15
2.3.1 Commutation Strategy for Single Phase Matrix Converter	16
2.3.2 Commutation Strategy for Three-Phase MC	19
Chapter 3	20-64
Analytical Analysis, Results and discussions	20-64
3.1 PWM Generation for the Single Phase Matrix Converter	21
3.1.1 Simulation of the Single Phase Matrix Converter	23
3.2 Generation of Modulating Signal for the Three Phase MC	25
3.2.1 Modulation Technique for the Three Phase Matrix Converter	25
3.2.1.1 Transfer Function of the Indirect PWM Equivalent Model	26
3.2.1.2 Space Vector Modulation for the Inverter Stage	28
3.2.1.2.1 abc to $\alpha\beta$ Transformation for the Inverter Stage	31
3.2.1.2.2 Sector Selection for the Inverter Stage	32

3.3.1.2.3 Duty Period of Switch for the Inverter Stage	32
3.3.1.2.4 Duty Cycle Calculation for the Inverter Stage	36
3.3.1.2.5 Switching Duration of the Switches for the Inverter Stage	37
3.3.1.2.6 Switching Sequence of the Inverter Stage	38
3.3.3.2 SVM for the Rectifier Stage	42
3.3.2.1.1 abc into $\alpha\beta$ Transformation for the Rectifier Stage	44
3.3.2.1.2 Selector Selection for the Rectifier Stage	45
3.3.3.1.3 Duty Period of the Switch for the Rectifier Stage	46
3.3.3.1.4 Duty Cycle Calculation for the Rectifier Stage	48
3.3.3.1.5 Switching Duration of the Switches for Rectifier Stage	48
3.3.3.1.6 Switching Sequence for the Rectifier Stage	50
3.3.1.3 Space Vector Modulation for the Entire Matrix Converter	53
3.3.1.3.1 Switch Configuration for the Matrix Converter	54
3.3.1.3.1 Duty Cycle of the Matrix Converter	57
3.3.1.3.3 Matrix Converter Switching States Selection	61
3.2.2 Simulation of the Three Phase Matrix Converter:	62
Chapter 4	65
Conclusion and future scope	65
4.1 Conclusion	65
4.2 Future Work	65
References	66-67
Plagrism certificate	68

LIST OF FIGURES

Figure 1.1 Single-phase load fed from a three-pulse cyclo-converter	2
Figure 1.2 Structure of MC	3
Figure 1.3 RFIS Converter with blocking diode in Rectifier and IGBT at inverter stage	4
Figure 1.4 RFIS Converter with PWM based switches at rectifier and inverter stage	5
Figure 1.5 Simplified representation of MC system	5
Figure 2.1 Circuit Configuration of SPMC	9
Figure 2.2 Sinusoidal Input and Synthesized Output at 100 hertz	10
Figure 2.3 (a) Mode 1 operation of SPMC (b) Mode 2 operation of SPMC (c) Mode 2 operation of SPMC (d) Mode 2 operation of SPMC	12
Figure 2.4 3X3 Matrix Converter	12
Figure 2.5 Diode Bridge Arrangement of the Bidirectional Switches Configuration	14
Figure 2.6 Anti-Parallel Configuration of IGBTs and Diodes	14
Figure 2.7 Anti-Parallel reverse blocking IGBT's configuration of the Bidirectional Switches Configuration	15
Figure 2.8 Simple circuit where commutation problem exists	15
Figure 2.9 Duty cycle of the high-frequency switch	16
Figure 2.10 Current Flow during DT time interval in (a) and (1-D)T time interval in (b) in mode- 1 operation	17
Figure 2.11 Current Flow during DT time interval in (a) and (1-D) time interval in (b) in mode-3 operation	17
Figure 2.12 Current Flow during DT time interval in (a) and (1-D)T time interval in (b) in mode- 4 operation	17
Figure 2.13 Current Flow during DT time interval in (a) and (1-D)T time interval in (b) in mode- 4 operation	18
Figure 2.14 Simulation result of the output during all four modes of operation	18
Figure 2.15 Three Phase MC Semi-soft commutation process	19
Figure 3.1 Sinusoidal PWM Signal Generation at 100 Hz output Frequency	21
Figure 3.2 Switching Sequence of SPMC at 100 Hz Output frequency	23
Figure 3.3 Output Voltage and Current when load is Resistive of 50 W without filters	23
Figure 3.4 Output Voltage and Current when load is RL 50 W and 10 mH without filters	24
Figure 3.5 Output current and voltage of the SPMC for the resistive load of 50 W with filters.	24

Figure 3.6 Output current and voltage of the SPMC for the resistive load of 50 W and 10 mH without Filter with filters	24
Figure 3.7 Three Phase to Three Phase Matrix Converter	26
Figure 3.8 Indirect PWM Equivalent model	27
Figure 3.9 Random Switching States timing of the TPMC	28
Figure 3.10 Inverter stage from the equivalent model	28
Figure 3.11 Inverter Stage when switches S_7, S_{10}, S_{12} are on in the Equivalent model of the Inverter Stage	29
Figure 3.12 Sector representation during inverter stage (a) wrt angle (b) wrt time	32
Figure 3.13 Voltage Hexagon of inverter	33
Figure 3.14 Synthesis of reference voltage vector	33
Figure 3.15 At Sector-1, On switches in Inverter stage	37
Figure 3.16 Switching Sequence and Sequence in the Inverter Stage	38
Figure 3.17 Switching Sequence of switches in the Inverter Stage	40
Figure 3.18 Six sectors in the output voltages	41
Figure 3.19 Three Phase Output Voltage of Inverter Stage	41
Figure 3.20 Rectifier stage from the equivalent model	42
Figure 3.21 Equivalent circuits for rectifier stage when Switches S_1 and S_4 are closed	43
Figure 3.22 Sector Representation in Rectifier stage (a) wrt angle (b) wrt time	45
Figure 3.23 Current Hexagon of Rectifier stage	47
Figure 3.24 Synthesis of reference current vector	47
Figure 3.25 In Sector-1, On switches in Rectifier stage	49
Figure 3.26 Switching Sequence and Sequence in the Inverter Stage	50
Figure 3.27 Switching Sequence of switches in the Rectifier Stage	52
Figure 3.28 Input phase voltage sectors	53
Figure 3.29 Output DC voltage of Rectifier Stage	53
Figure 3.30 Transformation from equivalent circuit to matrix converter in phase a	54
Figure 3.31 Graphical interpretation of: (a) sectors and direction of the output voltage vectors of the MC (b) sectors and directions of the input line current vectors of the MC	55
Figure 3.32 Vector 1 of Inverter and Rectifier Stage of MC	55
Figure 3.33 $V-I$ pair during +1 active vector condition	56
Figure 3.34 Sector 1 of rectifier and Inverter stage of MC	59
Figure 3.35 $V_1 - I_1$ pair during d_{13}	59
Figure 3.36 $V_2 - I_1$ pair during d_{24}	60

Figure 3.37 $V_2 - I_2$ pair during d_{14}	60
Figure 3.38 $V_1 - I_2$ pair during d_{24}	60
Figure 3.39 $V_0 - I_0$ pair during d_0	61
Figure 3.40 TPMC output voltage and current of phase a of 50 W and 10 mH without Filter	62
Figure 3.41 MC Output Voltage and current of 50 W and 10 mH without Filters	63
Figure 3.42 TPMC output voltage and current of Ia phase without Filter	63
Figure 3.43 TPMC Output Voltage and current of 50 W and 10 mH with Filters	64

LIST OF TABLES

Table 2.1 Switching states of SPMC during Commutation processes	18
Table 3.1 Simulation parameters for SPMC	20
Table 3.2 Simulation parameters for TPMC	20
Table 3.3 SPMC Active Switches	22
Table 3.4 Switching Vectors and Switching States for the Inverter side	30
Table 3.5 abc to $\alpha\beta$ transformation	31
Table 3.6 Duty period of the Switching Vectors of Inverter Stage	36
Table 3.7 Switching Timing of the switches	37
Table 3.8 Switching Sequence and period of each switch in sector1 from output	39
Table 3.9 Switching vectors and Switch States Rectifier stage	43
Table 3.10 abc to $\alpha\beta$ Transmission	45
Table 3.11 Time Duration of the Switching Vectors of Rectifier Stage	48
Table 3.12 switching timing of switches in Rectifier stage	49
Table 3.13 Switching Sequence and period of each switch for sector-1	50
Table 3.14 Switches configuration of the MC	56
Table 3.15 Switching sequence of MC in current and voltage both are in sector 1	61
Table 3.16 Selection of Combination of Switching state configuration of Inverter and Rectifier stages-1	61
Table 3.17 Selection of Combination of Switching state configuration of Inverter and Rectifier stages-2	62

NOMENCLATURE

Symbol	Description	Units
V_s	Source Voltage	Volts
V_o	Output Voltage	Volts
I_s	Source Current	Ampere
I_o	Output Current	Ampere
D	Duty Cycle	No units
T_s	Switching time period	seconds
I_L	Inductor Current	Ampere
V_L	Voltage across Inductor	Volts
f_s	Switching Frequency	Hertz
Q	Charge	Coulomb
C_{eq}	Equivalent Capacitance	Farad
Hz	Frequency	Cycles/seconds
θ_i	Input current phase angle	Electrical Degrees
θ_o	Output Voltage Phase angle	Electrical Degrees
V_a	Output Voltage a Phase	Volts
V_b	Output Voltage b Phase	Volts
V_c	Output Voltage c Phase	Volts
V_A	Input Voltage A Phase	Volts
V_B	Input Voltage B Phase	Volts
V_C	Input Voltage C Phase	Volts

LIST OF ABBREVIATIONS

ACRONYMS	FULL FORM
AC	Alternating Current
DC	Direct Current
MOSFET	Metal Oxide Semiconductor Field Effect Transistor
IGBT	Insulated Gate Bipolar Transistor
MC	Matrix Converter
SPMC	Single Phase Matrix Converter
TPMC	Three Phase Matrix Converter
RFIS	Rectifier Fed Inverter System
SPWM	Sinusoidal Pulse Width Modulation
SVM	Space Vector Modulation
PWM	Pulse Width Modulation
VSC	Voltage Source Converter
VSI	Voltage Source Inverter
IEEE	Institute of Electrical and Electronics Engineers
MATLAB	Matrix Laboratory

ORGANISATION OF THESIS

This thesis is organized in Four chapters

- **Chapter 1** of this thesis work provides Introduction of the MC, Modulations, Literature survey, objective and organization of the thesis.
- **Chapter 2** aims to stretch a systemic description of the grassroots features of a Single phase and three phase MC in terms of performance and of technological issues. The MC has various advantages over traditional rectifier-inverter type frequency power converters. It provides output waveforms, with least high order harmonics and no sub-harmonics; it has implicit bi-directional current flow capability. Finally, but not slightest, it has not required any energy storage devices, which helps to make this converter less bulky capacitor.
But the MC has also some disadvantages. First of all, the maximum sinusoidal input and output waveforms transfer ratio restricted to $\cong 87\%$ [4]. Second one, it requires more semiconductor devices than an old conventional RFIC system; third one is till today there is not any bi-directional switch available in the market and hence they are constructed from the discrete unidirectional switches.
- **Chapter 3** of this thesis helps to find and study suitable modulation strategies for both the MC. In SPMC the sinusoidal PWM has been used whereas in the case of the TPMC the Indirect SVM Space Vector Modulation (SVM) has been used. In the Section 3.1, the Sinusoidal PWM has been discussed deeply, there is a comparison between the sinusoidal reference signal and the high-frequency triangular carrier signal, in comparison with this, the signal is generated that are used as the switching gate signal for the switches. The Indirect SVM process is the matrix combination of the Inverter stage modulation and Rectifier stage modulation, which is further explained briefly in Section 3.2 and 3.3. In both the Sections, suitable mathematical calculations and simulation results has been discussed.
- **Chapter 4** describes the results that has concluded in the entire thesis and tell the in which field the futher research can be possible.

1.1 Background

The Matrix Converter (MC) is the type of a forced commutated cyclo-converter alternative of the Rectifier Fed Inverter systems technology (RFIS) [23]. This converter has the ability to replace RFIS system. MC fed system is more reliable than the conventional RFIS system because of the following reasons.

- They have the capability to provide bi-directional power flow.
- They can deliver all silicon solution by converting the input frequency and magnitude into desired output magnitude and frequency.
- They don't have any intermediate DC link, hence they lead to a compact design as compared to RFIS.

With all these merits they have few demerits which are as follows:

- They have a problem in commutation of switches.
- The number of power electronics devices has been increased as compared to traditional RFIS.
- The switching algorithm and timing of the switches are quite complicated as compared to the traditional one.

The main focus of this thesis is to examine the Implementation of MC for frequency changing applications in the single phase and three phase MC, usually, this type of applications is used by changing the speed of the motor. In SPMC, it has four whereas in TPMC nine bi-directional switches, that has been commutated in such a right way that their switches sequence generates minimum switching losses and generate the high quality desired waveforms in input and output[23,24,26] In the early 1930's, after the development of controlled rectifiers, it has been realized that it could possible to generate AC of variable frequency directly from fixed AC with the help of a new device called Cyclo-converter and the cyclo-converter arrangements are shown in Figure 1.1.

Now, these devices are so appropriate that they are still used in many high power applications. Mostly frequencies in the range 50 to 60 Hz [9] is required in the industrial applications, these can be easily achieved with the help of cyclo-converter. In three phase to three phase cyclo-converter

requires 36 thyristors, which make the circuit complicated and large. Some common applications where we use cyclo-converter are as follows:

- In aircraft as a Variable speed and constant frequency (VSCF) power generator where the 400Hz power supply is required.
- Rolling mill drives,
- Cement mill drives.

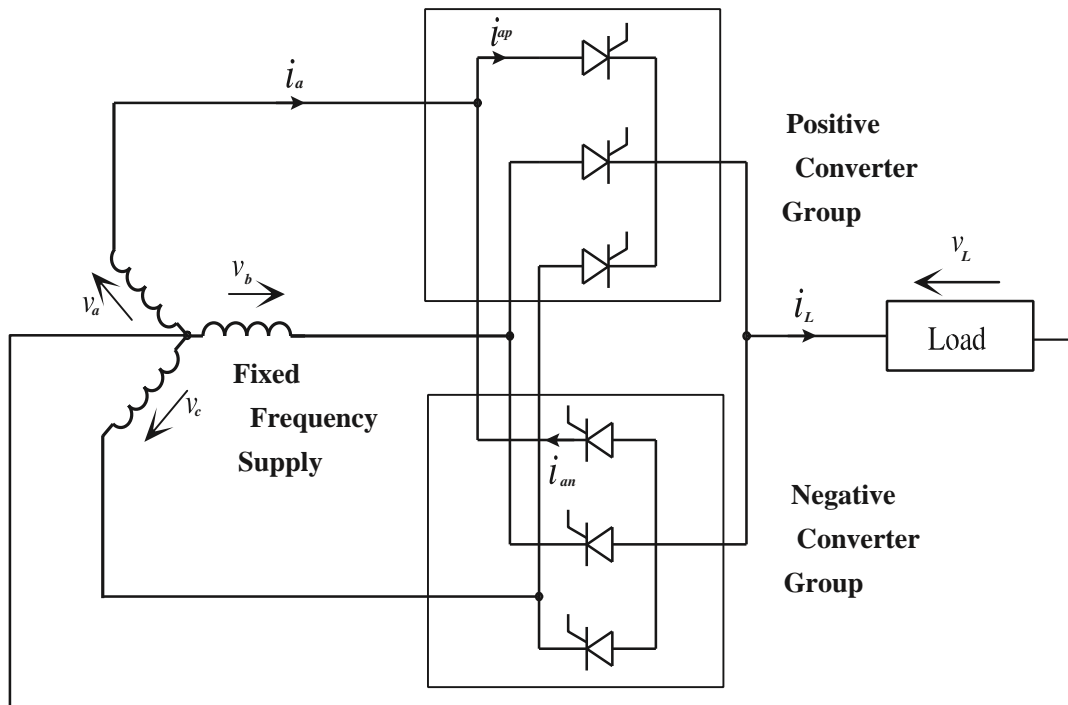


Figure 1.1 Single-phase load fed from a three-pulse cyclo-converter

MC was firstly mentioned by the two scientists namely “Alesina” and Venturini in the early of 1980’s. They proposed a general model of the MC and its relative Mathematical theory. They got the result that maximum AC to AC voltage transfer ratio is $(\sqrt{3}/2)$ which nearly equals to 0.866. on comparison to Three phase to three phase cyclo-converter, they usually have a minimum number of switches but in comparison with the traditional RFIS model, they require more semiconductor power electronics devices. In SPMC consists of four and The TPMC consists of nine bidirectional switches that are arranged in such a way that any of the input phases are connected to any of the output phases at an instant. Such arrangements are shown in Figure 1.2. In MC the input mains fed up with the constant frequency and supply. The amplitude of this MC can step up or down the frequency by synthesized output voltage equals to the multipliers of the input fundamentals.

For step up frequency operations: $F_o = n' F_i$ and (1.1)

For Step down frequency operations: $F_o = \frac{F_i}{n}$, where $n=1,2,3,\dots$ (1.2)

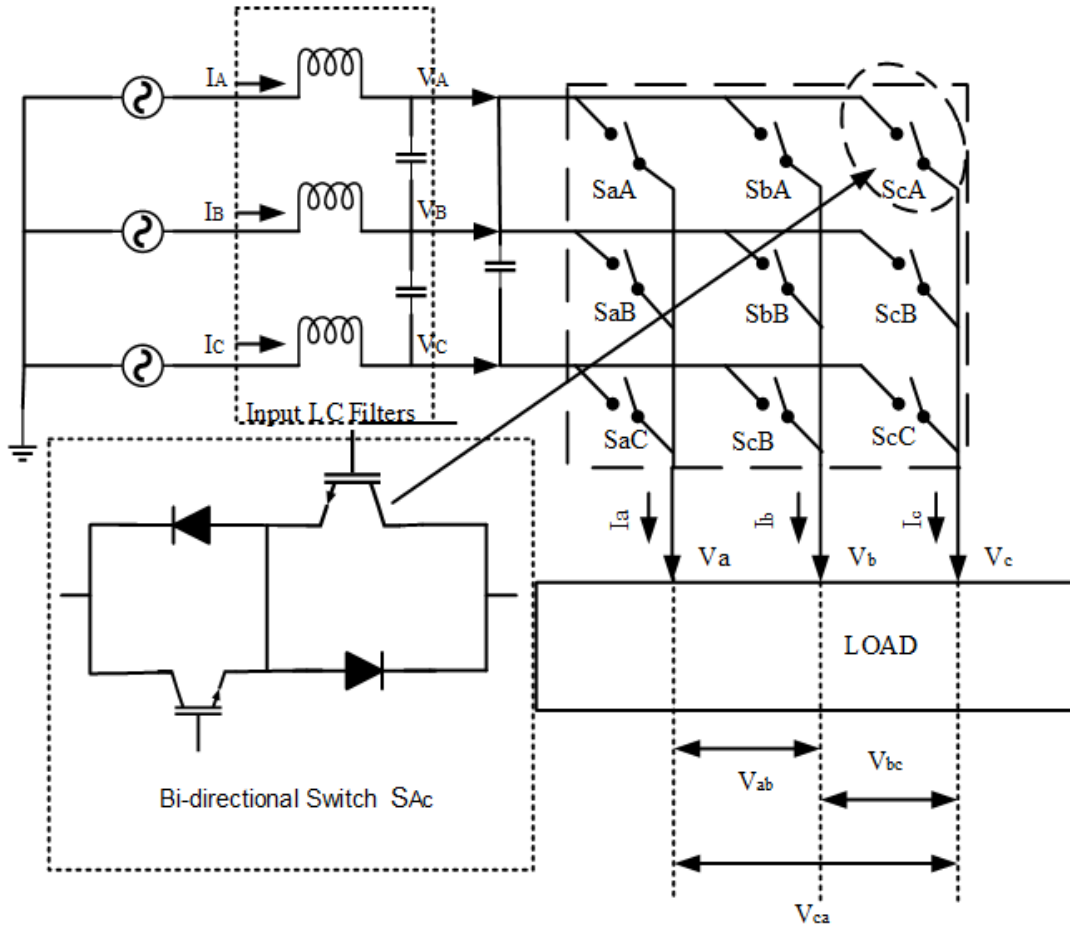


Figure 1.2 Structure of MC

1.2 Modulation

The area of Power Electronics Application as a converter has been expanding on a great scale all thanks to the great improvement in the Power Electronic switches and still, many research has been going for offering better voltage and current rating and switching characteristics and the advantages of these converters are as below:

- Dimension of the switches is less
- Low weight
- highly efficient
- high power applications
- low switching time.

The mode of operation of this converter is switch mode operation, which operates in the turn off and turn on manner, which can give generation to the Pulse width modulation technique, this technique is high-speed process that is applied to the power converter switches that are ranging from kilohertz (in motor control application) to several Megahertz (resonant converters).

The traditional RFIS controller which is provided by the fixed AC voltage and provides us desired output voltage and current are shown in Figure 1.3. These are mainly applied in variable speed drives applications. According to Figure 1.3, at the initial stage the rectification process has been done on the input side then the output of the rectifier is fed with intermediate DC link and that act as an input to the inverter stage. Hence this process will provide the nearly sinusoidal voltage output waveform at desired frequency and the large capacitor has been placed in between the input and output of RFIS converter which acts as a storage of energy and provides VSI the constant DC source voltage.

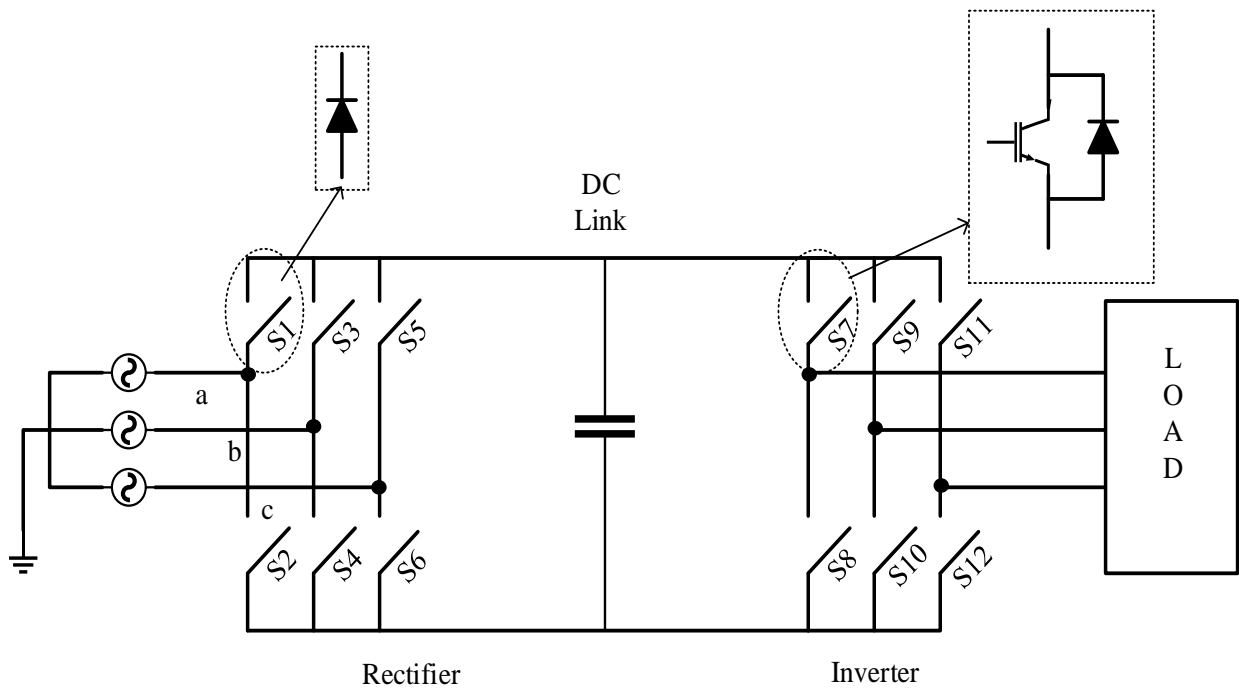


Figure 1.3 RFIS Converter with blocking diode in Rectifier and IGBT at inverter stage

Generally, the capacitor is so large that it can occupy a total volume of the converter by 30 to 50 % that would withstand for the few kilowatt power level and another demerit of this converter is they are temperature sensitive. The bridge VSI draws generally input current that contains lots of 5th and 7th order harmonics, which becomes a burden for the converter and injected back to the mains supply and can cause severe power losses in the system. To get rid of this problem, the use of PWM based switches to the rectifier, that helps to modulate nearly input sinusoidal current is shown in Figure 1.4 [23].

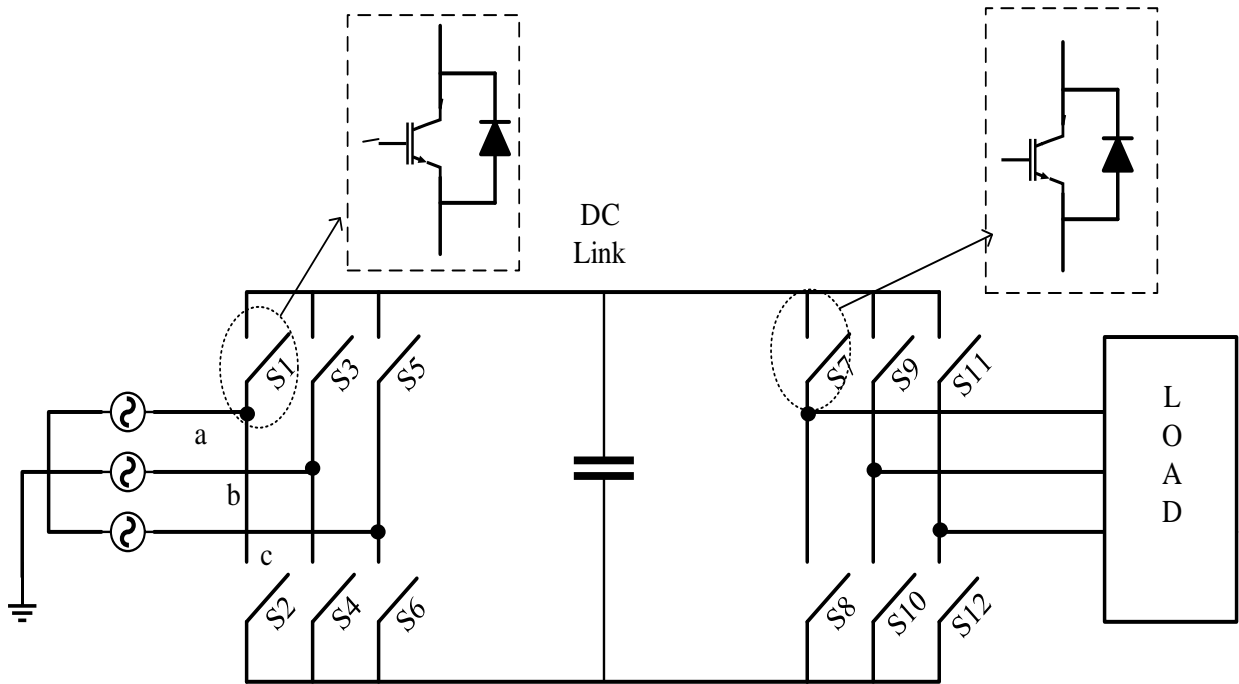


Figure 1.4R FIS Converter with PWM based switches at rectifier and Inverter stage

To get rid of these bulky intermediate DC link and multi step conversion, there is an alternative AC to AC converter, MC, this converter has been analyzed for single and three phase RL load in the thesis. The MC, as shown in Figure 1.5. The desired output frequency and voltage have been generating through the duty cycle of the switch.

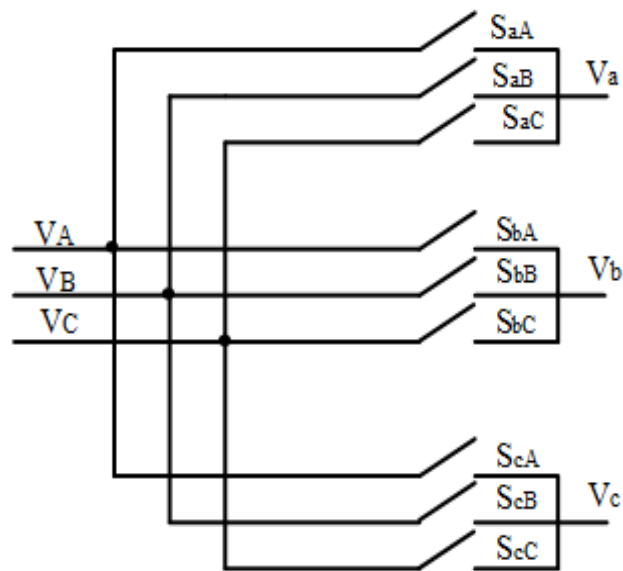


Figure 1.5 Simplified representation of MC system

1.3 Literature survey

The paper [2] concluded that it is possible to convert frequency from one form to another frequency without having an intermediate DC link in between them or not by traditional method Rectifier

Inverter Frequency Changers (RFIS), The proposed converter has improved structure and switching scheme of proposed model is the combination of rectifier and inverter. Merits of these papers are to eliminate unwanted DC link components that will help to make the converter less bulky, having bi-directional power flow capability and very less voltage output distortion and also have demerits that it requires high switching frequency this will get this model work only on low and medium power applications.

The papers [10][11][17] presents 4 quadrant operation of semiconductor switches in power converter devices. The paper described the possible solution of safe commutation of the switches. These switches have been constructed from the two-quadrant switches that are separately controllable. The merits of this paper is to provide 4 quadrant switches from the MC with safe commutation strategy. Along with that it had some demerits also that the load current flows and switching sequence all are dependent on each other, like if one switch gets turn off before turning off of another switch cause open circuit in output give rise to voltage spikes and if one switch will turn on before turning off of another switch cause short-circuited in the input side give rise to current spikes.[9], it describes the method of ‘overlap’ current commutation. In this method, the incoming switch is just turned on before the outgoing switch gets turn off. There is some short circuit has been taken place for the short interval of time between the two phase. In this process, during short circuit there is an extra inductance is required just to stop the current rise to the destruction level. This proposed technique is barely used as the inductor is too costly and make the system bulky.

In the papers[20],[6] the outgoing switch is turned off before the incoming switch is turned on, and proposed method is commonly known as dead time method of current commutation. In this method there is a requirement of the Snubber circuit, that will provide the path to the current. This method has some limitations as Snubber design complicates the bidirectional switches, require more area and method have a poor response.

[20],[8]proposed a method as “semi-soft commutation method”, this method is the most reliable method to commutate the current for bi-directional switches and depends upon the direction of the current. As they have merits that they don’t require any Snubber or inductance to decrease the losses. For the TPMC topology, this commutation technique has been used. In the proposed commutation method, as this commutation process does not require any Snubber circuit and energy storing device for the necessity of the dead time. This proposed method requires an optimal sequence of the switches so that it is possible to achieved optimal operation, the only demerit of this it’s difficult to achieve optimal operation. For the direction of the load current in this proposed model, it depends upon the input and output voltages.

The paper [13] is the inherent limitation of AC-AC MC. In MC there is the unavailability of the natural freewheeling path, the paper is more concerned about providing freewheeling path to the SPMC through simple commutation strategy. This strategy provides the path to the current to dissipate in the dead time and helps in reducing the voltage spikes. The merits of this proposed model are to provide a free-wheeling path through the bidirectional switches that provide switching sequences carefully.

This paper [9] is all about design and realization the direct AC to AC SPMC topology, having four bi-directional switches. The input is fed from the mains supply at a constant frequency and output frequency is synthesized as per our demand. The operation has been done on the RL circuit. The merits of this topology is to provide variable frequency and voltage at the output end and the only demerit of this topology is to get the output frequencies which are the multiple of the input frequency, not any frequency i.e. if input frequency is 50 Hz the Output must be natural number multiplication or division of 50Hz i.e. 12.5, 25,100 etc.

The papers[14,20,16] help to investigate SPMC fed R-L load and asynchronous motor. It presents analysis of Single phase AC-AC converter drive characteristics on square wave modulation and sinusoidal wave modulation. It also analyses harmonics effects on output voltages. As PWM shows poor response towards output voltage as it generates distorted voltage output and doesn't reduce the harmonics content. So, in place of PWM generator, the authors have used sinusoidal PWM. This paper investigated that it shows good results in low output synthesized output but there is an increase in the lower order harmonics as we increase the frequency. The merits of the proposed model is to provide an alternative to indirect DC link for low output frequencies and demerits of this model is that there is an increase in the lower order harmonics in the converter when there is decrease in the output synthesized frequency. The main purposes of the papers [4] and [7] is the analysis and implementation of the novel new space vector modulation technique for the Forced Commutatedcyclo-converter, which is Indirect SVM. This modulation helps to attain nearly sinusoidal output voltage waveform and help to cover up the harmonics. The merits of this proposed modulation are THD of this model is independent of output and switching frequency, there is notably decrement in THD by using a filter at the output side. The demerits of this proposed modulation are the value of THD for FCC is slightly higher and changes with the change in voltage transfer ratio of input and output.

[10],[21]proposes a space vector Modulation control topology to control variable speed drives in AC/DC/AC applications. These papers proposed the calculations of time duration on zero states and reference vector for each switching states. The current and voltage regulation are done on rectifier and inverter respectively. This proposed scheme shows low harmonics because of

symmetrical distribution of the switches, especially on high Modulating Index. The merits of this topology are these will provide us nearly sinusoidal waveform and having lesser harmonics whereas disadvantages were requiring separately SVM for each Rectifier and Inverter that will add up the cost along with the intermediate DC link. The paper[22] examines various approaches of SVM technique. The schemes have 512 maximum States but possibly it has 27 switching states that are useful and among them 21 having 18 active vector states and 3 zero vector states and has 6 synchronous configuration states due to their variable direction of output voltage and input current they are not synthesized reference vectors, that are usefully implemented in SVM strategy. This strategy has reference voltage and current at any instant of time. This important feature of this strategy is to select four active states having suitable time during the cycle interval T_s . [18] proposed a novel technique of commutation for the bi-directional switches and improvement in the output voltage errors, the proposed method is based on the duty cycle of the converter. The merits of proposed commutation are that they suppressed the input current vibrations in the motor and doesn't require any damping circuit and there is low THD realization in the waveform.

FUNDAMENTALS OF THE MATRIX CONVERTER(MC)

2.1 Matrix Converter

In the MC, for 3 phase, it consists of 9 bi-directional switches which allow connection of output phase to any input phase. The three-phase voltage source system is connected to the input terminal, generally, grid, whereas the output terminals are connected to the 3 phase load system, like Induction motor. With its nine bi-directional switches, it's theoretically assumed that the MC can have 2^9 i.e. 512 possible combinations, but actually, not all are applicable. Considering two basic rules of the converter, first one is input current never be short-circuited and second one, the output voltage should never be open circuited. Due to these two constraints, there are possibly 27 switching combinations are permitted. Moreover, there are non-availability of bi-directional switches, hence monolithic bi-directional switches have been prepared and used for this switching purpose of MC. In this section, it will describe the SPMC switching pattern[9] of the converters in various conditions and furthermore, basics of TPMC is explained in[5].

2.1.1 Single Phase Matrix Converter (SPMC)

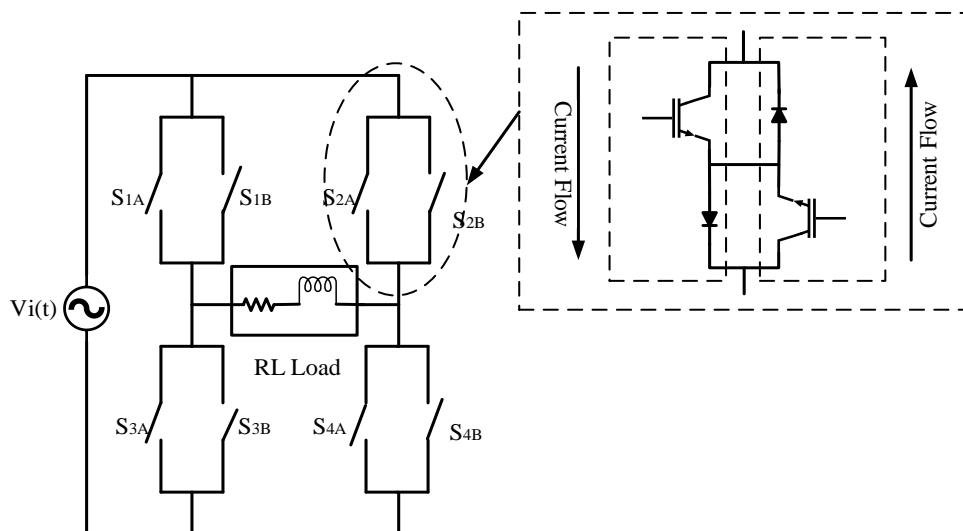


Figure 2.1 Circuit Configuration of SPMC

In SPMC, there is a single phase Single-step direct and single step AC to AC power frequency converter having bi-directional switches in the form of 2×2 array combinations without any DC

link, the circuit configuration of SPMC is shown in Figure 2.1. The comparison between Fundamental Input of 50 Hz and Synthesized Output of desired 100 Hz is shown in Figure 2.2.

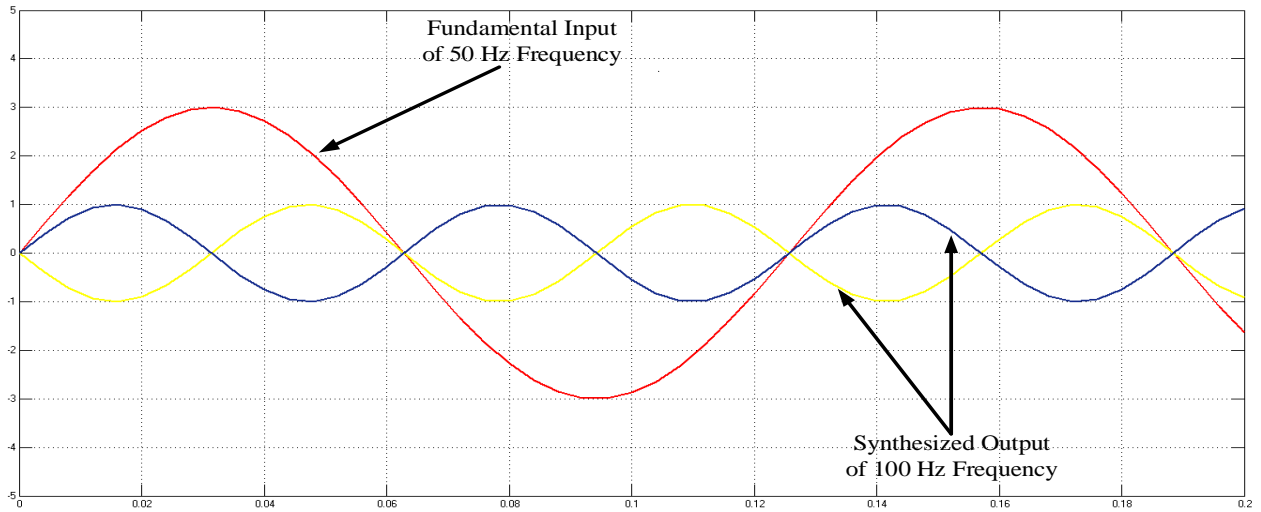
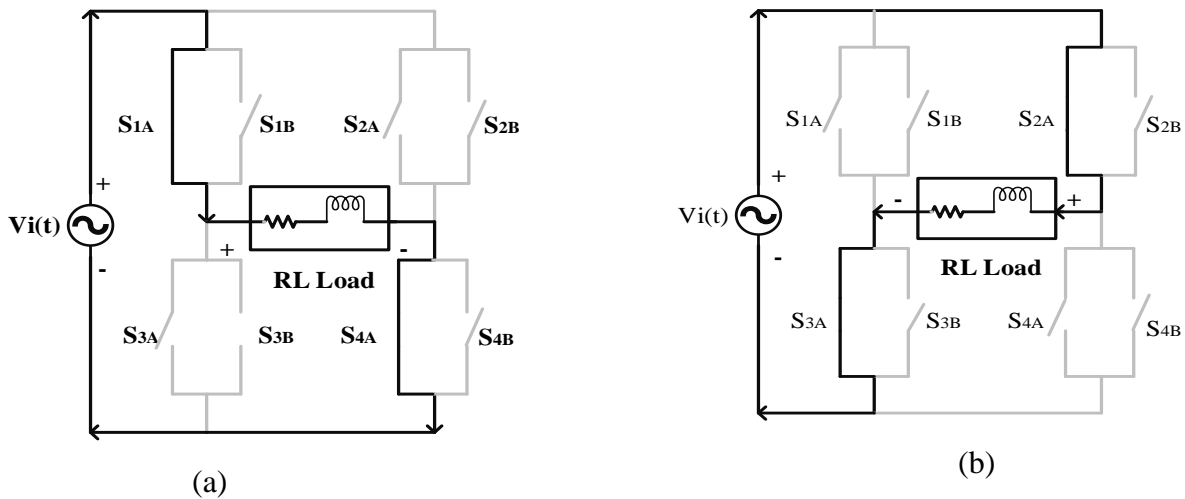


Figure 2.2 Sinusoidal Input and Synthesized Output at 100 hertz

In 50 Hz to 100 Hz frequency changer SPMC generally, has 4 modes of operations. These all modes of operation are shown in Figure 2.3 (a) to (d).

Mode 1: When The Input and output both are in the positive half cycle: In this mode of operation of SPMC, the Switches S_{4A} and S_{1A} are switched on and all other are off. So, the direction of current flowing from S_{1A} to RL load to S_{4A} as shown in Figure 2.3 (a). A similar process is followed in all other three modes of operation. Mode 2 operation of SPMC is shown in Figure 2.3(b), Mode 3 in Figure 2.3 (c) and Mode 4 in Figure 2.3 (d).



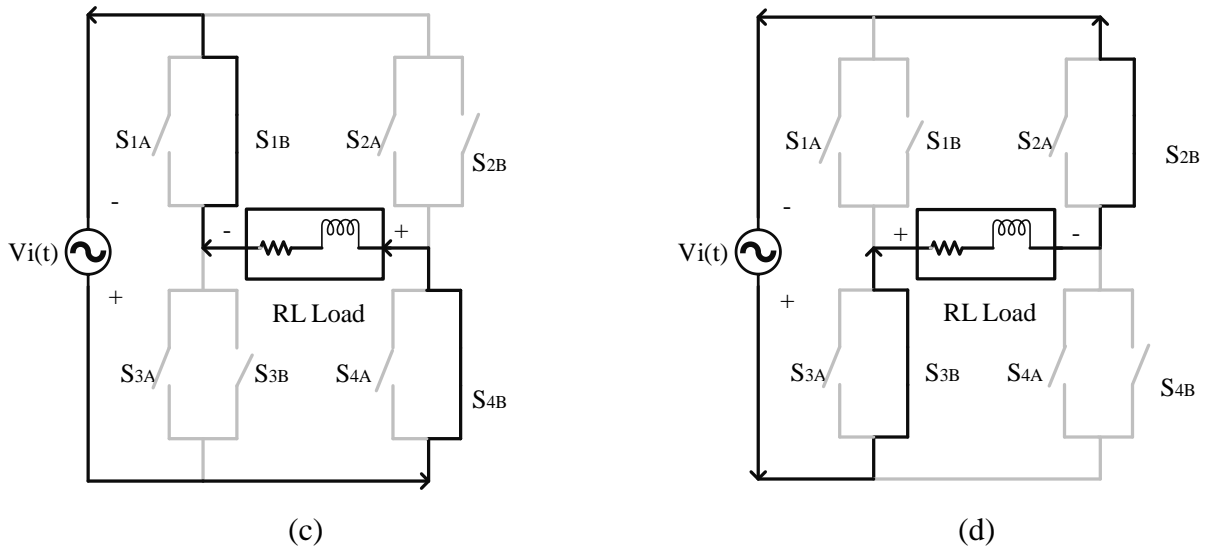


Figure 2.3 (a) Mode 1 operation of SPMC (b) Mode 2 operation of SPMC (c) Mode 2 operation of SPMC (d) Mode 2 operation of SPMC

2.1.2 Three Phase Matrix Converter (TPMC)

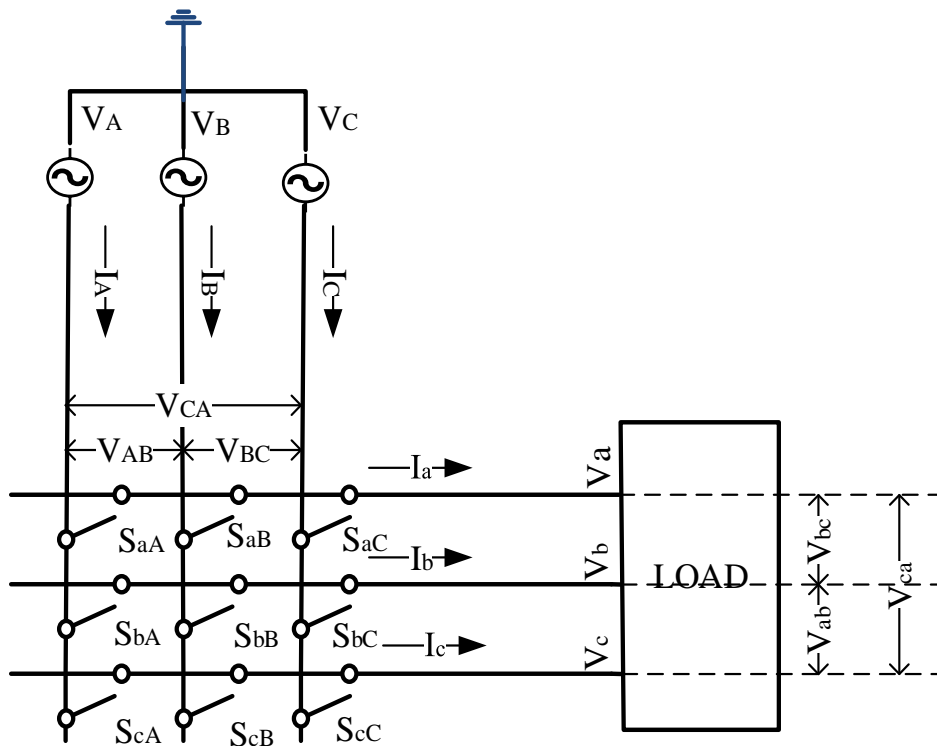


Figure 2.4 3X3 Matrix Converter

At any instant of time, power flow from the input does not equal to the power output. This difference in power losses that must be absorbed or delivered by the DC storage link in between

the converter. The MC succeed to replace the multiple stage conversions and get rid of the intermediate DC energy storage devices or element through a single stage power converter and hence they have uses the bidirectional switches in matrix form by connecting input terminals and output terminals as shown in Figure 2.4. Assuming ideal switches of the MC, the typical arrangement of the bi-directional switches, the power can flow through the converter and can be in reversed direction. Due to the absence of any intermediate DC link in between them, the input power flow must be equal to output power flow. However practically, due to the presence of the reactive filter and switching losses in the MC, the input power is not equal to the output power. The TPMC consists of nine bidirectional switches that are arranged in such a way that they are divided into three groups of three switches. In each group of the TPMC, each output phase can be connected to any input phase. In TPMC there are maximum possible 512 (2^n where $n=9$) switching states. But among all of them, there are only 27 possible switching states that are permitted and to operate for this converter [1], because for the TPMC safety, the switching state should follow these given following rules:

- The two different input lines are never being short-circuited.
- There should not be any discontinuity of inductor load output line i.e. they should not be open circuited.

Looking at the features of the MC that have been briefly described in the early sections. Till date, there has not been much utilization found yet.

2.2 Bi-directional Switch Realization

To construct the MC there is a requirement of bi-directional switches, that generally conducts current and block voltage in both the directions. But still, there is not any true bi-directional switch available. The realization of these bi-directional switches is a combination of different switching arrangements, which are presented below.

Diode bridge arrangement:

It is possible to construct bi-directional switch by using single switching device like MOSFET, IGBT as shown in Figure 2.5. This arrangement has few advantages that it requires only one switching device to turn on and off cause low switching losses but due to conduction of three devices at the same time, this will cause in large conduction losses.

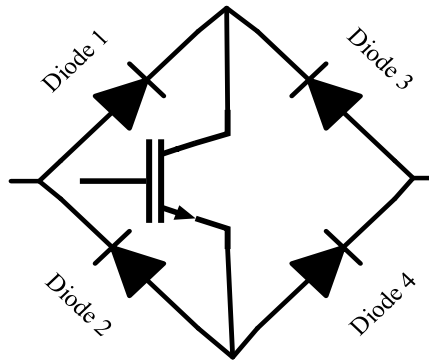


Figure 2.5 Diode Bridge Arrangement of the Bidirectional Switches Configuration

Two Anti-Parallel Igbts and Series Diodes Configuration:

In this arrangement, it consists of two IGBT's that are united in an anti-parallel combination and both are in series with the diodes as shown in Figure 2.6 This arrangement has some advantages that only one diode and one Switch is conducting at any instant of time. The diodes present in this have reverse blocking capabilities. This configuration requires isolating gate drive for the each switch. There are several advantages of this type of configuration, that it can lower down the conduction losses and have independent control of negative and positive currents.

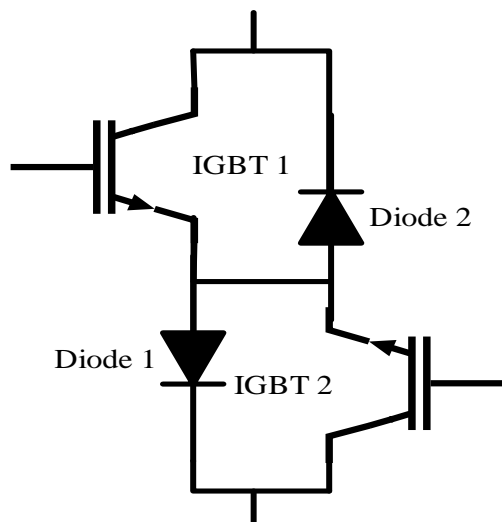


Figure 2.6 Anti-Parallel Configuration of IGBTs and Diodes

Anti-Parallel IGBT's Configuration:

In this configuration, it's practically possible to connect two reverse blocking devices in anti parallel manner and form bi-directional switches as shown Figure 2.7. In this manner of combination of switches, the efficiency of the converter is improved and possibly decrease in the

size of the converter. However, till now the IGBT's has not been used practically implemented due to they showed a poor reverse blocking capabilities. The most common and preferable configuration is common emitter configuration and is the most preferred solution for the low conduction losses as two devices are conducting at any instant of time and to control the direction of the current. But the main disadvantages of that type of configuration is that there is a requirement of the isolated power supply of each bidirectional switches for gate drive unit.

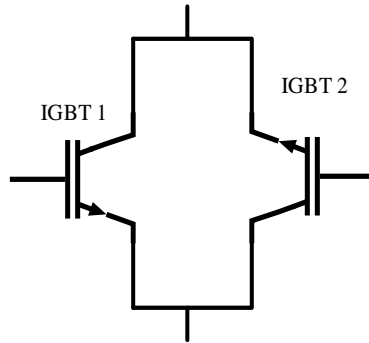


Figure 2.7 Anti-Parallel reverse blocking IGBT's configuration of the Bidirectional Switches Configuration

2.3 Commutation Strategy

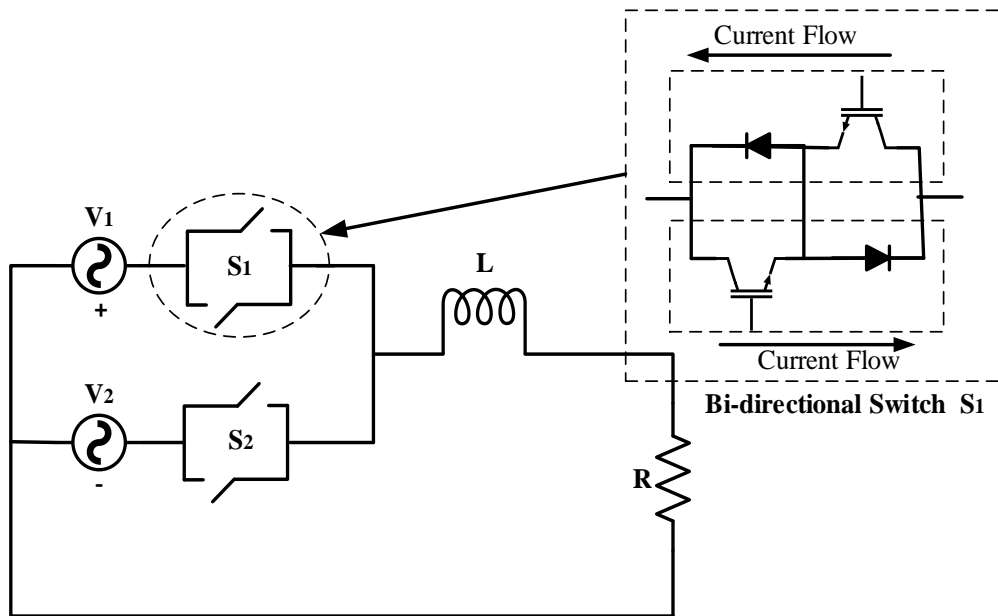


Figure 2.8 Simple circuit where commutation problem exists

It is not possible to define a timing which allows to carry out a safe commutation of the load current between two diode bridge switches. However, the commutation process can't be based on a switching method other than the Notwithstanding, the commutation process isn't based on a

switching method which is generally other than the “break-before-make” one or “make-before-break” one as shown in Figure 2.8. In the case of a make-before-break switching method, if the switch is turned on but the off-going switch is still off. In this way, the both the bi-directional switches S_1 and S_2 create a short-circuited path in between the V_1 and V_2 voltage sources that are the resultant of generation of current spikes, anyhow if these spikes are not limited, would be the cause of the destruction of switches. Similarly in the case of a break-before-make switching method, in this situation, if the off-going switch is turned off before turn on of the on-coming switch, results in the open path for induction load. It causes voltage spikes on the open switch.

2.3.1 Commutation Strategy for Single Phase Matrix Converter

In SPMC, there are no freewheeling diodes available for the proper commutation of bi-directional switches. In order to avoid this, problem the switches S_3 and S_4 are operated at high frequency. These switches have DT and $(1-D)T$ on and off time respectively as shown in Figure 2.9.

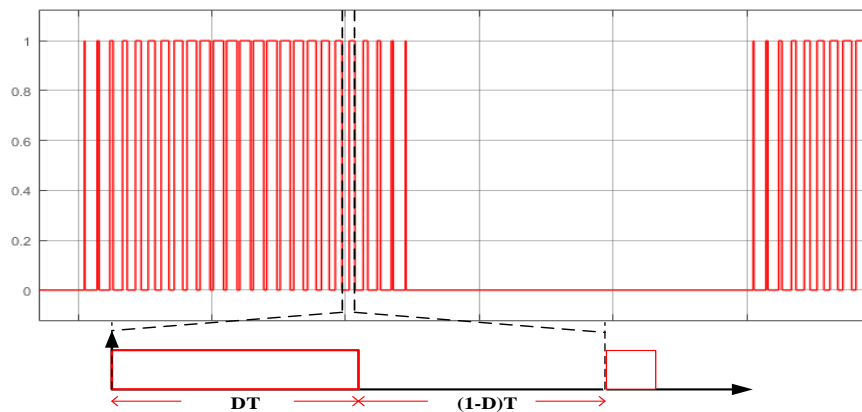


Figure 2.9 Duty cycle of the high-frequency switch

The mode-1 operation of SPMC is divided into two parts. Here switches S_{1A} and S_{2B} are switched on and S_{4A} is operated at high-frequency as shown in Figure 2.10. In part 1, the time interval is DT , during this time high-frequency switch S_{4A} is switched on and the current flows in the direction of S_{1A} to RL load to S_{4A} to During this period, the load inductor gets charged. In part 2, the time interval is $(1-D)T$, during this time high frequency switches S_{4A} is switched off and the charge stored in the inductor is freewheeled through S_{2B} as shown in Figure 2.10 (b). The Commutation of SPMC in all four mode of operations are shown in Figure 2.11 to 2.13. In the Figure 2.14, shows the simulation result of the output during all four modes of operation and the switching pattern of the SPMC is explained deeply in Chapter 3.

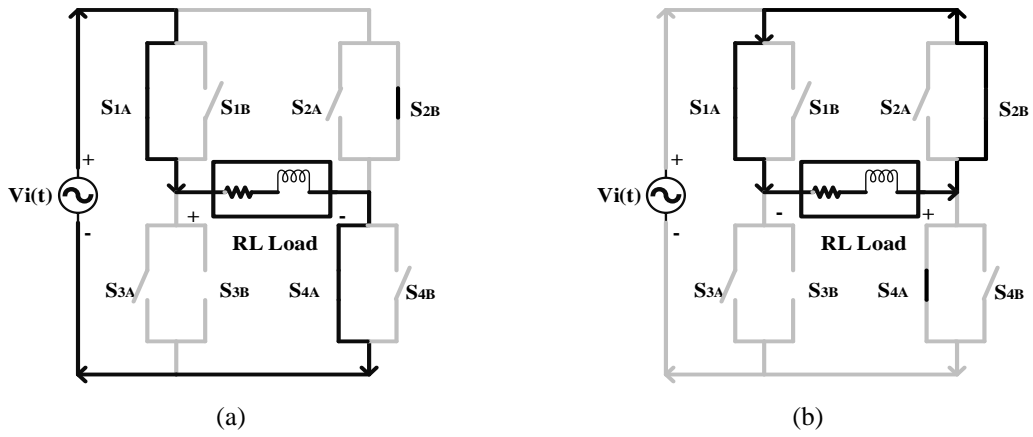


Figure 2.10 Current Flow during DT time interval in (a) and $(1-D)T$ time interval in (b) in mode-1 operation

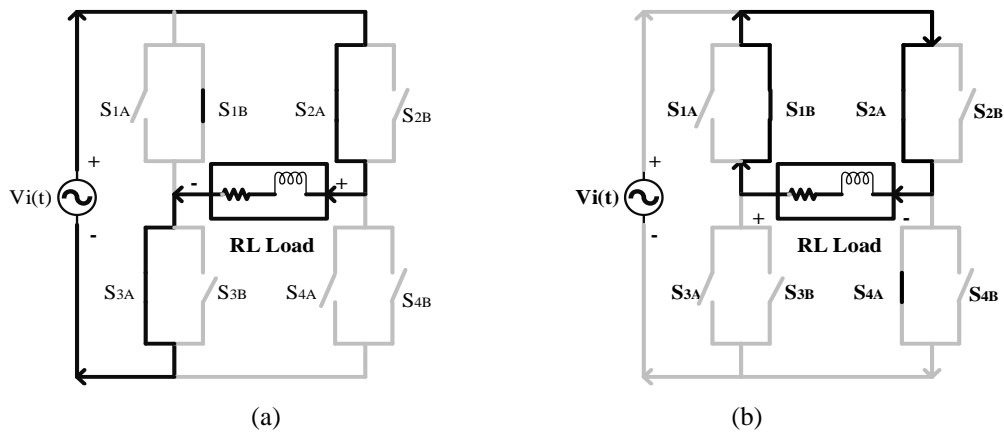


Figure 2.11 Current Flow during DT time interval in (a) and $(1-D)T$ time interval in (b) in mode-2 operation

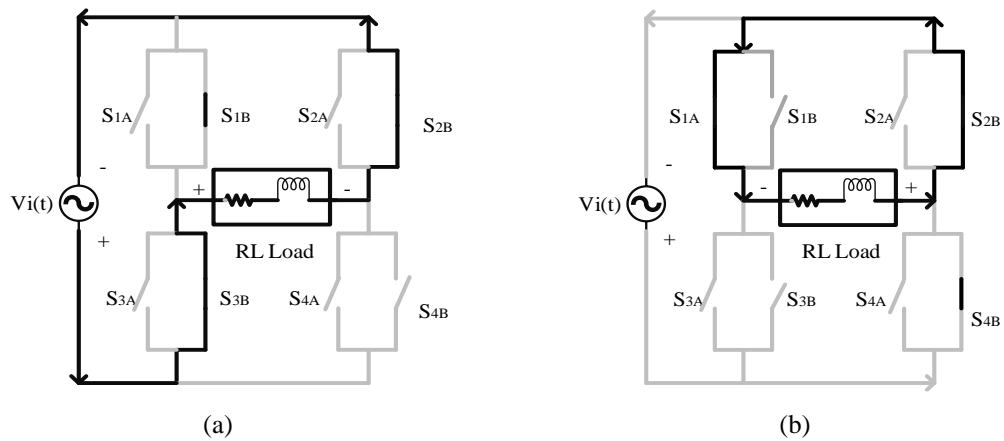


Figure 2.12 Current Flow during DT time interval in (a) and $(1-D)T$ time interval in (b) in mode-3 operation

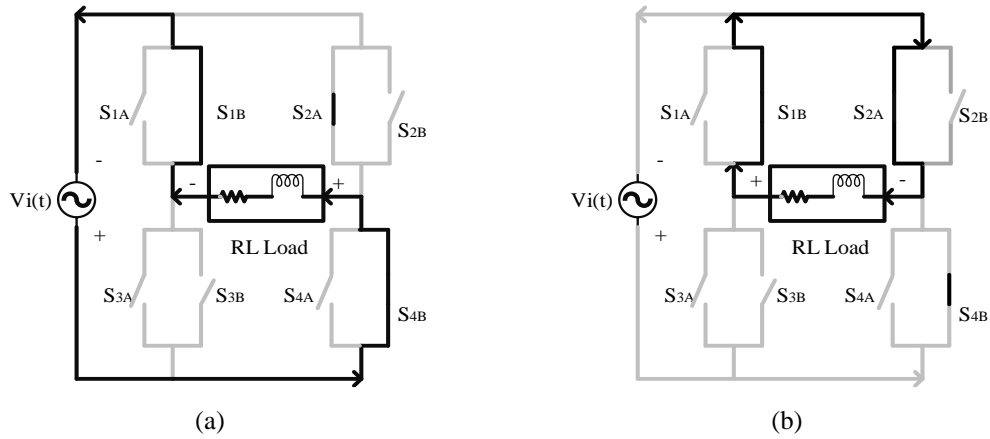


Figure 2.13 Current Flow during DT time interval in (a) and (1-D)T time interval in (b) in mode-4 operation

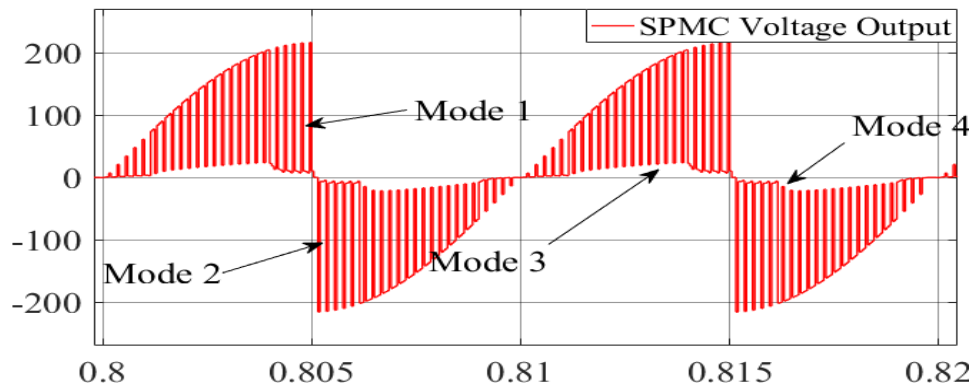


Figure 2.14 Simulation result of the output during all four modes of operation

Table 2.1 Describes all the switches that are on and off during DT and (1-D)T duration in all the 4 modes of operations and again in the Figure 2.14 when the current is passing through the switch, that switch is represented by '1' and otherwise it is represented by '0'.

Table 2.1 Switching states of SPMC during Commutation processes

Mode	DT period								(1-D)T period							
	S _{1A}	S _{1B}	S _{2A}	S _{2B}	S _{3A}	S _{3B}	S _{4A}	S _{4B}	S _{1A}	S _{1B}	S _{2A}	S _{2B}	S _{3A}	S _{3B}	S _{4A}	S _{4B}
1	1	0	0	0	0	0	1	0	1	0	0	1	0	0	0	0
2	0	0	1	0	1	0	0	0	0	1	1	0	0	0	0	0
3	0	0	0	1	0	1	0	0	1	0	0	1	0	0	0	0
4	0	1	0	0	0	0	0	1	0	1	1	0	0	0	0	0

2.3.2 Commutation Strategy for Three-Phase MC

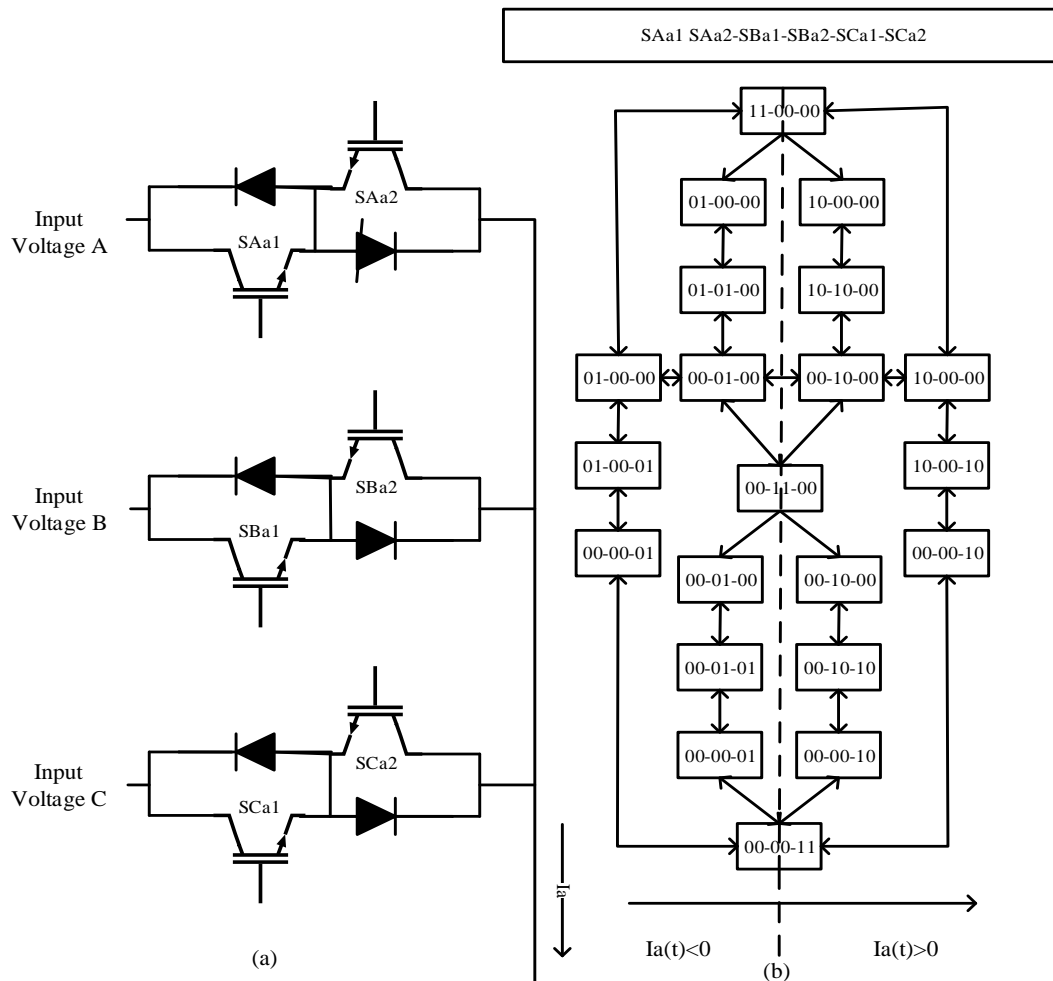


Figure 2.15 Three Phase MC Semi-soft commutation process

In TPMC, this process is the most common commutation process and known to be a Semi-Soft Commutation process is illustrated in Figure 2.15 and the main principle of this process is to disconnect one input phase and connect another input-phase without violating the rules of commutation of the MC e.g. disconnection of input phase A and connection of input phase B with the output phase a. This process of commutation has been done in several steps and these steps have shown below:

- In the initial stage, consider that gate pulses have been given to the switch S_{Aa} this bi-directional switch is the combination of the mono directional switches S_{Aa1} and S_{Aa2} . In the next state, the output current will tell that input current will pass through which mono directional switch like if the output current is > 0 , then current will pass from S_{Aa1} otherwise it will pass through S_{Aa2} .

- In the next stage, along with the switch S_{Aa} , a gate pulse is provided to switch on the Switch S_{Ba} . The direction of flow of current in this switch also depends upon the output current, like if the output current is > 0 , then current will pass from S_{Ba1} otherwise it will pass through S_{Ba2} . During this stage, the current is passing not only from S_{Aa} but also from S_{Ba} .
- In the Final Stage, the gate pulse has been removed switch S_{Aa} and turn this switch OFF. Now all the current will shift to the switch S_{Ba} . In this stage, the current has been shifted from one switch to another completely. Similar commutation process will take place in all the switches while shifting current from one switch to another and this process of commutation does not violate any of the two rules of the commutation of the switches.

There is 6 transition state for each switch that is represented by when a transient is off by '0' and when a transient is on by "1".

ANALYTICAL ANALYSIS, RESULTS AND DISCUSSIONS

In MC topologies, it is a complex task to find and study suitable modulation strategies. In SPMC the sinusoidal PWM has been used whereas in the case of the TPMC the Indirect SVM Space Vector Modulation(SVM) has been used. In Section 3.2, a detail description of switching pulse of SPWM generation is presented. The Indirect SVM process is the matrix combination of the Inverter stage modulation and Rectifier stage modulation, which is further explained briefly in Section 3.3 and 3.4. In both the Sections, suitable mathematical calculations and simulation results have been discussed. The simulation is done in MATLAB environment with the parameters for SPMC is shown in Table 3.1 and for TPMC is shown in Table 3.2.

Table 3.1 Simulation parameters for SPMC

Input Voltage	220 Volts
Input Frequency	50 Hz
R load	50 W
RI load	50 W and 10 mH
Output Frequencies	50 Hz, 100 Hz and 25 Hz
Switching Frequency	5000 Hz
LC Filters	$L = 136 \times 10^{-6}$ H; $C = 64.5 \times 10^{-6}$ F
Modulating Index	0.8

Table 3.2 Simulation parameters for TPMC

Input Voltage	220 Volts per phase
Input Frequency	50 Hz
R load	50 W
RI load	50 W and 10 mH
Output Frequencies	100 Hz, 50 Hz, 25 Hz
Switching Frequency	5000 Hz
LC Filter	$L = 125 \times 10^{-6}$ H; $C = 68.5 \times 10^{-6}$ F
Modulating Index	0.866

3.1 PWM Generation for the Single Phase Matrix Converter

In SPMC, there are no freewheeling diodes available for the proper commutation of bi-directional switches. In order to avoid this, problem the switches S_3 and S_4 are operated at high frequency. These switches have DT and $(1-D)T$ on and off time respectively as shown in Figure 2.9.

The mode-1 operation of SPMC is divided into two parts. Here switches S_{1A} and S_{2B} are switched on and S_{4A} is operated at high-frequency as shown in Figure 2.10. In part 1, the time interval is DT , during this time high-frequency switch S_{4A} is switched on and the current flows in the direction of S_{1A} to RL load to S_{4A} to During this period, the load inductor gets charged.

In part 2, the time interval is $(1-D)T$, during this time high frequency switches S_{4A} is switched off and the charge stored in the inductor is freewheeled through S_{2B} as shown in Figure 2.10 (b).

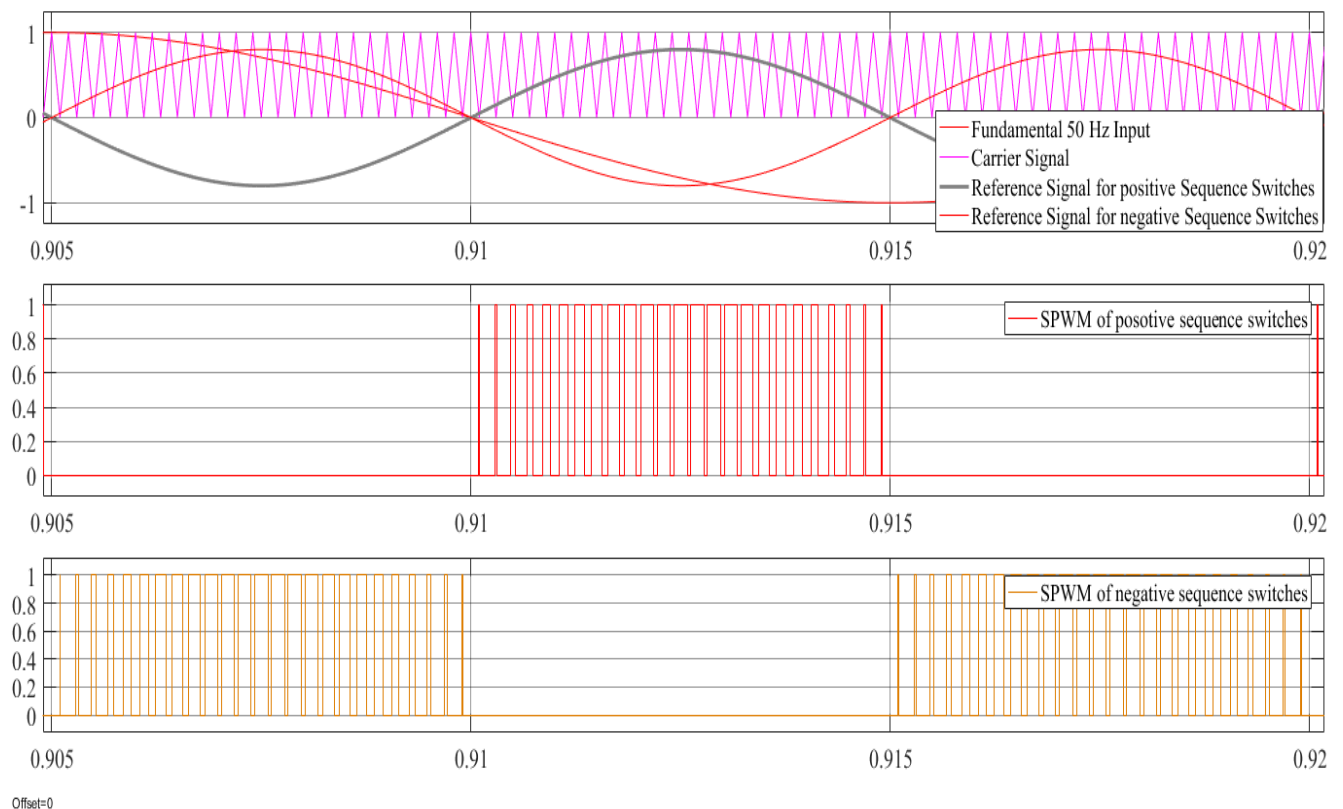


Figure 3.1 Sinusoidal PWM Signal Generation at 100 Hz output Frequency

In the Generation of Sinusoidal PWM, the two sinusoidal signals have been compared to the reference signal. Both the reference signal is in 180-degrees phase with each other, the main reason using two reference signal with 180-degrees phase shift is the amplitude of the carrier signal is 0 to +1 So, on comparing it with carrier signal one reference signal will give the signal for the

positive cycle and another for the negative cycle. In Figure 3.1, it shows the SPWM generation when output frequency is 100 Hz and Figure 3.2, shows the switching sequence of the gate pulse provided to all the switches of the SPMC.

Table 3.3 SPMC Active Switches

Input Frequency	Output Frequency	Mode	Active Switches		PWM Switches
50 Hz	50 Hz	1	S _{1A}	S _{2B}	S _{4A}
		2	S _{2B}	S _{1B}	S _{3B}
	100 Hz	1	S _{1A}	S _{2A}	S _{4A}
		2	S _{2A}	S _{1B}	S _{3A}
		3	S _{2B}	S _{1A}	S _{3B}
		4	S _{1B}	S _{2A}	S _{4A}
	25 Hz	1	S _{1A}	S _{2B}	S _{4A}
		2	S _{1B}	S _{2A}	S _{4B}
		3	S _{2A}	S _{1B}	S _{3A}
		4	S _{2B}	S _{1A}	S _{3B}

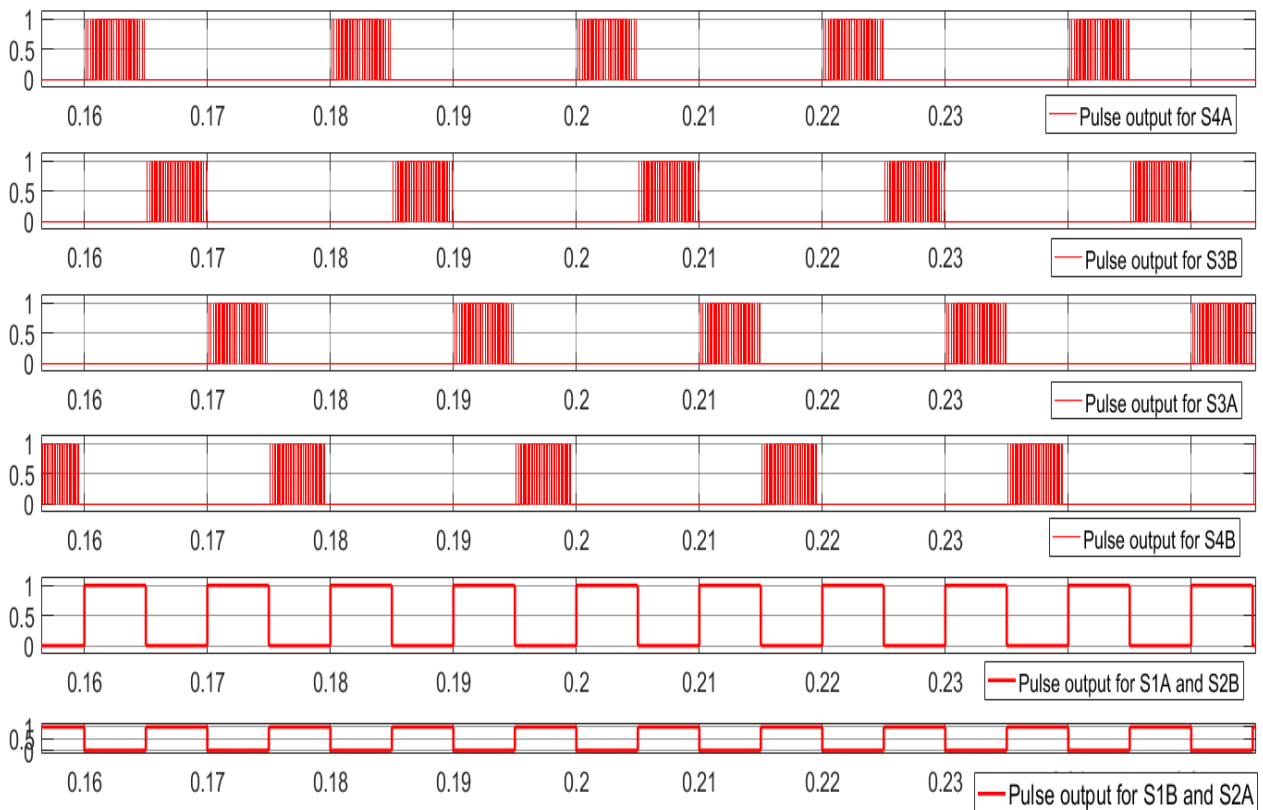


Figure 3.2 Switching Sequence of SPMC at 100 Hz Output frequency

3.1.1 Simulation of the Single Phase Matrix Converter

Figure 3.3 shows the output current and voltage of the SPMC for the resistive load of 50 W without filters through Simulation model in MATLAB.

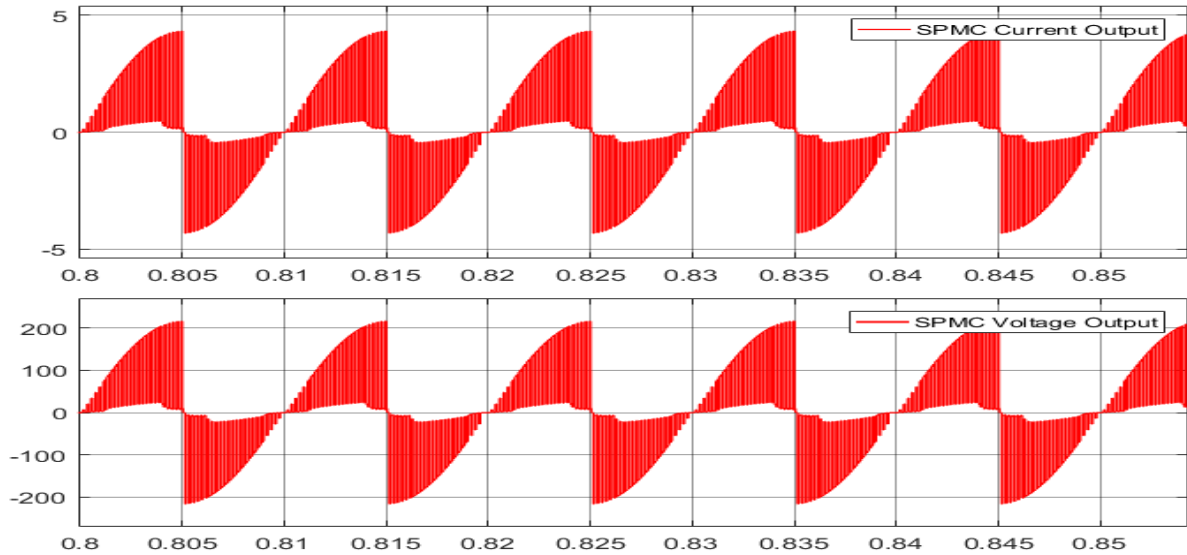


Figure 3.3 Output Voltage and Current when load is Resistive of 50 W without filters

Figure 3.4 shows the output current and voltage for the resistive inductive of 50 W and 10 mH load without filters through Simulation model in MATLAB.

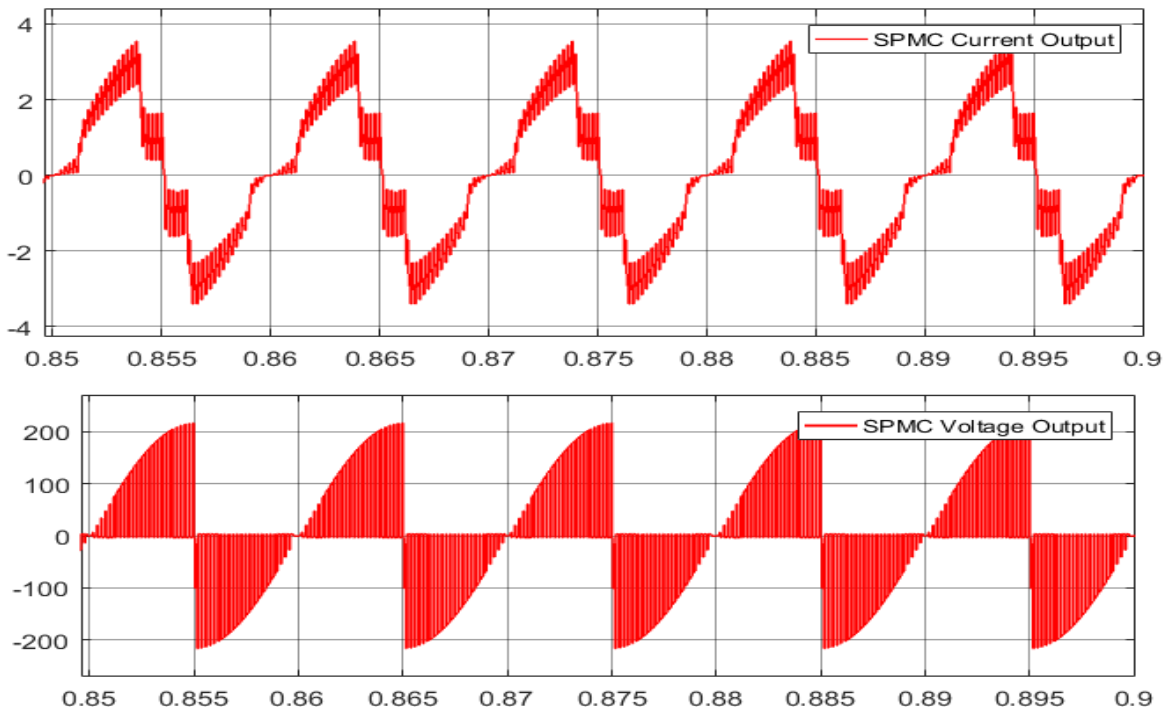


Figure 3.4 Output Voltage and Current when load is RL 50 W and 10 mH without filters

Figure 3.5 shows the output current and voltage of the SPMC for the resistive load of 50 W with Filter through Simulation model in MATLAB.

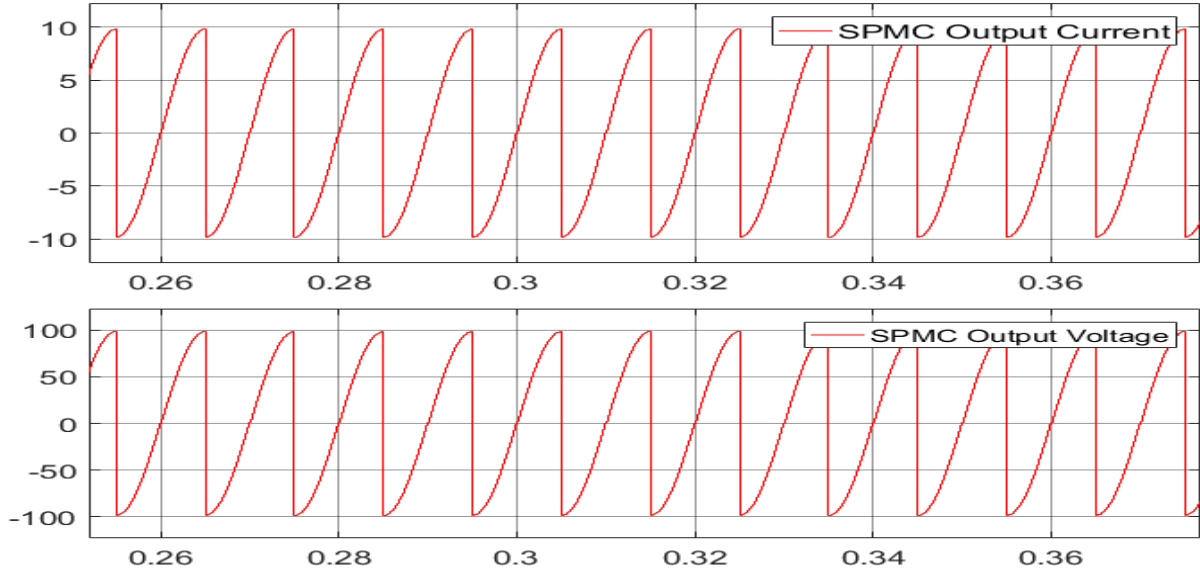


Figure 3.5 Output current and voltage of the SPMC for the resistive load of 50 W with filters.

Figure 3.6 output current and voltage of the SPMC for the resistive load of 50 W and 10 mH without Filter with filters through Simulation model in MATLAB.

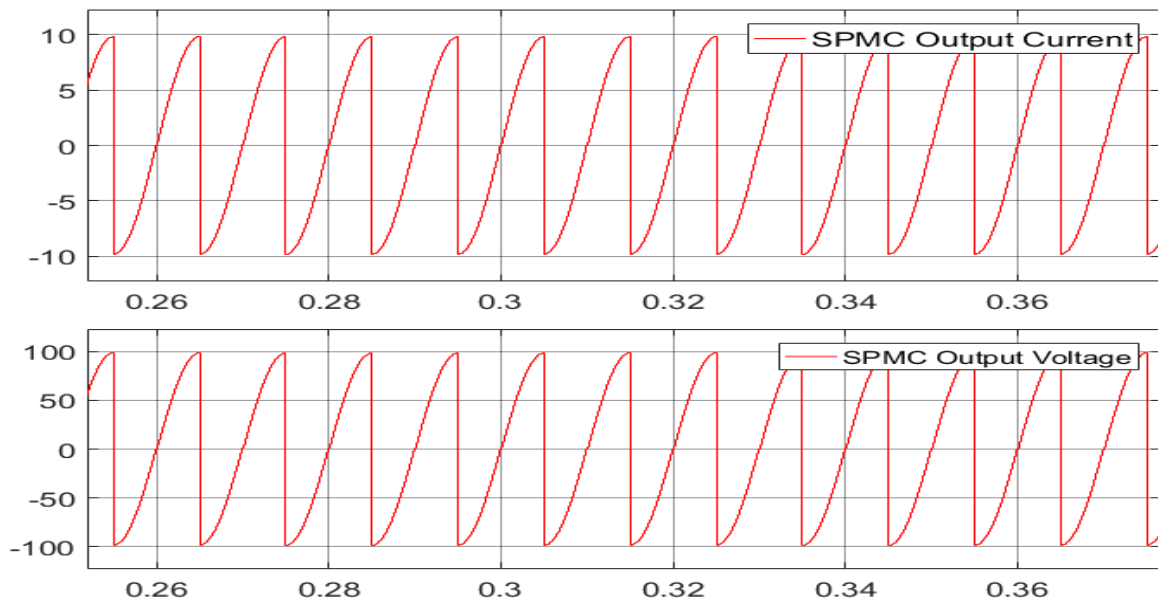


Figure 3.6 Output current and voltage of the SPMC for the resistive load of 50 W and 10 mH without Filter with filters

3.2 Generation of Modulating Signal for the Three Phase MC

There is a technique that was proposed in the year 1989 by the scientist Borojevic-et-al[18], then further research had been done by the Ziogas et al and Huber-et-al[19]. In this technique, he proposed an equivalent MC modulation strategy which is the combination of rectifier and inverter modulation strategy and proposed that there was a “DC link” in between Rectifier Stage and Inverter Stage. This Modulation scheme is also called as “fictitious DC link modulation topology”. This modulation topology has been divided into two parts. Part one Inverter Stage; Part two Rectifier Stage:

The Inverter stage has 3 phase Inverter stage topology that has 6 switches namely S_7 to S_{12} . Rectifier stage had another six switches S_1 to S_6 and has Rectifier stage topology.

Consider that input voltage of the MC in each phase is

$$\begin{aligned} V_A &= V_I \sin \omega t \\ V_B &= V_I \sin(\omega t + 120^\circ) \\ V_C &= V_I \sin(\omega t + 240^\circ) \end{aligned} \quad (3.1)$$

3.2.1 Modulation Technique for the Three Phase Matrix Converter

The representation of three phase MC is 3×3 matrix form, since there is no energy storing element and all nine bi-directional switches are connected in the sequence that every input is connected to every output phase is shown in Figure 3.7. Therefore, the input currents and output voltages of the MC thus characterized in the form of transfer function T is shown in Equation (3.6)

Output Voltage of the MC

$$V_0 = T * V_I \quad (3.2)$$

$$V_a = S_{aA} V_A + S_{aB} V_B + S_{aC} V_C ; \quad (3.3)$$

$$V_b = S_{bA} V_A + S_{bB} V_B + S_{bC} V_C ; \quad (3.4)$$

$$V_c = S_{cA} V_A + S_{cB} V_B + S_{cC} V_C ; \quad (3.5)$$

In Matrix Form;

$$\begin{bmatrix} V_a \\ V_b \\ V_c \end{bmatrix} = \begin{bmatrix} S_{aA} & S_{aB} & S_{aC} \\ S_{bA} & S_{bB} & S_{bC} \\ S_{cA} & S_{cB} & S_{cC} \end{bmatrix} \cdot \begin{bmatrix} V_A \\ V_B \\ V_C \end{bmatrix} ; \quad (3.6)$$

Similarly, for the input current

$$I_I = T^T * I_0 ; \quad (3.7)$$

$$\begin{bmatrix} I_A \\ I_B \\ I_C \end{bmatrix} = \begin{bmatrix} S_{aA} & S_{bA} & S_{cA} \\ S_{aB} & S_{bB} & S_{cB} \\ S_{aC} & S_{bC} & S_{cC} \end{bmatrix} \begin{bmatrix} I_a \\ I_b \\ I_c \end{bmatrix} \quad (3.8)$$

where V_A , V_B and V_C are input voltages phase, I_A , I_B and I_C are input currents V_a , V_b and V_c are output voltages phase, I_a , I_b and I_c are output currents and. All these elements of transfer matrix T_{ij} represented the instantaneous input voltage to the instantaneous voltage output of the switch function.

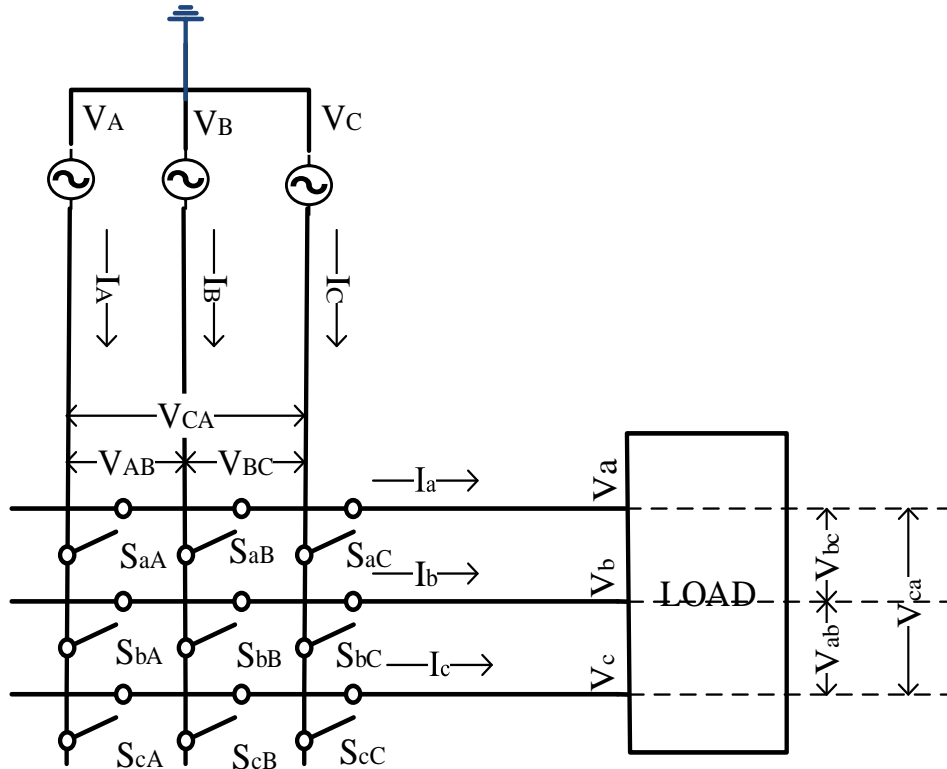


Figure 3.7 Three Phase to Three Phase Matrix Converter

3.2.1.1 Transfer Function of the Indirect PWM Equivalent Model

Considered the AC to AC power frequency conversion system and having virtual DC link in between the Input and output side. This converter has two AC to AC conversion stages, first stage is the rectifier stage and second stage is inverter stage as shown in Figure 3.8. In rectifier stage, the process of conversion of DC from AC takes place and Energy stored in the virtual DC link. In the another stage, the energy stored in the virtual DC link becomes the input for Inverter stage and hence here DC to AC conversion takes place.

In Invertersion stage,

$$\begin{bmatrix} V_a \\ V_b \\ V_c \end{bmatrix} = \begin{bmatrix} S_7 & S_8 \\ S_9 & S_{10} \\ S_{11} & S_{12} \end{bmatrix} \cdot \begin{bmatrix} V_{DC+} \\ V_{DC-} \end{bmatrix} \quad (3.9)$$

For Rectification stage,

$$\begin{bmatrix} V_{DC+} \\ V_{DC-} \end{bmatrix} = \begin{bmatrix} S_1 & S_3 & S_5 \\ S_2 & S_4 & S_6 \end{bmatrix} \begin{bmatrix} V_A \\ V_B \\ V_C \end{bmatrix} \quad (3.10)$$

On Comparing Equation (3.9) and Equation (3.10), we get

$$\begin{bmatrix} V_a \\ V_b \\ V_c \end{bmatrix} = \begin{bmatrix} S_7 & S_8 \\ S_9 & S_{10} \\ S_{11} & S_{12} \end{bmatrix} \cdot \begin{bmatrix} S_1 & S_3 & S_5 \\ S_2 & S_4 & S_6 \end{bmatrix} \cdot \begin{bmatrix} V_A \\ V_B \\ V_C \end{bmatrix} \quad (3.11)$$

$$\begin{bmatrix} V_a \\ V_b \\ V_c \end{bmatrix} = \begin{bmatrix} S_7.S_1 & S_8.S_2 & S_7.S_3 & S_8.S_4 & S_7.S_5 & S_8.S_6 \\ S_9.S_1 & S_{10}.S_2 & S_9.S_3 & S_{10}.S_6 & S_9.S_5 & S_{10}.S_6 \\ S_{11}.S_1 & S_{12}.S_2 & S_{11}.S_3 & S_{12}.S_8 & S_{11}.S_5 & S_{12}.S_6 \end{bmatrix} \cdot \begin{bmatrix} V_A \\ V_B \\ V_C \end{bmatrix} \quad (3.12)$$

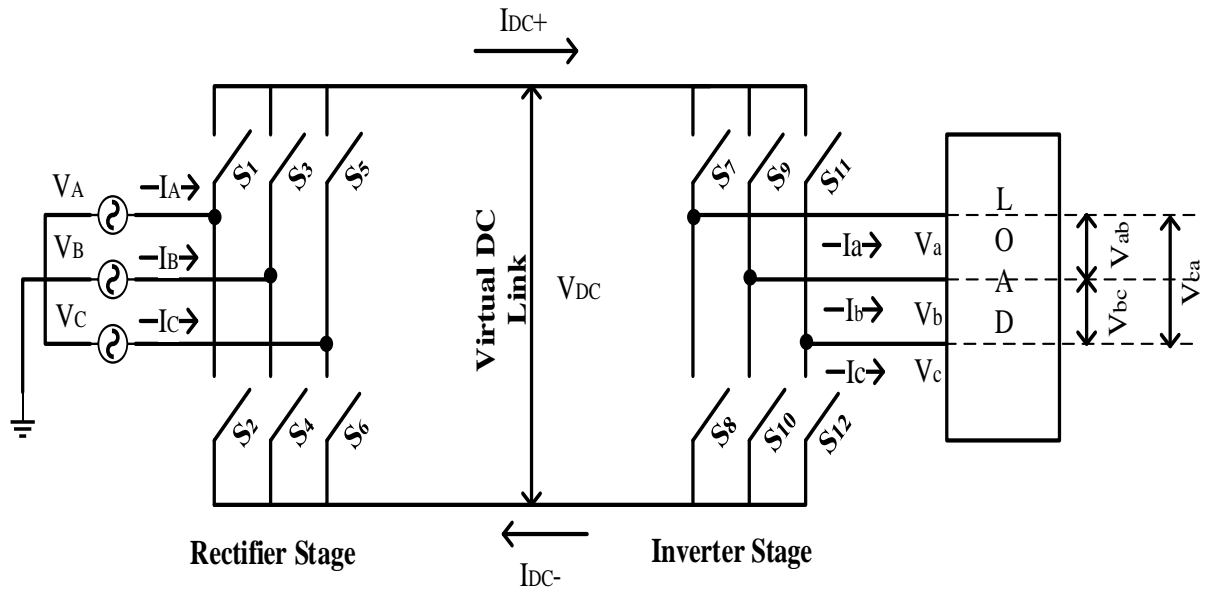


Figure 3.8 Indirect PWM Equivalent model

It is concluded from the Equation (3.12) the equivalent Switches all the 9 MC Switches from the Virtual DC link Equivalent mode switches. The TPMC topology has been shown in Figure 3.8 the two possible constraints that should not be during switching of switches that input phase should not be short-circuited whereas having an inductive load in output phase, hence the output phase

should never be open circuited. The switching function of S_{ij} switch is described in the Equation (3.13)

$$\begin{aligned} S_{ij}=1, & \quad \text{Switch } S_{ij} \text{ is closed} \\ =0, & \quad \text{Switch } S_{ij} \text{ is open} \end{aligned} \quad (3.13)$$

where $i \in \{a, b, c\}$ is the output phase, $j \in \{A, B, C\}$ is the input phase. Taking the details that there must not be short-circuited in input phase cause rise in current spikes and the inductor load output never be open circuited cause rise in voltage spikes and above Equation (3.13) is expressed in Equation (3.14) as a switching function

$$S_{iA} + S_{iB} + S_{iC} = 1, \quad (3.14)$$

where $i \in \{a, b, c\}$ is the output phase

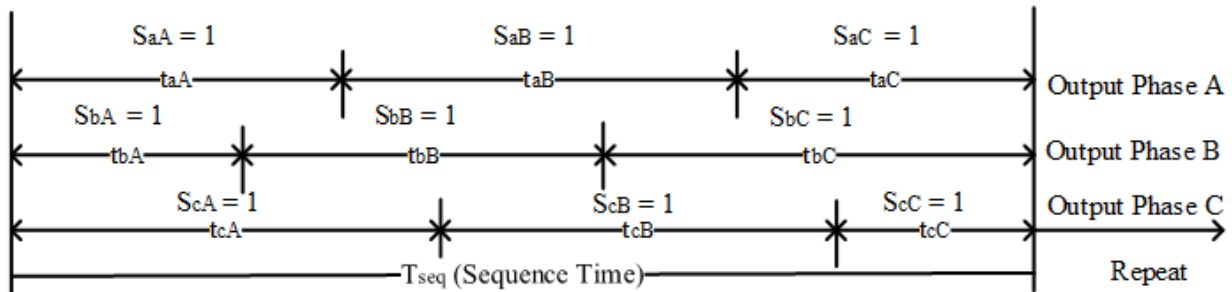


Figure 3.9 Random Switching States timing of the TPMC

3.3.2.1 Space Vector Modulation for the Inverter Stage

In this section, the introduction of SVM in the Inverter stage. Assume that SVM of inverter stage of the equivalent circuit and the DC voltage is supplied virtual DC link, then $V_{DC} = (V_{DC+}) - (V_{DC-})$ is shown in Figure 3.10.

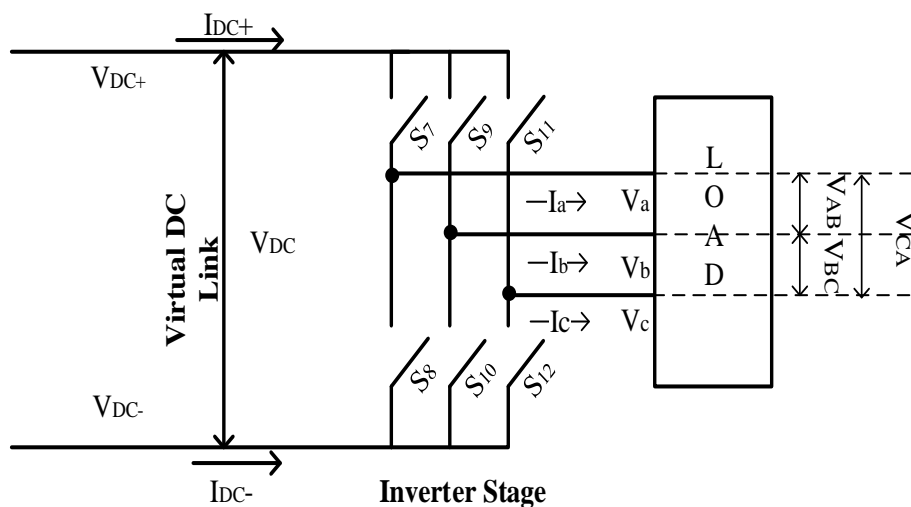


Figure 3.10 Inverter stage from the equivalent model

The output voltages are represented by multiplying inverter transfer function \mathbf{I} to virtual DC-link voltage V_{DC} . On the same time, I_{DC} which is the DC link current has been represented by \mathbf{I}^T .

$$\begin{bmatrix} V_a \\ V_b \\ V_c \end{bmatrix} = \begin{bmatrix} S_7 & S_8 \\ S_9 & S_{10} \\ S_{11} & S_{12} \end{bmatrix} \begin{bmatrix} V_{DC+} \\ V_{DC-} \end{bmatrix} \quad (3.15)$$

$$\begin{bmatrix} I_{DC+} \\ I_{DC-} \end{bmatrix} = \begin{bmatrix} S_7 & S_9 & S_{11} \\ S_8 & S_{10} & S_{12} \end{bmatrix} \begin{bmatrix} I_a \\ I_b \\ I_c \end{bmatrix} \quad (3.16)$$

To know the values of the output voltage and output voltage phase angle, there are 6 switches in inverter stage that is represented in order $S_7, S_8, S_9, S_{10}, S_{11}$, and S_{12} and when a switch is off by it is denoted by '0' and when a switch is on it is denoted by "1" and. Consider that inverter stage of the active vector $V_1[1 \ 0 \ 0]$. In this active stage, switch number 7 has been switched on from the upper part and switch number 10 and 12 from the lower part is shown in Figure 3.11

$$V_a = \left(\frac{2}{3}\right) V_{dc}; \quad (3.17)$$

$$V_b = V_c = -\left(\frac{1}{3}\right) V_{dc}; \quad (3.18)$$

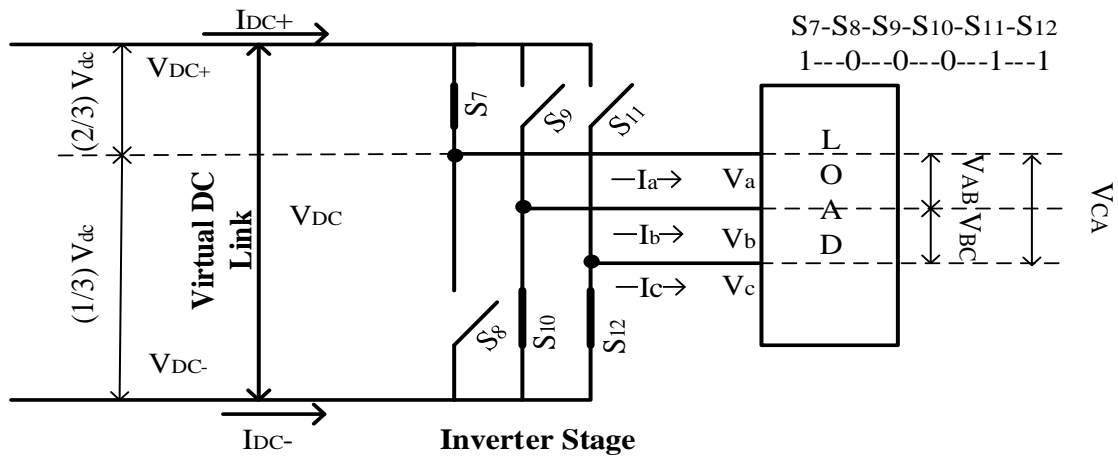


Figure 3.11 Inverter Stage when switches S_7, S_{10}, S_{12} are on in the Equivalent model of the Inverter Stage

In this voltage space vector, it reveals that output voltage V_A is connected to $(2/3) V_{DC+}$ and output voltages V_B and V_C are connected to $(1/3) V_{DC-}$ and their vector magnitude is represented as

$$V_1 = \frac{2}{3} \left(V_a + V_b \cdot e^{i\frac{2\pi}{3}} + V_c \cdot e^{i\frac{4\pi}{3}} \right) \quad (3.19)$$

$$= \frac{2}{3} \left(\frac{2}{3} V_{DC} - \frac{1}{3} V_{DC} \cdot e^{i\frac{2\pi}{3}} - \frac{1}{3} V_{DC} \cdot e^{i\frac{4\pi}{3}} \right) \quad (3.20)$$

$$V_1 = \left(\frac{2}{3} \right) \cdot V_{DC} \cdot e^{i0} \quad (3.21)$$

Hence the output voltage phase angle of the Inverter stage is start at 0^0 and magnitude of voltage output is $\frac{2\sqrt{3}}{3} V_{DC}$. In Table 3.4, it displays the output voltage magnitudes and output voltage angles of all the six active and 2 zero states of the Inverter stage.

Table 3.4 Switching Vectors and Switching States for the Inverter side

Type	Vector	$\begin{bmatrix} S_7 & S_9 & S_{11} \\ S_8 & S_{10} & S_{12} \end{bmatrix}^T$	$\begin{bmatrix} V_a & V_b & V_c \\ V_{ab} & V_{bc} & V_{ac} \end{bmatrix}$	$ V_{out} $	$\angle\theta_0$	I_{DC+}
Active	$V_1[1\ 0\ 0]$	$\begin{bmatrix} 1 & 0 & 0 \\ 0 & 1 & 1 \end{bmatrix}^T$	$\begin{bmatrix} \frac{2}{3}V_{DC} & -\frac{1}{3}V_{DC} & -\frac{1}{3}V_{DC} \\ V_{DC} & 0 & -V_{DC} \end{bmatrix}$	$\frac{2}{3}V_{DC}$	0	I_A
Active	$V_2[1\ 1\ 0]$	$\begin{bmatrix} 1 & 1 & 0 \\ 0 & 0 & 1 \end{bmatrix}^T$	$\begin{bmatrix} \frac{1}{3}V_{DC} & \frac{1}{3}V_{DC} & -\frac{2}{3}V_{DC} \\ 0 & V_{DC} & -V_{DC} \end{bmatrix}$	$\frac{2}{3}V_{DC}$	$\frac{\pi}{3}$	$-I_C$
Active	$V_3[0\ 1\ 0]$	$\begin{bmatrix} 0 & 1 & 0 \\ 1 & 0 & 1 \end{bmatrix}^T$	$\begin{bmatrix} -\frac{1}{3}V_{DC} & \frac{2}{3}V_{DC} & -\frac{1}{3}V_{DC} \\ -V_{DC} & V_{DC} & 0 \end{bmatrix}$	$\frac{2}{3}V_{DC}$	$\frac{2\pi}{3}$	I_B
Active	$V_4[0\ 1\ 1]$	$\begin{bmatrix} 0 & 1 & 1 \\ 1 & 0 & 0 \end{bmatrix}^T$	$\begin{bmatrix} \frac{2}{3}V_{DC} & -\frac{1}{3}V_{DC} & -\frac{1}{3}V_{DC} \\ V_{DC} & 0 & -V_{DC} \end{bmatrix}$	$\frac{2}{3}V_{DC}$	π	$-I_A$
Active	$V_5[0\ 0\ 1]$	$\begin{bmatrix} 0 & 0 & 1 \\ 1 & 1 & 0 \end{bmatrix}^T$	$\begin{bmatrix} -\frac{1}{3}V_{DC} & \frac{2}{3}V_{DC} & -\frac{1}{3}V_{DC} \\ 0 & -V_{DC} & V_{DC} \end{bmatrix}$	$\frac{2}{3}V_{DC}$	$\frac{-2\pi}{3}$	I_C

Active	$V_6[1\ 0\ 1]$	$\begin{bmatrix} 1 & 0 & 1 \\ 0 & 1 & 0 \end{bmatrix}^T$	$\begin{bmatrix} \frac{1}{3}V_{DC} & -\frac{2}{3}V_{DC} & \frac{1}{3}V_{DC} \\ V_{DC} & -V_{DC} & 0 \end{bmatrix}$	$\frac{2}{3}V_{DC}$	$-\frac{\pi}{3}$	$-I_B$
Zero	$V_0[0\ 0\ 0]$ $V_7[1\ 1\ 1]$	$\begin{bmatrix} 0 & 0 & 0 \\ 1 & 1 & 1 \end{bmatrix}^T$	$\begin{bmatrix} 1 & 1 & 1 \\ 0 & 0 & 0 \end{bmatrix}^T$	0		0

3.3.1.2.1 abc to $\alpha\beta$ Transformation for the Inverter Stage

The $\alpha\beta$ conversion from abc is the mathematical transformation helps for the analysis and simplification of three phase circuits, the main usefulness of this conversion is helping to generate a reference signal that has been used in SVM control in inverter stage.

$$V_\alpha + jV_\beta = \frac{2}{3} \left[V_a + V_b e^{j\frac{2\pi}{3}} + V_c e^{j\frac{4\pi}{3}} \right] \quad (3.22)$$

$$= \frac{2}{3} \left[V_a + V_b \cos \frac{2\pi}{3} + V_c \cos \frac{4\pi}{3} \right] - j \frac{2}{3} \left[V_a + V_b \sin \frac{2\pi}{3} + V_c \sin \frac{4\pi}{3} \right] \quad (3.23)$$

$$\begin{bmatrix} V_\alpha \\ V_\beta \end{bmatrix} = \begin{bmatrix} 1 & \cos \frac{2\pi}{3} & \cos \frac{4\pi}{3} \\ 0 & j \sin \frac{2\pi}{3} & j \sin \frac{4\pi}{3} \end{bmatrix} = \frac{2}{3} \begin{bmatrix} 1 & -\frac{1}{2} & -\frac{1}{2} \\ 0 & \frac{\sqrt{3}}{2} & -\frac{\sqrt{3}}{2} \end{bmatrix} \cdot \begin{bmatrix} V_a \\ V_b \\ V_c \end{bmatrix} \quad (3.24)$$

$$V_\alpha = \frac{2}{3} \left[V_a - \frac{1}{2} V_b - \frac{1}{2} V_c \right]; \quad (3.25)$$

$$= \frac{2}{3} \left[\frac{\sqrt{3}}{2} V_b - \frac{\sqrt{3}}{2} V_c \right]; \quad (3.26)$$

In Table 3.5, the transformation of abc to alpha beta at all various output phase angles.

Table 3.5 abc to $\alpha\beta$ transformation

q	V_a	V_b
0	$\frac{2}{3} V_a - \frac{1}{3} V_b - \frac{1}{3} V_c$	$\frac{1}{\sqrt{3}} V_b - \frac{1}{\sqrt{3}} V_c$
$\frac{p}{3}$	$\frac{1}{3} V_a - \frac{2}{3} V_b + \frac{1}{3} V_c$	$\frac{1}{\sqrt{3}} V_a - \frac{1}{\sqrt{3}} V_c$
$\frac{2p}{3}$	$-\frac{1}{3} V_a - \frac{1}{3} V_b + \frac{2}{3} V_c$	$\frac{1}{\sqrt{3}} V_a - \frac{1}{\sqrt{3}} V_b$

p	$-\frac{2}{3}V_a + \frac{1}{3}V_b + \frac{1}{3}V_c$	$-\frac{1}{\sqrt{3}}V_b + \frac{1}{\sqrt{3}}V_c$
$-\frac{2p}{3}$	$-\frac{1}{3}V_a + \frac{2}{3}V_b - \frac{1}{3}V_c$	$-\frac{1}{\sqrt{3}}V_a + \frac{1}{\sqrt{3}}V_c$
$\frac{p}{3}$	$\frac{1}{3}V_a + \frac{1}{3}V_b - \frac{2}{3}V_c$	$-\frac{1}{\sqrt{3}}V_a + \frac{1}{\sqrt{3}}V_b$

3.3.1.2.2 Sector Selection for the Inverter Stage

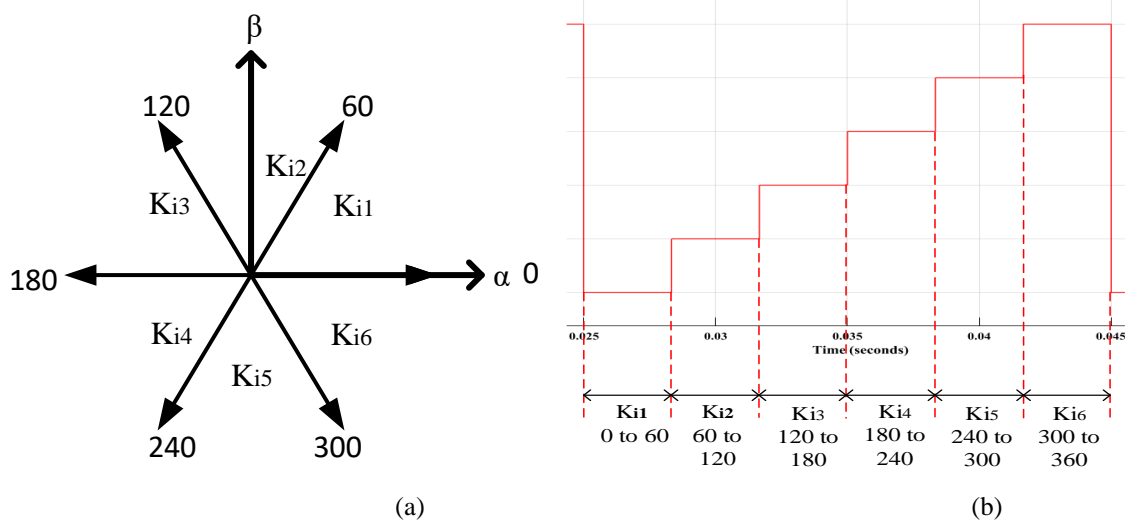


Figure 3.12 Sector representation during inverter stage (a) wrt angle (b) wrt time

In this section, this describes that angle of the Inverter stage exists in which sector out of the 6 Sectors. The 6 sectors of the inverter stage each sector has 60 degrees angle as shown in Figure 3.12. The sector of the Inverter stage is represented by K_i where $i \in \{1, 2, \dots, 6\}$. The Sector 1 of the Inverter stage lies in between 0 to 60 degrees, Sector 2 of the Inverter stage lies in between 60 to 120 degrees, Sector 3 of the Inverter stage lies in between 120 to 240 degrees, Sector 4 of the Inverter stage lies in between 180 to 240 degrees, Sector 5 of the Inverter stage lies in between 240 to 300 degrees and Sector 6 of the Inverter stage lies in between 300 to 360 or 0 degree.

3.3.1.2.3 Duty Period of Switch for the Inverter Stage

There are 8 space vectors that have been arranged in a hexagon. This hexagon having 6 sectors of 60 degrees each shown in the Figure 3.13 and Figure 3.14 provide the synthesis of the reference voltage V_0^* in sector 1, this vector is within the voltage hexagon. V_0^* has been concluded from

the V_1 and V_2 have the d_1 and d_2 duty cycle respectively. Let us considered T_s is the constant time interval and the reference Voltage V_0^* is expressed in the Equation (3.27)

$$V_0^* T_s = V_1 T_1 + V_2 T_2 + V_{0v} T_{0v} \quad (3.27)$$

$$T_s = T_1 + T_2 + T_{0v} \quad (3.28)$$

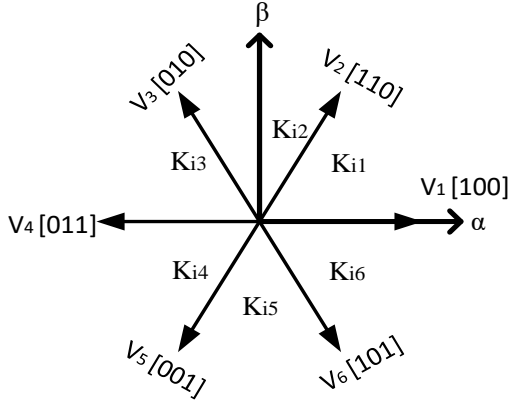


Figure 3.13 Voltage Hexagon of inverter

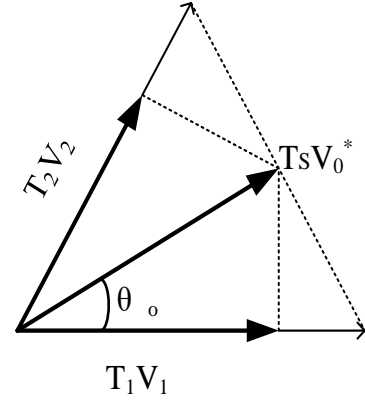


Figure 3.14 Synthesis of reference voltage vector

Considered the case when Inverter stage is in the Sector 1 as shown in Figure 3.14. At that time, $V_0^* = V_0^* \angle \theta_o$; $V_1 = V_{dc} \angle 0^\circ$; $V_2 = V_{dc} \angle \frac{\pi}{3}$; $V_{0v} = 0 \angle 0^\circ$. The duty Period of the inverter Stage is Expressed in the Equation (3.29).

$$T_s V_0^* \begin{bmatrix} \cos \theta_o \\ j \sin \theta_o \end{bmatrix} = \left(\frac{2}{3}\right) T_1 V_{dc} \begin{bmatrix} 1 \\ 0 \end{bmatrix} + \left(\frac{2}{3}\right) T_2 V_{dc} \begin{bmatrix} \cos \frac{\pi}{3} \\ j \sin \frac{\pi}{3} \end{bmatrix} \quad (3.29)$$

On comparing real and imaginary terms, we get

$$T_s V_0^* \cos \theta_o = \left(\frac{2}{3}\right) T_1 V_{dc} + \left(\frac{2}{3}\right) \left(\frac{1}{2}\right) T_2 V_{dc} = \left(\frac{2}{3}\right) T_1 V_{dc} + \left(\frac{1}{3}\right) T_2 V_{dc} \quad (3.30)$$

$$T_s V_0^* \sin \theta_o = \left(\frac{2}{3}\right) \left(\frac{\sqrt{3}}{2}\right) T_2 V_{dc} = \left(\frac{1}{\sqrt{3}}\right) T_2 V_{dc} \quad (3.31)$$

$$T_2 = \sqrt{3} \left(\frac{V_0^*}{V_{dc}}\right) T_s \sin \theta = M_v T_s \sin \theta \quad (3.32)$$

$$T_1 = \sqrt{3} \left(\frac{V_0^*}{V_{dc}}\right) T_s \sin \left(\frac{\pi}{3} - \theta\right) = M_v T_s \sin \left(\frac{\pi}{3} - \theta\right) \quad (3.33)$$

$$M_v = \sqrt{3} \left(\frac{V_0^*}{V_{dc}} \right) \quad (3.34)$$

Where M_v is the Modulation Index of Inverter Stage.

$$T_{0v} = T_s - T_1 - T_2 \quad (3.35)$$

Now the resultant space vector V_0^* is the vector sum of $\frac{T_1}{T_s}(V_1)$ and $\frac{T_2}{T_s}(V_2)$; where V_1 and V_2 are space vectors.

For Maximum Modulation Index

For the maximum modulation index the timing of the T_1 and T_2 are equally divided

$$\frac{T_{0v}}{2} = 0.5 (T_s - T_1 - T_2) \quad (3.36)$$

$$\begin{aligned} \frac{T_{0v}}{T_s} &= 0.5 - \frac{T_1}{T_s} - \frac{T_2}{T_s} = 0.5 - \frac{M_v \sin \theta}{\sin \frac{p}{3}} - \frac{M_v \sin \left(\frac{2\pi}{3} - \theta \right)}{\sin \frac{p}{3}} \\ &= 0.5 - M_v \frac{\sin \theta}{\sin \frac{p}{3}} - \frac{\sin \left(\frac{2\pi}{3} - \theta \right)}{\sin \frac{p}{3}} \end{aligned} \quad (3.37)$$

Maximum value of M_v

$$M_v \frac{\sin \theta}{\sin \frac{p}{3}} - \frac{\sin \left(\frac{2\pi}{3} - \theta \right)}{\sin \frac{p}{3}} = 1; \quad (3.38)$$

$$M_v = \frac{\sin \left(\frac{2\pi}{3} - \theta \right)}{\sin \frac{p}{3} - \sin \theta} \quad (3.39)$$

For maximum value of M_v , θ is $\frac{p}{3}$ and equals to 0.866.

For the calculation of time interval for the n th sector is described below in Equation (3.38) and Equation (3.41) and Equation (3.43) describes the duty period of zero vector of Inverter stage.

Time interval of the Inverter stage for n th Sector;

$$T_1 = M_v T_s \sin\left(\frac{\pi}{3} - \theta_0 + (n-1)\frac{\pi}{3}\right) \quad (3.40)$$

$$= M_v T_s \left[\sin\left(\frac{n\pi}{3} \cos \theta_0 - \cos\left(\frac{n\pi}{3}\right) \sin \theta_0\right) \right] \quad (3.41)$$

$$T_2 = M_v T_s \sin\left(\theta_0 - (n-1)\frac{\pi}{3}\right) \quad (3.42)$$

$$= M_v T_s \left[-\cos \theta_0 \sin\left((n-1)\frac{\pi}{3}\right) + \sin \theta_0 \cos\left((n-1)\frac{\pi}{3}\right) \right] \quad (3.43)$$

In the Table 3.6, Explains the duty period of the Vectors active V_1 , V_2 and Zero vector V_{0v} having a time interval of T_1 , T_2 and T_0 respectively.

Table 3.6 Duty period of the Switching Vectors of Inverter Stage

Sector	T_1	T_2	T_{0v}
1	$M_v T_s \sin\left(\frac{\pi}{3} - \theta_0\right)$	$M_v T_s \sin \theta_0$	$T_s - T_1 - T_2$
2	$M_v T_s \sin\left(\frac{2\pi}{3} - \theta_0\right)$	$M_v T_s \sin\left(\theta_0 - \frac{\pi}{3}\right)$	
3	$M_v T_s \sin(\pi - \theta_0)$	$M_v T_s \sin\left(\theta_0 - \frac{2\pi}{3}\right)$	
4	$M_v T_s \sin\left(\frac{4\pi}{3} - \theta_0\right)$	$M_v T_s \sin(\theta_0 - \pi)$	
5	$M_v T_s \sin\left(\frac{5\pi}{3} - \theta_0\right)$	$M_v T_s \sin\left(\theta_0 - \frac{4\pi}{3}\right)$	
6	$M_v T_s \sin(2\pi - \theta_0)$	$M_v T_s \sin\left(\theta_0 - \frac{5\pi}{3}\right)$	

3.3.1.2.4 Duty Cycle Calculation for the Inverter Stage

The duty cycle of the active vectors is calculated and Shown in Equation (3.44) –(3.47) introduces the duty cycle generation in the Simulink model in one Sector. The duty cycle is defined to be a time period of current vector to the total time interval.

$$V_0^* = d_1 V_1 + d_2 V_2 \quad (3.44)$$

$$d_1 = \frac{T_1}{T_s} = M_v \cdot \sin\left(\frac{\pi}{3} - \theta_o\right) \quad (3.45)$$

$$d_2 = \frac{T_2}{T_s} = M_v \cdot \sin(\theta_o) \quad (3.46)$$

$$d_{0v} = \frac{T_{0v}}{T_s} = 1 - d_1 - d_2 \quad (3.47)$$

3.3.1.2.5 Switching Duration of the Switches for the Inverter Stage

In this section, the switching Patterns of the which switches and examine that the switches are whose are turned on and off during each sector. Let us consider a case when the inverter stage is in the sector 1 as shown in Figure 3.14. In the sector 1, active voltage vectors are $V_1[100]$ and $V_2[110]$. For the sector 1, In the active vector V_1 switches: S_7, S_9, S_{12} are at on condition rest all are off. Similarly in the active vector V_2 switches: S_7, S_{10}, S_{12} is on condition rest all are off. In the zero vector V_7 all lower switches are turned on and during zero vector V_0 , all upper switches are turned on. Hence duty period of the switches S_7 and S_{12} are $T_1 + T_2 + T_0/2$, whereas for switch S_9 is $T_1 + T_0/2$ and for S_{10} is $T_2 + T_0/2$ and for the rest of the switches duty period is $T_0/2$.

Table 3.7 Switching Timing of the switches, this explains the switching states of each switch of the switches S_7 to S_{12} in the all six sectors of the Inverter stage. In the Figure 3.15, it describes the Switching timing of the Inverter Stage in sector 1.

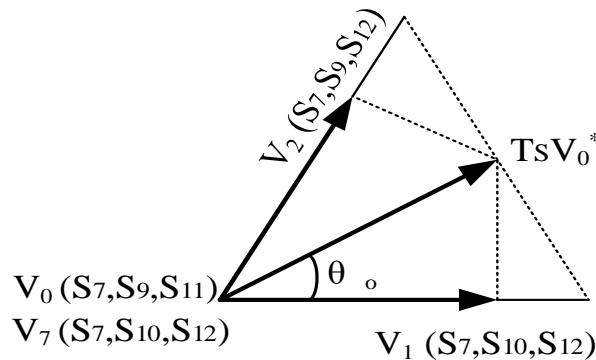


Figure 3.15 At Sector-1, On switches in Inverter stage

Table 3.7 Switching Timing of the switches

K_i	Switching timing for upper switch	Switching timing for lower switch
1	$S_7(t) = T_1 + T_2 + \frac{T_{0v}}{2}; S_9(t) = T_2 + \frac{T_{0v}}{2}; S_{11}(t) = \frac{T_{0v}}{2}$	$S_8(t) = \frac{T_{0v}}{2}; S_{10}(t) = T_1 + \frac{T_{0v}}{2}; S_{12}(t) = T_1 + T_2 + \frac{T_{0v}}{2}$

2	$S_7(t) = T_2 + \frac{T_{0v}}{2}; S_9(t) = T_1 + T_2 + \frac{T_{0v}}{2}; S_{11}(t) = \frac{T_{0v}}{2}$	$S_8(t) = T_1 + \frac{T_{0v}}{2}; S_{10}(t) = \frac{T_{0v}}{2}; S_{12}(t) = T_1 + T_2 + \frac{T_{0v}}{2}$
3	$S_7(t) = \frac{T_{0v}}{2}; S_9(t) = T_1 + T_2 + \frac{T_{0v}}{2}; S_{11}(t) = T_2 + \frac{T_{0v}}{2}$	$S_8(t) = T_1 + T_2 + \frac{T_{0v}}{2}; S_{10}(t) = \frac{T_{0v}}{2}; S_{12}(t) = T_1 + \frac{T_{0v}}{2}$
4	$S_7(t) = \frac{T_{0v}}{2}; S_9(t) = T_1 + T_2 + \frac{T_{0v}}{2}; S_{11}(t) = T_2 + \frac{T_{0v}}{2}$	$S_8(t) = T_1 + T_2 + \frac{T_{0v}}{2}; S_{10}(t) = T_1 + \frac{T_{0v}}{2}; S_{12}(t) = \frac{T_{0v}}{2}$
5	$S_7(t) = T_2 + \frac{T_{0v}}{2}; S_9(t) = \frac{T_{0v}}{2}; S_{11}(t) = T_1 + T_2 + \frac{T_{0v}}{2}$	$S_8(t) = T_1 + \frac{T_{0v}}{2}; S_{10}(t) = T_1 + T_2 + \frac{T_{0v}}{2}; S_{12}(t) = \frac{T_{0v}}{2}$
6	$S_7(t) = T_1 + T_2 + \frac{T_{0v}}{2}; S_9(t) = \frac{T_{0v}}{2}; S_{11}(t) = T_2 + \frac{T_{0v}}{2}$	$S_8(t) = \frac{T_{0v}}{2}; S_{10}(t) = T_1 + T_2 + \frac{T_{0v}}{2}; S_{12}(t) = T_2 + \frac{T_{0v}}{2}$

3.3.1.2.6 Switching Sequence of the Inverter Stage

In the Figure 3.16, it shows the switching sequence of the Inverter stage. In this process, the duty cycle value has been compared with triangular carrier waveform to generate the -phase output voltage. The output phase is changed during the switching pattern from $T_0/4 \rightarrow T_1/2 \rightarrow T_2/2 \rightarrow T_0/4 \rightarrow T_0/4 \rightarrow T_2/2 \rightarrow T_1/2 \rightarrow T_0/4$, consequently and Table 3.8 describes the switching sequence of the Inverter stage.

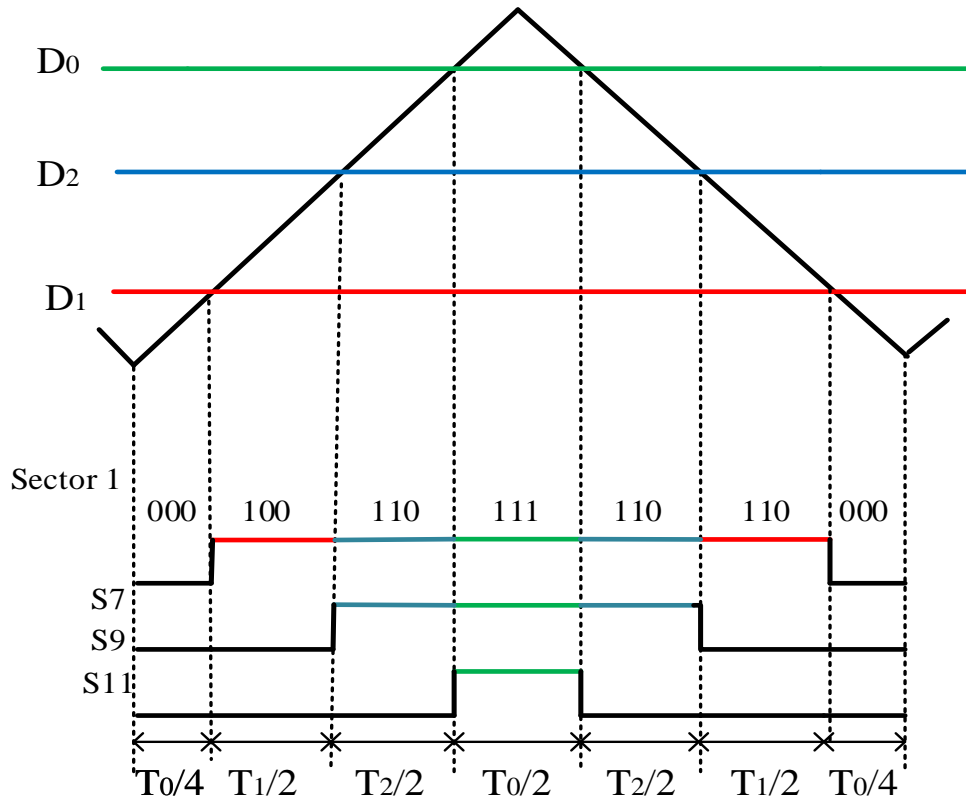


Figure 3.16 Switching Sequence and Sequence in the Inverter Stage

Table 3.8 Switching Sequence and period of each switch in sector1 from output

Sample Number	T0/4 in ns	T1/2 in ns	T2/2 in ns	T0/4 in ns	T0/4 in ns	T2/2 in ns	T1/2 in ns	T0/4 in ns
	V0/4	V1/2	V2/2	V7/4	V7/4	V2/2	V1/2	V0/4
1	13.59	74.78	0	11.59	11.59	0	74.78	13.59
	1	1	0	1	0	1	1	1
2	12.2	73.85	5.99	10.99	10.99	5.99	73.85	12.2
	1	1	1	1	1	1	1	1
3	9.964	68.01	13.86	9.097	9.097	13.86	68.01	9.964
	1	1	1	1	1	1	1	1
4	9.964	64.11	17.76	9.097	9.097	17.76	64.11	9.964
	1	1	1	1	1	1	1	1
5	10.44	60.00	21.81	9.091	9.091	21.81	60.00	10.44
	1	1	1	1	1	1	1	1
6	8.184	58.18	28.18	7.045	7.045	28.18	58.18	8.184
	1	1	1	1	1	1	1	1
7	8.13	52.13	33.96	6.916	6.916	33.96	52.13	8.13
	1	1	1	1	1	1	1	1
8	7.654	48.3	38.26	6.936	6.936	38.26	48.31	7.654
	1	1	1	1	1	1	1	1
9	8.224	43.8	42.03	7.082	7.082	42.03	43.86	8.224
	1	1	1	1	1	1	1	1
10	8.224	37.9	47.97	7.082	7.082	47.97	37.92	8.224
	1	1	1	1	1	1	1	1
11	8.08	34.01	51.87	7.018	7.018	51.87	34.01	8.08
	1	1	1	1	1	1	1	1
12	8.079	28.06	57.82	7.018	7.018	57.82	28.06	8.079
	1	1	1	1	1	1	1	1
13	9.485	22.13	60.07	8.98	8.98	60.07	22.13	9.485
	1	1	1	1	1	1	1	1
14	9.486	18.06	64.13	9.033	9.033	64.13	18.06	9.486
	1	1	1	1	1	1	1	1

15	10.35	14.04	67.56	9.05	9.05	67.56	14.04	10.35
	1	1	1	1	1	1	1	1
16	12.41	5.762	72.24	10.85	10.85	72.24	5.762	12.41
	1	1	1	1	1	1	1	1
17	14.62	0	74.01	13.07	13.07	74.01	0	14.62
	1	0	1	1	1	1	0	1

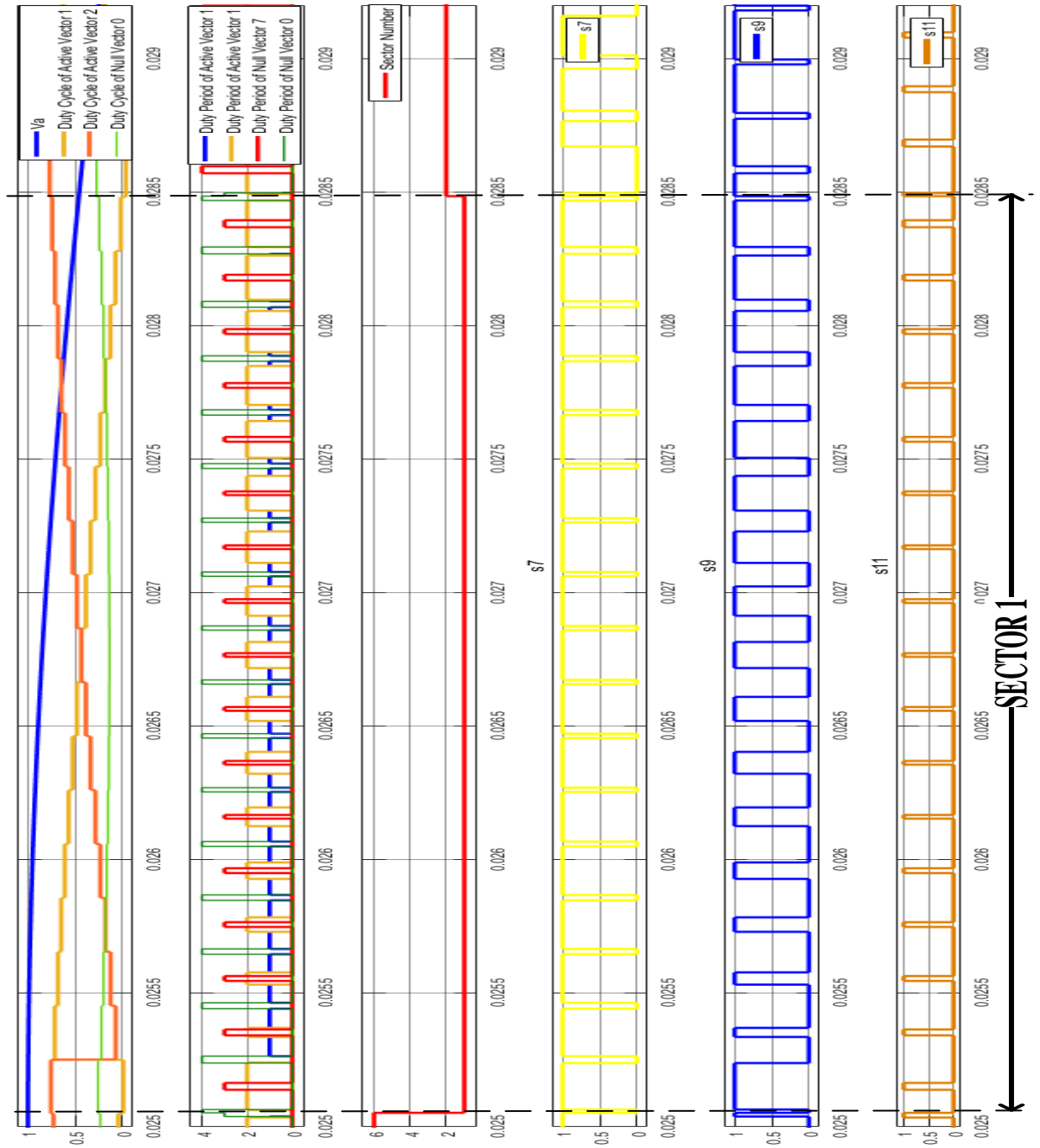


Figure 3.17 Switching Sequence of switches in the Inverter Stage

The six sectors in Figure 3.18 means directly means to the 60° six segments of 3 phase desired output voltage within the period. where V_{DC} is the average value of the virtual dc-link voltage.

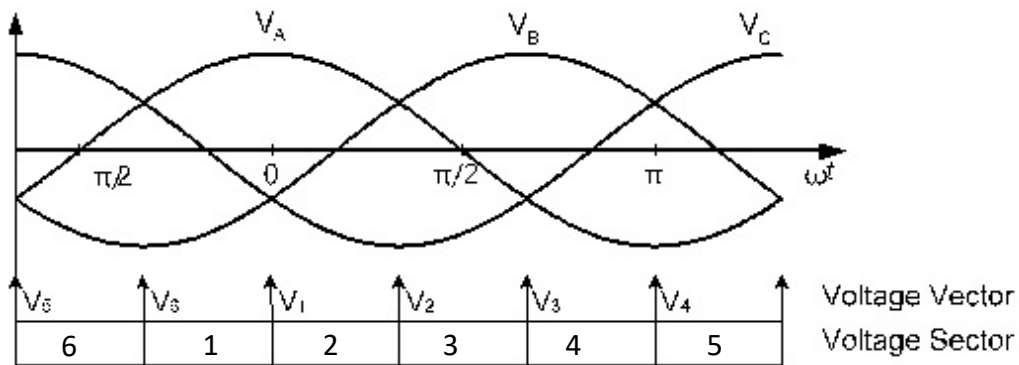


Figure 3.18 Six sectors in the output voltages

Let us take an example of the output voltage phase for a switching cycle of voltage sector K_{i1} . In the voltage sector K_{i1} , the two active vectors are V_1 and V_2 shown in Figure 3.18, the mean value of the dc-link current and voltages output is written as follows

$$\begin{bmatrix} V_A \\ V_B \\ V_C \end{bmatrix} = d_1 \cdot V_6 + d_2 \cdot V_1 = \left(d_1 \cdot \begin{bmatrix} 1 & 0 \\ 1 & 0 \\ 0 & 1 \end{bmatrix} + d_2 \cdot \begin{bmatrix} 1 & 0 \\ 0 & 1 \\ 0 & 1 \end{bmatrix} \right) \cdot \begin{bmatrix} V_{DC+} \\ V_{DC-} \end{bmatrix} \quad (3.48)$$

The three phase output voltage waveforms V_A , V_B and V_C in the inverter stage is shown in Figure 3.19.

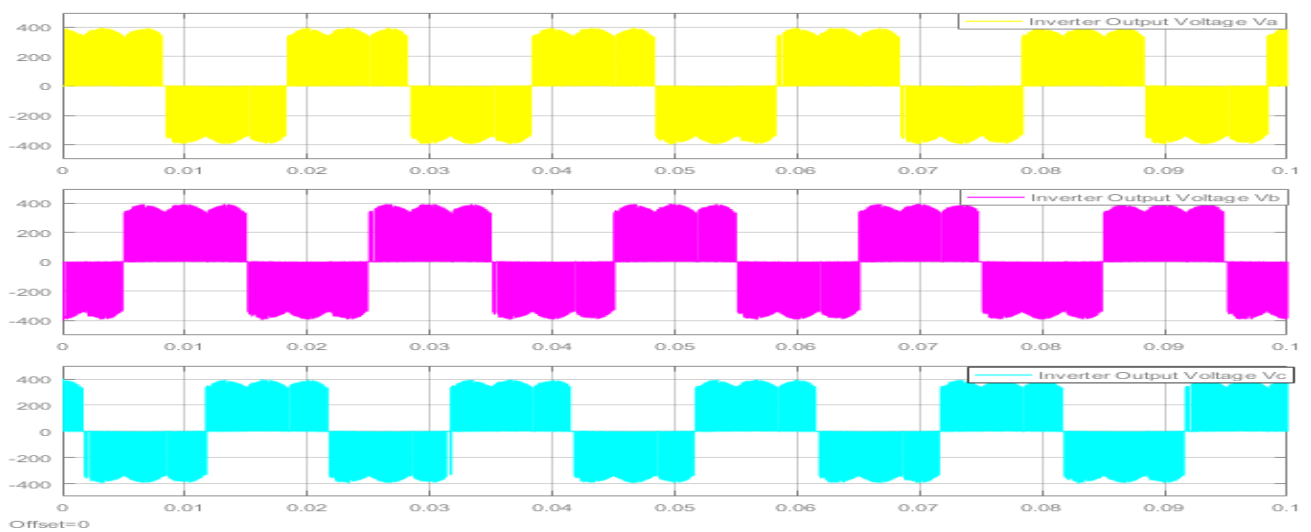


Figure 3.19 Three Phase Output Voltage of Inverter Stage

3.3.3.2 SVM for the Rectifier Stage

This section introduces SVM for the Rectifier stage, In the previous section, the research and analysis have been done on the inverter stage, Similarly, in this section the research and analysis has been done on rectifier stage. The equivalent circuit of this part is shown in Figure 3.20 and assume this as a standalone rectifier.

In this SVM, there is a virtual DC link that is taken into account as an all quantities reference. The input currents are shown below in the Equation (3.49) and DC link Voltage is derived in Equation (3.50).

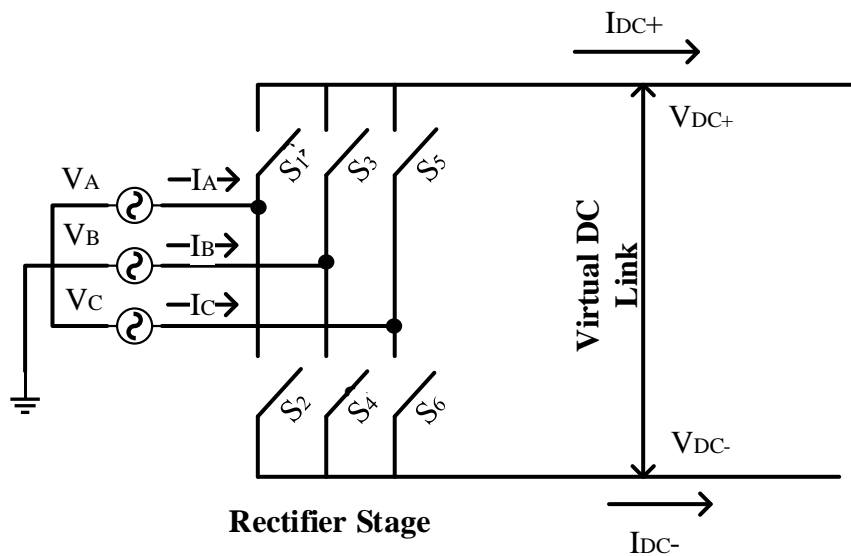


Figure 3.20 Rectifier stage from the equivalent model

$$\begin{bmatrix} I_A \\ I_B \\ I_C \end{bmatrix} = \begin{bmatrix} S_1 & S_2 \\ S_3 & S_4 \\ S_5 & S_6 \end{bmatrix} \cdot \begin{bmatrix} I_{DC+} \\ I_{DC-} \end{bmatrix} \quad (3.49)$$

$$\begin{bmatrix} V_{DC+} \\ V_{DC-} \end{bmatrix} = \begin{bmatrix} S_1 & S_3 & S_5 \\ S_2 & S_4 & S_6 \end{bmatrix} \quad (3.50)$$

To know the values of the Input Current and Input Current phase angle. In Rectifier we have two output DC values. Consider that inverter stage of the active vector $I_1[AB]$. In this active stage, switch number 1 has been switched on from the upper part and switch number 4 from the lower part shown in Figure 3.21

Then I_1 is expressed using the transformation of space vector is shown in Equation (3.51) respectively, let us considered that the rectifier is in sector 1

$$I_1 = \frac{2}{3} \left(I_A + I_B \cdot e^{i\frac{2\pi}{3}} + I_C \cdot e^{i\frac{4\pi}{3}} \right) = \frac{2}{3} \left(I_{DC} - I_{DC} \cdot e^{i\frac{2\pi}{3}} - 0 \cdot e^{i\frac{4\pi}{3}} \right) \quad (3.51)$$

$$I_1 = \frac{2}{\sqrt{3}} \cdot I_{DC} \cdot e^{i\frac{\pi}{6}} \quad (3.52)$$

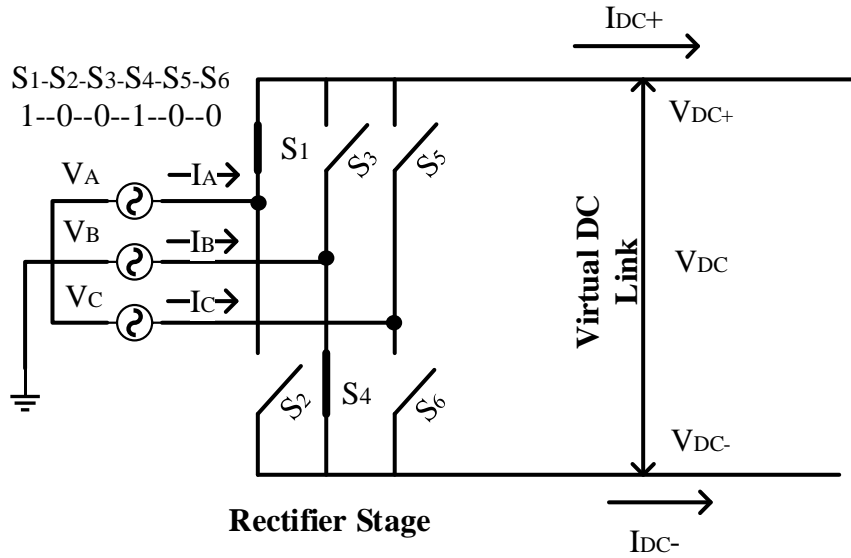


Figure 3.21 Equivalent circuits for rectifier stage when Switches S_1 and S_4 are closed

Hence the Input Current angle of the Rectifier stage current input angle $\frac{\pi}{6}$ and magnitude of current input is $\frac{2}{\sqrt{3}} I_{DC}$. Table 3.9 shows the Input current magnitude and Input current phase angles of all the six active and three zero states of the Rectifier stage. the vector [P N] represents the positive and Negative terminal of DC side. There are 6 switches in rectifier stage that are represented in such a way that when a switch is off by '0' and when a switch is on by "1" and shown in order S_1, S_2, S_3, S_4, S_5 and S_6 .

Table 3.9 Switching vectors and Switch States Rectifier stage

Type	Vector I [P N]	$\begin{bmatrix} S_1 & S_3 & S_5 \\ S_2 & S_4 & S_6 \end{bmatrix}^T$	$[I_a, I_b, I_c]$	$ I_{in} $	$ \angle I_{in} $	V_{DC}
	I_1 [AB]	$\begin{bmatrix} 1 & 0 & 0 \\ 0 & 1 & 0 \end{bmatrix}^T$	$[I_{DC+} \ I_{DC-} \ 0]$	$\frac{2}{\sqrt{3}} I_{DC}$	$-\frac{\pi}{6}$	V_{AB}

ACTIVE	$I_2[AC]$	$\begin{bmatrix} 1 & 0 & 0 \\ 0 & 0 & 1 \end{bmatrix}^T$	$[I_{DC+} \ 0 \ I_{DC-}]$	$\frac{2}{\sqrt{3}} I_{DC}$	$\frac{\pi}{6}$	$-V_{CA}$
	$I_3[BC]$	$\begin{bmatrix} 0 & 1 & 0 \\ 0 & 0 & 1 \end{bmatrix}^T$	$[I_{DC+} \ 0 \ I_{DC-}]$	$\frac{2}{\sqrt{3}} I_{DC}$	$\frac{\pi}{2}$	V_{BC}
	$I_4[BA]$	$\begin{bmatrix} 0 & 1 & 0 \\ 1 & 0 & 0 \end{bmatrix}^T$	$[I_{DC-} \ I_{DC+} \ 0]$	$\frac{2}{\sqrt{3}} I_{DC}$	$\frac{5\pi}{6}$	$-V_{AB}$
	$I_5[CA]$	$\begin{bmatrix} 0 & 0 & 1 \\ 1 & 0 & 0 \end{bmatrix}^T$	$[I_{DC-} \ 0 \ I_{DC+}]$	$\frac{2}{\sqrt{3}} I_{DC}$	$\frac{-5\pi}{6}$	V_{CA}
	$I_6[CB]$	$\begin{bmatrix} 0 & 0 & 1 \\ 0 & 1 & 0 \end{bmatrix}^T$	$[0 \ I_{DC-} \ I_{DC+}]$	$\frac{2}{\sqrt{3}} I_{DC}$	$\frac{-\pi}{2}$	$-V_{BC}$
ZERO	$I_0[AA]$	$\begin{bmatrix} 1 & 0 & 0 \\ 1 & 0 & 0 \end{bmatrix}^T$	$\begin{bmatrix} 0 & 1 & 0 \\ 0 & 1 & 0 \end{bmatrix}^T$	0		0
	$I_0[BB]$					
	$I_0[CC]$	$\begin{bmatrix} 0 & 0 & 1 \\ 0 & 0 & 1 \end{bmatrix}^T$				

3.3.2.1.1 abc into $\alpha\beta$ Transformation for the Rectifier Stage

The alpha beta conversion from abc is the mathematical transformation helps for the analysis and simplification of three phase circuits, the main usefulness of this conversion is helping to generate a reference signal that has been used in SVM control in Rectifier Stage.

$$I_\alpha + jI_\beta = \frac{2}{3} \left[I_A + I_B e^{j\frac{2\pi}{3}} + I_C e^{j\frac{4\pi}{3}} \right] \quad (3.53)$$

$$= \frac{2}{3} \left[I_A + I_B \cos \frac{2\pi}{3} + I_C \cos \frac{4\pi}{3} \right] - j \frac{2}{3} \left[I_A + I_B \sin \frac{2\pi}{3} + I_C \sin \frac{4\pi}{3} \right]; \quad (3.54)$$

$$\begin{bmatrix} I_\alpha \\ I_\beta \end{bmatrix} = \begin{bmatrix} 1 & \cos \frac{2\pi}{3} & \cos \frac{4\pi}{3} \\ 0 & j \sin \frac{2\pi}{3} & j \sin \frac{4\pi}{3} \end{bmatrix} \cdot \begin{bmatrix} I_A \\ I_B \\ I_C \end{bmatrix} = \frac{2}{3} \begin{bmatrix} 1 & -\frac{1}{2} & -\frac{1}{2} \\ 0 & \frac{\sqrt{3}}{2} & -\frac{\sqrt{3}}{2} \end{bmatrix} \cdot \begin{bmatrix} I_A \\ I_B \\ I_C \end{bmatrix} \quad (3.55)$$

$$I_\alpha = \frac{2}{3} \left[I_A - \frac{1}{2} I_B - \frac{1}{2} I_C \right]; \quad (3.56)$$

$$I_\beta = \frac{2}{3} \left[\frac{\sqrt{3}}{2} I_B - \frac{\sqrt{3}}{2} I_C \right]; \quad (3.57)$$

Table 3.10 abc to $\alpha\beta$ Transmission

q	I_a	I_b
0	$\frac{2}{3}I_A - \frac{1}{3}I_B - \frac{1}{3}I_C$	$\frac{1}{\sqrt{3}}I_B - \frac{1}{\sqrt{3}}I_C$
$\frac{p}{3}$	$\frac{1}{3}I_A - \frac{2}{3}I_B + \frac{1}{3}I_C$	$\frac{1}{\sqrt{3}}I_A - \frac{1}{\sqrt{3}}I_C$
$\frac{2p}{3}$	$-\frac{1}{3}I_A - \frac{1}{3}I_B + \frac{2}{3}I_C$	$\frac{1}{\sqrt{3}}I_A - \frac{1}{\sqrt{3}}I_B$
p	$-\frac{2}{3}I_A + \frac{1}{3}I_B + \frac{1}{3}I_C$	$-\frac{1}{\sqrt{3}}I_B + \frac{1}{\sqrt{3}}I_C$
$-\frac{2p}{3}$	$-\frac{1}{3}I_A + \frac{2}{3}I_B - \frac{1}{3}I_C$	$-\frac{1}{\sqrt{3}}I_A + \frac{1}{\sqrt{3}}I_C$
$\frac{p}{3}$	$\frac{1}{3}I_A + \frac{1}{3}I_B - \frac{2}{3}I_C$	$-\frac{1}{\sqrt{3}}I_A + \frac{1}{\sqrt{3}}I_B$

3.3.2.1.2 Selector Selection for the Rectifier Stage

In this section, this describes that angle of the Inverter stage exists in which sector out of the 6 Sectors. The 6 sectors of the inverter stage each sector has 60 degrees angle as shown in Figure 3.22. The sector of the Inverter stage is represented by K_r where $r \in \{1, 2, \dots, 6\}$.

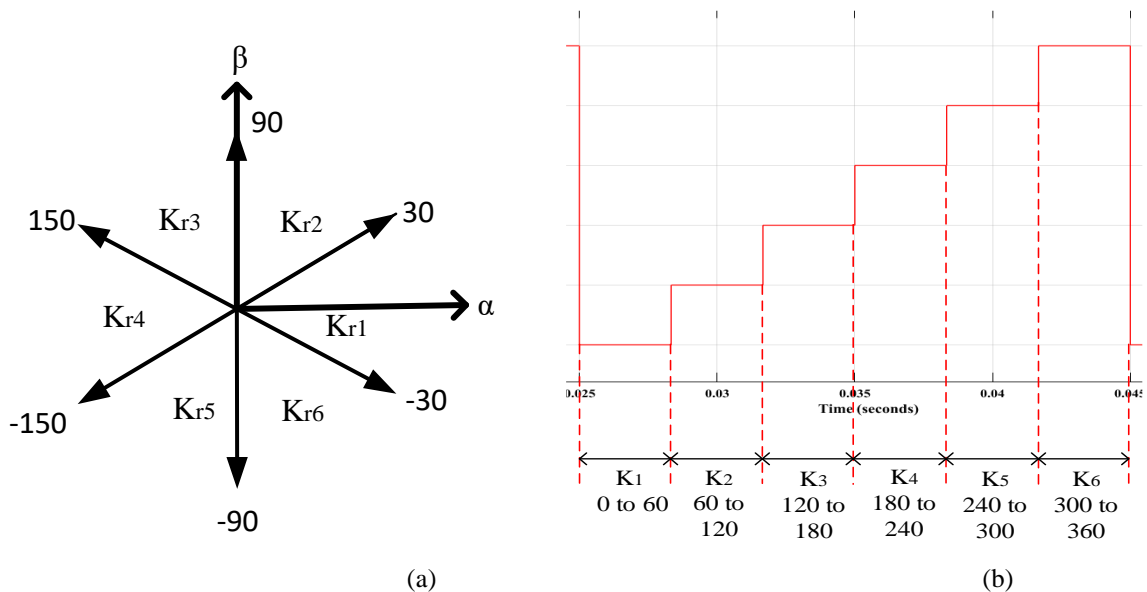


Figure 3.22 Sector Representation in Rectifier stage (a) wrt angle (b) wrt time

The Sector 1 of the Inverter stage lies in between -30 to 30 degrees, Sector 2 of the Inverter stage lies in between 30 to 90 degrees, Sector 3 of the Inverter stage lies in between 90 to 150 degrees, Sector 4 of the Inverter stage lies in between 150 to 210 degrees, Sector 5 of the Inverter stage lies in between 210 to 270 degrees and Sector 6 of the Inverter stage lies in between 270 to 330 or -30 degree.

3.3.3.1.3 Duty Period of the Switch for the Rectifier Stage

There are 9 space vectors that have been arranged in a hexagon that the synthesis of the reference Current I_0^* , this vector is within the voltage hexagon. I_0^* has been concluded from the I_1 and I_2 having the d_3 and d_4 duty cycle respectively. Let us considered T_s is the constant time interval for the input Current, than the I_0^* is expressed in the Equation (3.57)

$$I_0^* T_s = I_1 T_1 + I_2 T_2 + I_{0c} T_0; \quad (3.58)$$

$$T_s = T_3 + T_4 + T_{0c}; \quad (3.59)$$

Considered the case when Rectifier stage is in the Sector 1 as shown in Figure 3.24. At that time,

$$I_0^* = I_0^* \angle \theta_i; \quad I_1 = \frac{2}{\sqrt{3}} I_{DC} \angle 0^\circ; \quad I_2 = \frac{2}{\sqrt{3}} I_{DC} \angle \frac{\pi}{3}; \quad I_{0c} = 0; \quad \text{and The duty Period of the}$$

Rectifier Stage is Expressed in Equation (3.60)

$$T_s I_0^* \begin{bmatrix} \cos \theta_i \\ j \sin \theta_i \end{bmatrix} = T_1 \left(\frac{2}{\sqrt{3}} I_{dc} \right) \begin{bmatrix} \cos \left(-\frac{\pi}{6} \right) \\ j \sin \left(-\frac{\pi}{6} \right) \end{bmatrix} + T_2 \left(\frac{2}{\sqrt{3}} I_{dc} \right) \begin{bmatrix} \cos \frac{\pi}{6} \\ j \sin \frac{\pi}{6} \end{bmatrix} \quad (3.60)$$

On comparing real and imaginary terms, we get

$$T_s I_0^* \cos \theta_i = T_1 \left(\frac{2}{\sqrt{3}} I_{dc} \right) \left(\frac{\sqrt{3}}{2} \right) + T_2 \left(\frac{2}{\sqrt{3}} I_{dc} \right) \left(\frac{\sqrt{3}}{2} \right) = T_1 (I_{dc}) + T_2 (I_{dc}) \quad (3.61)$$

$$T_s I_0^* \sin \theta_i = T_1 \left(\frac{2}{\sqrt{3}} I_{dc} \right) \left(-\frac{1}{2} \right) + T_2 \left(\frac{2}{\sqrt{3}} I_{dc} \right) \left(\frac{1}{2} \right) = \left(-\frac{1}{\sqrt{3}} \right) T_1 I_{dc} + \left(\frac{1}{\sqrt{3}} \right) T_2 I_{dc} \quad (3.62)$$

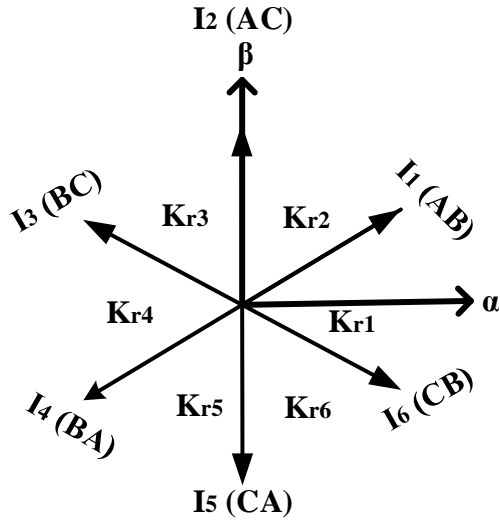


Figure 3.23 Current Hexagon of Rectifier stage

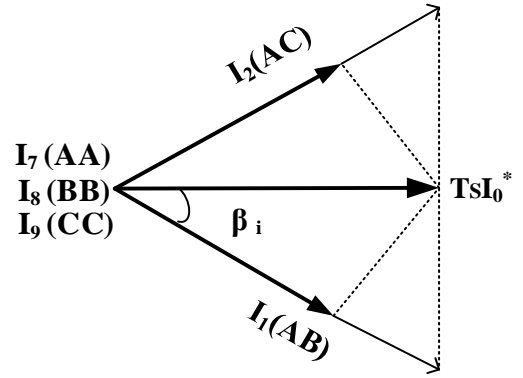


Figure 3.24 Synthesis of reference current vector

$$T_2 = \left(\frac{I_0^*}{I_{dc}} \right) T_s \sin \theta_i = M_v T_s \sin \theta_i; \quad (3.63)$$

$$T_1 = \left(\frac{I_0^*}{I_{dc}} \right) T_s \sin \left(\frac{\pi}{3} - \theta_i \right) = M_v T_s \sin \left(\frac{\pi}{3} - \theta_i \right); \quad (3.64)$$

Where, $M_c = \left(\frac{I_0^*}{I_{dc}} \right);$

Where M_1 is the Modulation Index of Rectifier Stage.

For the calculation of time interval for the n th sector it's described below in Equation (3.65) and Equation (3.66)

For n th Sector;

$$\begin{aligned} T_3 &= M_c T_s \sin \left(\frac{\pi}{3} - \theta_i + (n-1) \frac{\pi}{3} \right) \\ &= M_c T_s \left[\sin \left(\frac{n\pi}{3} \cos \theta - \cos \left(\frac{n\pi}{3} \right) \sin \theta_i \right) \right] \end{aligned} \quad (3.65)$$

$$\begin{aligned} T_4 &= M_c T_s \sin \left(\theta_i - (n-1) \frac{\pi}{3} \right) \\ &= M_c T_s \left[-\cos \theta_i \sin \left((n-1) \frac{\pi}{3} \right) + \sin \theta_i \cos \left((n-1) \frac{\pi}{3} \right) \right] \end{aligned} \quad (3.66)$$

$$T_{0c} = T_s - T_3 - T_4 \quad (3.67)$$

Table 3.11 Time Duration of the, Explains the time interval of the Vectors active I_3 , I_4 and Zero vector I_{0c} having a time interval of T_3 , T_4 and T_{0c} respectively.

Table 3.11 Time Duration of the Switching Vectors of Rectifier Stage

Sector	T_3	T_4	T_{0c}
1	$M_c T_s \sin\left(\frac{\pi}{3} - \theta_i\right)$	$M_c T_s \sin \theta_i$	$T_s - T_3 - T_4$
2	$M_c T_s \sin\left(\frac{2\pi}{3} - \theta_i\right)$	$M_c T_s \sin\left(\theta_i - \frac{\pi}{3}\right)$	
3	$M_c T_s \sin(\pi - \theta_i)$	$M_c T_s \sin\left(\theta_i - \frac{2\pi}{3}\right)$	
4	$M_c T_s \sin\left(\frac{4\pi}{3} - \theta_i\right)$	$M_c T_s \sin(\theta_i - \pi)$	
5	$M_c T_s \sin\left(\frac{5\pi}{3} - \theta_i\right)$	$M_c T_s \sin\left(\theta_i - \frac{4\pi}{3}\right)$	
6	$M_s T_s \sin(2\pi - \theta_i)$	$M_c T_s \sin\left(\theta_i - \frac{5\pi}{3}\right)$	

3.3.3.1.4 Duty Cycle Calculation for the Rectifier Stage

The duty cycle of the active vectors is calculated and Shown in Equation (3.68) – (3.71) introduces the duty cycle generation in the Simulink model in one Sector. The duty cycle is defined to be a time period of current vector to the total time interval.

$$I_I^* = d_3 I_3 + d_4 I_4 \quad (3.68)$$

$$d_3 = \frac{T_3}{T_s} = M_c \cdot \sin\left(\frac{\pi}{3} - \theta_i\right) \quad (3.69)$$

$$d_4 = \frac{T_4}{T_s} = M_c \cdot \sin(\theta_i) \quad (3.70)$$

$$d_{0c} = \frac{T_{0c}}{T_s} = 1 - d_3 - d_4 \quad (3.71)$$

3.3.3.1.5 Switching Duration of the Switches for Rectifier Stage

In this section. the switching Patterns of the which switches and examine that the switches are whose are turned on and off during each sector. Let us consider a case when the inverter stage is in the sector 1. In the sector 1, active current vectors are I_1 [ab] and I_2 [ac]. For the sector 1 of the

Inverter stage, In the active vector I_1 the switches S_1, S_6 are at switched on condition rest all are off. Similarly, in the active vector I_2 switches: S_1, S_4 are at switched on condition rest all are off. In the zero vector, I_7 switches S_1 and S_2 are switched on whereas in I_8 switches S_3 and S_4 whereas I_9 switches S_5 and S_6 . Hence duty period of the switches S_1 is $T_1+T_2+T_0/2$, whereas for switch S_6 is $T_1+T_0/2$ and for S_4 is $T_2+T_0/2$ and for the rest of the switches duty period is $T_0/2$.

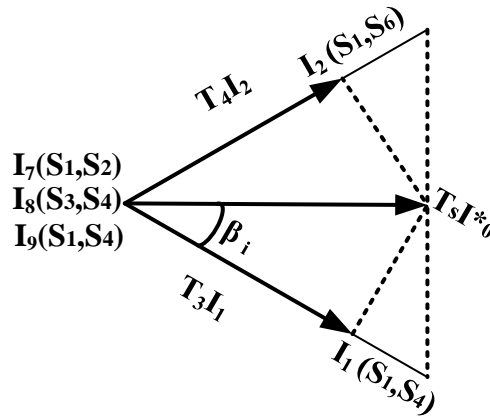


Figure 3.25 In Sector-1, On switches in Rectifier stage

Table 3.7 Switching Timing of the switches, this explains the switching states of each switch of the switches S_1 to S_6 in the all six sectors of the Rectifier Stage. In the Figure 3.25, it describes the Switching timing of the Inverter Stage in sector 1.

Table 3.12 switching timing of switches in Rectifier stage

Sector	Switching timing for upper switch	Switching timing for lower switch
1	$S_1 = T_3 + T_4 + \frac{T_{0c}}{2}; S_3 = \frac{T_{0c}}{2}; S_5 = \frac{T_{0c}}{2}$	$S_2 = \frac{T_{0c}}{2}; S_4 = T_3 + \frac{T_{0c}}{2}; S_6 = T_4 + \frac{T_{0c}}{2}$
2	$S_1 = T_3 + \frac{T_{0c}}{2}; S_3 = T_4 + \frac{T_{0c}}{2}; S_5 = \frac{T_{0c}}{2}$	$S_2 = \frac{T_{0c}}{2}; S_4 = \frac{T_{0c}}{2}; S_6 = T_3 + T_4 + \frac{T_{0c}}{2}$
3	$S_1 = \frac{T_{0c}}{2}; S_3 = T_3 + T_4 + \frac{T_{0c}}{2}; S_5 = \frac{T_{0c}}{2}$	$S_2 = T_4 + \frac{T_{0c}}{2}; S_4 = \frac{T_{0c}}{2}; S_6 = T_3 + \frac{T_{0c}}{2}$
4	$S_1 = T_3 + T_4 + \frac{T_{0c}}{2}; S_3 = \frac{T_{0c}}{2}; S_5 = \frac{T_{0c}}{2}$	$S_2 = \frac{T_{0c}}{2}; S_4 = T_3 + \frac{T_{0c}}{2}; S_6 = T_4 + \frac{T_{0c}}{2}$
5	$S_1 = T_3 + \frac{T_{0c}}{2}; S_3 = T_4 + \frac{T_{0c}}{2}; S_5 = \frac{T_{0c}}{2}$	$S_2 = \frac{T_{0c}}{2}; S_4 = \frac{T_{0c}}{2}; S_6 = T_3 + T_4 + \frac{T_{0c}}{2}$
6	$S_1 = T_4 + \frac{T_{0c}}{2}; S_3 = \frac{T_{0c}}{2}; S_5 = T_3 + \frac{T_{0c}}{2}$	$S_2 = \frac{T_{0c}}{2}; S_4 = T_3 + T_4 + \frac{T_{0c}}{2}; S_6 = \frac{T_{0c}}{2}$

3.3.3.1.6 Switching Sequence for the Rectifier Stage

In the Figure 3.26, it shows the switching sequence of the Inverter stage. In this process the phase duty ratio value has compared with triangular carrier waveform to generate the phase output voltage. The output phase is changed during the switching pattern from $T_0/4 \rightarrow T_1/2 \rightarrow T_2/2 \rightarrow T_0/4 \rightarrow T_0/4 \rightarrow T_2/2 \rightarrow T_1/2 \rightarrow T_0/4$, consequently and the Table 3.13 describes the switching sequence of the Inverter stage of the MC.

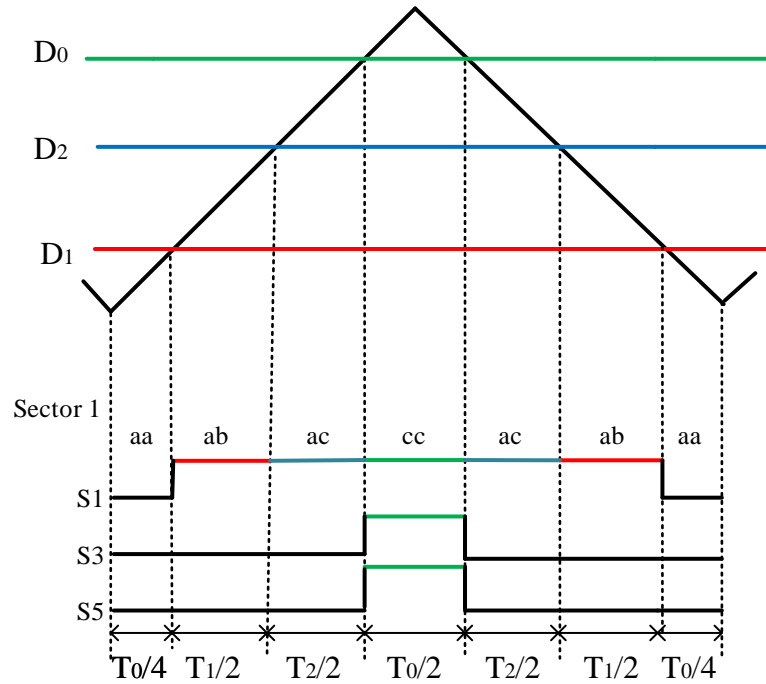


Figure 3.26 Switching Sequence and Sequence in the Inverter Stage

Table 3.13 Switching Sequence and period of each switch for sector-1

Sample Number	$T_0/4$	$T_1/2$	$T_2/2$	$T_0/4$	$T_0/4$	$T_2/2$ in	$T_1/2$	$T_0/4$
	in ns	in ns	in ns	in ns	in ns	ns	in ns	in ns
1	13.59	74.8	0	11.59	11.59	0	74.8	13.59
	1	1	0	1	1	0	1	1
2	12.25	74.1	4.5	10.99	10.99	4.5	74.1	12.25
	1	1	1	1	1	1	1	1
3	10.26	70.01	13.04	9.09	9.09	13.042	70.01	10.26
	1	1	1	1	1	1	1	1

4	10.96	66.11	16.16	9.29	9.20	16.162	66.11	10.96
	1	1	1	1	1	1	1	1
5	10.44	62.00	20.81	9.10	9.10	20.81	62.00	10.44
	1	1	1	1	1	1	1	1
6	9.184	60.19	26.18	7.45	7.45	26.18	60.19	9.184
	1	1	1	1	1	1	1	1
7	8.75	55.60	30.46	6.71	6.71	30.46	55.60	8.75
	1	1	1	1	1	1	1	1
8	8.956	49.31	36.88	6.55	6.55	36.88	49.31	8.956
	1	1	1	1	1	1	1	1
9	8.224	40.86	42.03	7.08	7.08	42.03	40.86	8.224
	1	1	1	1	1	1	1	1
10	8.08	34.01	50.87	7.01	7.01	50.873	34.01	8.08
	1	1	1	1	1	1	1	1
11	8.065	28.06	56.82	7.18	7.18	56.826	28.06	8.065
	1	1	1	1	1	1	1	1
12	9.55	23.13	60.03	8.42	8.42	60.033	23.13	9.55
	1	1	1	1	1	1	1	1
13	10.16	20.06	63.99	9.03	9.03	63.99	20.06	10.16
	1	1	1	1	1	1	1	1
14	10.38	12.04	66.56	9.05	9.05	66.56	12.04	10.38
	1	1	1	1	1	1	1	1
15	12.04	7.76	70.24	11.55	11.55	70.24	7.76	12.04
	1	1	1	1	1	1	1	1
16	13.05	5.54	70.45	13.55	13.55	70.45	5.54	13.05
	1	1	1	1	1	1	1	1
17	14.36	0	72.06	13.74	13.74	72.06	0	14.36
	1	0	1	1	1	1	0	1

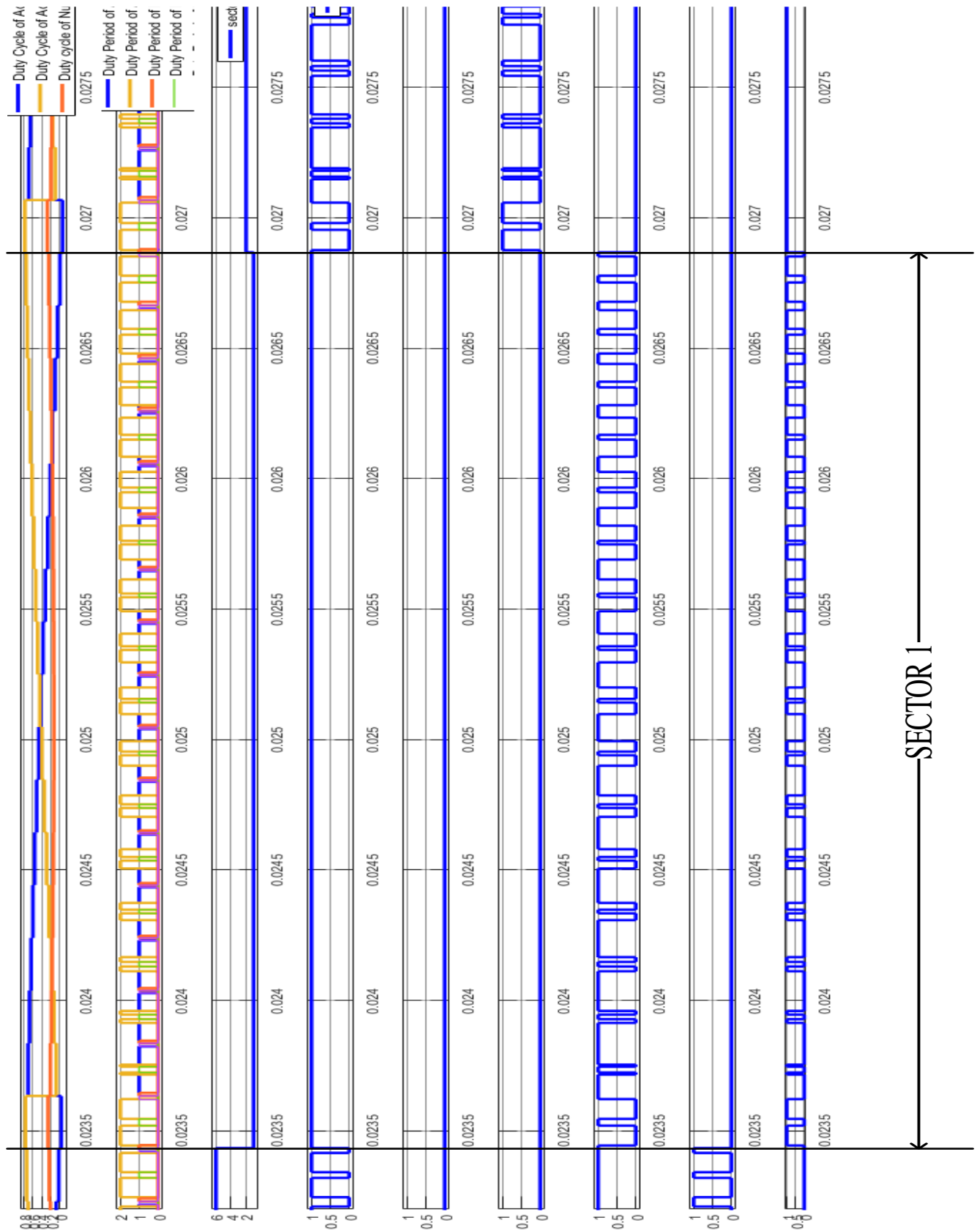


Figure 3.27 Switching Sequence of switches and Switching Duration for Rectifier Stage

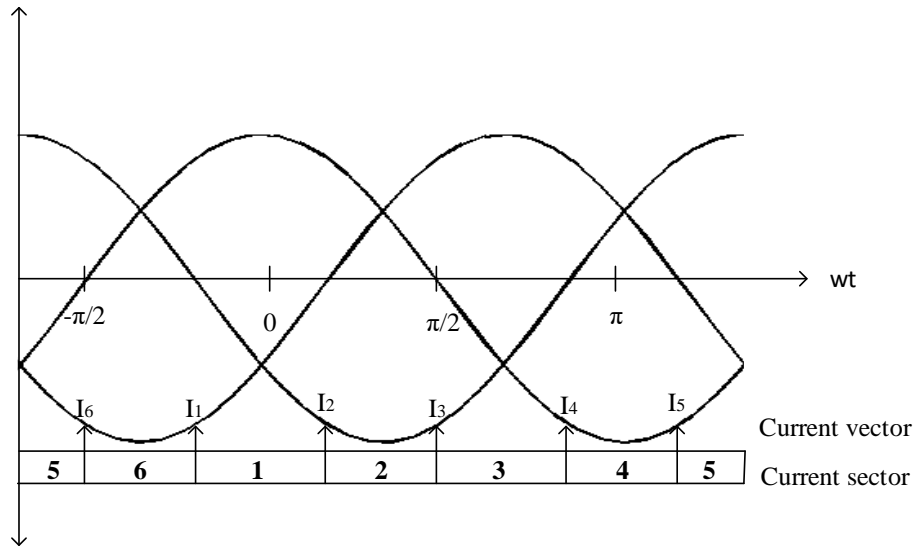


Figure 3.28 Input phase Current sectors

Let us take an example of the Input current phase for a switching cycle of current hexagon sector K_{r1} . In this sector, the active vectors are I_1 and I_2 respectively as shown in Figure 3.28, then the DC-link mean value of voltages output is written as follows

$$\begin{bmatrix} V_{DC+} \\ V_{DC-} \end{bmatrix} = \left(d_3 \cdot \begin{bmatrix} 1 & 0 & 0 \\ 0 & 1 & 0 \end{bmatrix} + d_4 \cdot \begin{bmatrix} 1 & 0 & 0 \\ 0 & 0 & 1 \end{bmatrix} \right) \cdot \begin{bmatrix} V_A \\ V_B \\ V_C \end{bmatrix} \quad (3.72)$$

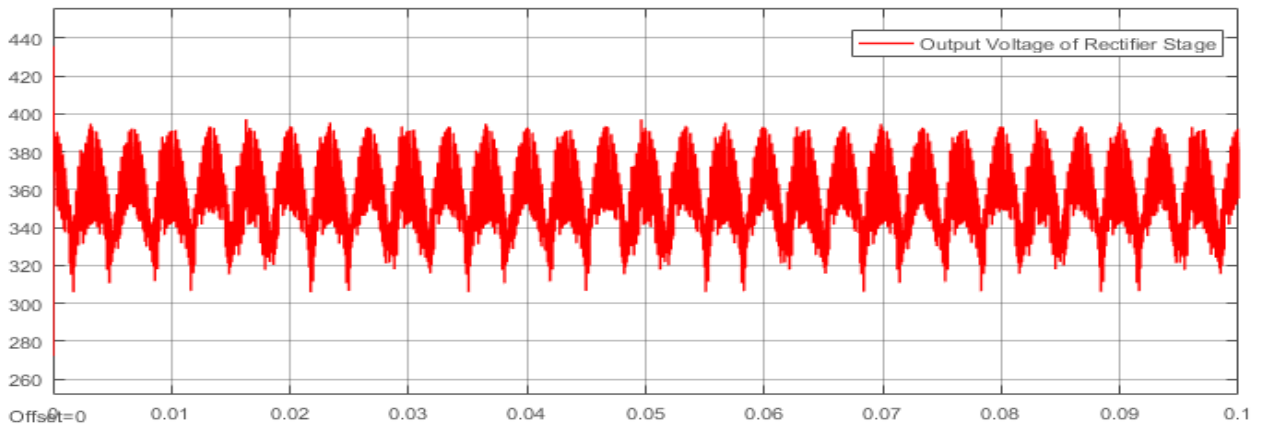


Figure 3.29 Output DC voltage of Rectifier Stage

3.3.1.3 Space Vector Modulation for the Entire Matrix Converter

In the previous sections, the derivation of switching vectors and duty cycle which are derived from the Inverter stage and Rectifier stage and these are used in the equivalent circuit of MC. Therefore, these two independent SVM merged into a single modulation and form indirect SVM

for the MC and this section describe the switching states of MC and how it is transformed from the Inverter and Rectifier stage.

On comparing Equation (3.11) and Equation (3.8), we get

$$\begin{matrix}
 \dot{e}_{aA} \\
 \dot{e}_{aB} \\
 \dot{e}_{aC}
 \end{matrix}
 \begin{matrix}
 S_{bA} \\
 S_{bB} \\
 S_{bC}
 \end{matrix}
 \begin{matrix}
 S_{cA} \\
 S_{cB} \\
 S_{cC}
 \end{matrix}
 \begin{matrix}
 \dot{e}_{7 \cdot S_1} \\
 \dot{e}_{9 \cdot S_1} \\
 \dot{e}_{11 \cdot S_1}
 \end{matrix}
 \begin{matrix}
 S_{8 \cdot S_2} \\
 S_{10 \cdot S_2} \\
 S_{12 \cdot S_2}
 \end{matrix}
 \begin{matrix}
 S_{7 \cdot S_3} \\
 S_{9 \cdot S_3} \\
 S_{11 \cdot S_3}
 \end{matrix}
 \begin{matrix}
 S_{8 \cdot S_4} \\
 S_{10 \cdot S_6} \\
 S_{12 \cdot S_8}
 \end{matrix}
 \begin{matrix}
 S_{7 \cdot S_5} \\
 S_{9 \cdot S_5} \\
 S_{11 \cdot S_5}
 \end{matrix}
 \begin{matrix}
 S_{8 \cdot S_6} \\
 S_{10 \cdot S_6} \\
 S_{12 \cdot S_6}
 \end{matrix}
 \quad (3.73)$$

From the Equation (3.73); Transfer Equation of matrix displays that's the output is the product of sum of the input phases. In the Figure 3.32 shows the switch that are on in the equivalent circuit that are transformed and relevant to the all nine bi-directional switches.

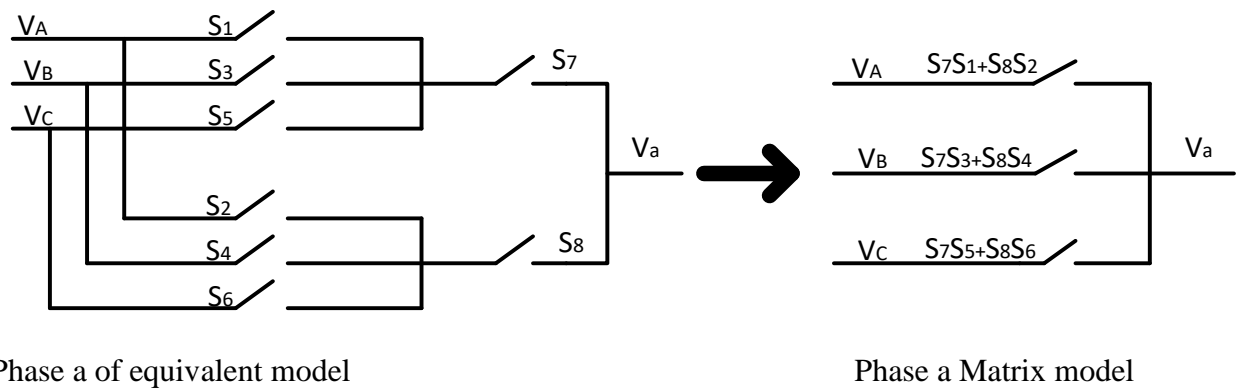


Figure 3.30 Transformation from equivalent circuit to matrix converter in phase a

3.3.1.3.1 Switch Configuration for the Matrix Converter

Previously it was mentioned that TPMC has maximum possible 27 switching states and they have categorized into three groups:

Group NO. I: this group contains 18 possible combinations of switches providing fixed output voltage vector which varies with input voltage angle and input current vectors that varies with output current angle. In this group any two phases of output of the converter, have been connected with single input phase.

Group NO. II: In this group containing 3 possible combination providing zero input current vector and output voltage vectors. In this the converter's all three phase are connected to single input phase.

Group NO. III: In this group containing 6 possible combination providing. In this group, the converters all output are connected to different outputs. In this group resultant of magnitude and

angle both are variables and it difficult to find reference of these values hence they are not used that much in the switching states of the matrix converter.

Table 3.14 represents the all the three groups switches configuration of the MC.

Consider that active vector state is +1 of MC, on comparing the Figures 3.31 (a) and (b) and 3.32, it shows that this active vector state of MC having V_1 active state of Inverter stage and I_1 active state of the rectifier stage. In the active vector $V_1[1\ 0\ 0]$ of the Inverter stage, switches S_7, S_{10} and S_{12} are turned on whereas in the active vector $I_1 [A\ B]$ of the rectifier stage S_1 and S_4 switches are turned on and So the equivalent of these switches that are switched on in MC form is shown in Figure 3.33.

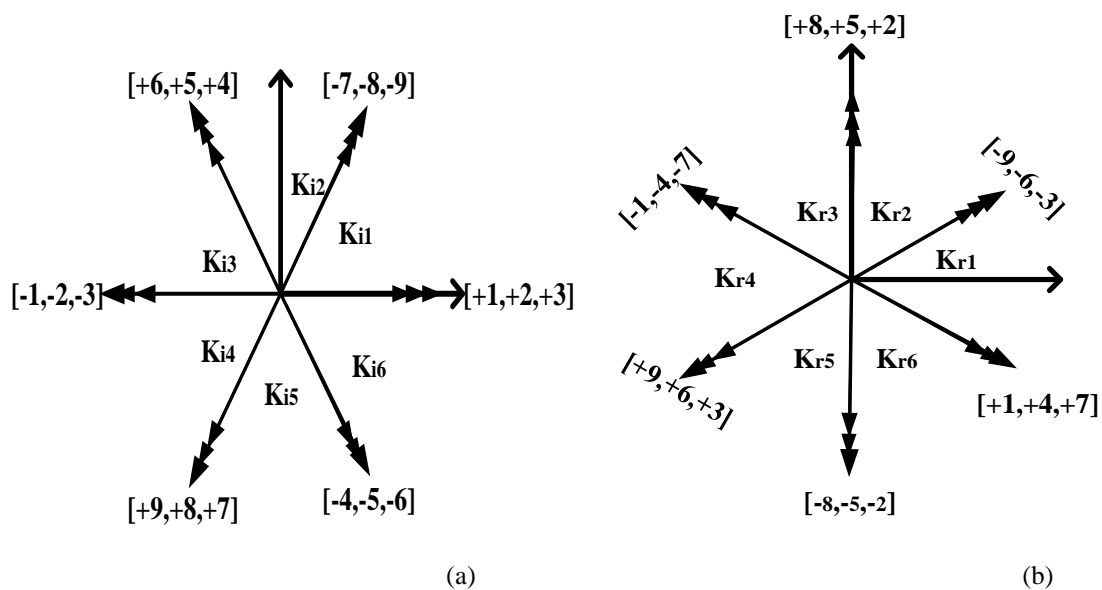


Figure 3.31 Graphical interpretation of: (a) sectors and direction of the output voltage vectors of the MC (b) sectors and directions of the input line current vectors of the MC

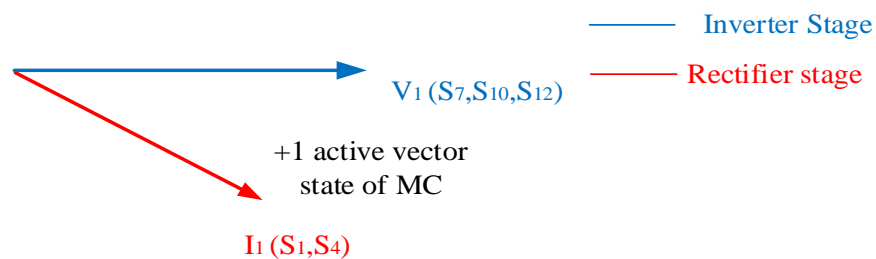


Figure 3.32 Vector 1 of Inverter and Rectifier Stage of MC

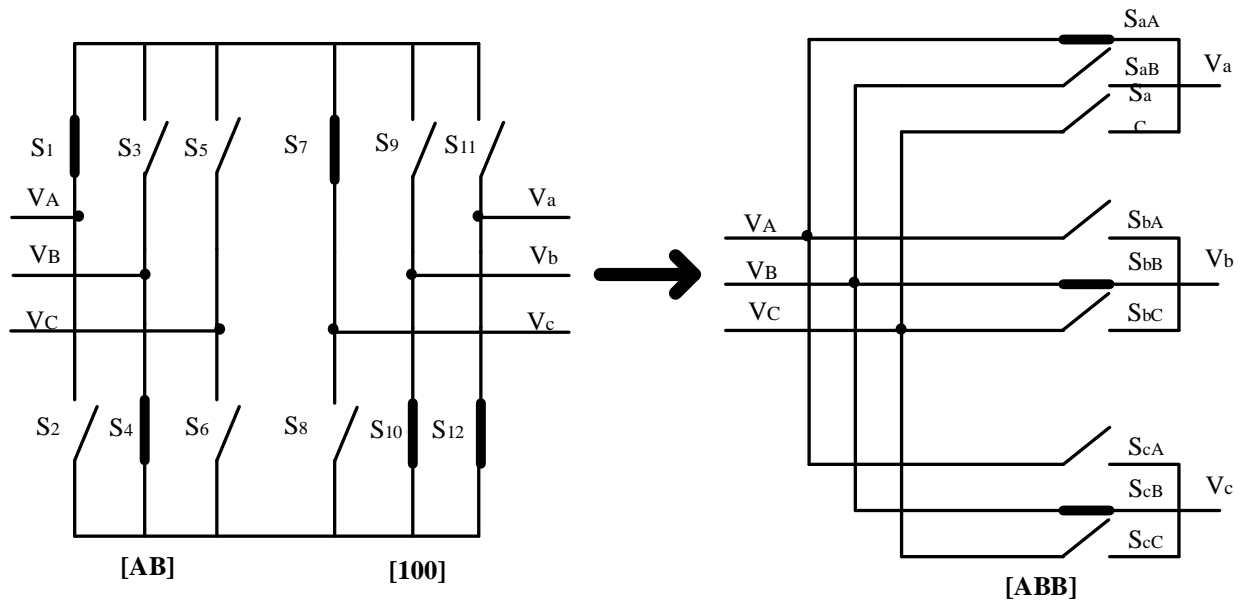


Figure 3.33 $V - I$ pair during +1 active vector condition

Table 3.14 Switches configuration of the MC

Active State	Converter State	Switches on	V_0	I_0	Θ_0	Θ_i
+1	S_{ABB}	$S_{11} S_{12} S_{32}$	$\frac{2}{3} V_{AB}$	$\frac{2}{\sqrt{3}} i_a$	0	$-\frac{1}{6} \pi$
-1	S_{BAA}	$S_{12} S_{21} S_{31}$	$-\frac{2}{3} V_{AB}$	$-\frac{2}{\sqrt{3}} i_a$	0	$-\frac{1}{6} \pi$
+2	S_{BCC}	$S_{12} S_{23} S_{33}$	$\frac{2}{3} V_{BC}$	$\frac{2}{\sqrt{3}} i_a$	0	$\frac{\pi}{2}$
-2	S_{CBB}	$S_{13} S_{22} S_{32}$	$-\frac{2}{3} V_{BC}$	$-\frac{2}{\sqrt{3}} i_a$	0	$\frac{\pi}{2}$
+3	S_{CAA}	$S_{11} S_{21} S_{31}$	$\frac{2}{3} V_{CA}$	$\frac{2}{\sqrt{3}} i_a$	0	$\frac{7\pi}{6}$
-3	S_{ACC}	$S_{11} S_{23} S_{33}$	$-\frac{2}{3} V_{CA}$	$-\frac{2}{\sqrt{3}} i_a$	0	$\frac{7\pi}{6}$
+4	S_{BAB}	$S_{12} S_{21} S_{32}$	$\frac{2}{3} V_{BA}$	$\frac{2}{\sqrt{3}} i_b$	$\frac{2}{3} \pi$	$-\frac{1}{6} \pi$
-4	S_{ABA}	$S_{11} S_{22} S_{31}$	$-\frac{2}{3} V_{AB}$	$-\frac{2}{\sqrt{3}} i_b$	$\frac{2}{3} \pi$	$-\frac{1}{6} \pi$
+5	S_{CBC}	$S_{13} S_{22} S_{33}$	$\frac{2}{3} V_{CB}$	$\frac{2}{\sqrt{3}} i_b$	$\frac{2}{3} \pi$	$\frac{\pi}{2}$

-5	S _{BCB}	S ₁₂ S ₂₃ S ₃₂	$-\frac{2}{3} V_{BC}$	$-\frac{2}{\sqrt{3}} i_b$	$\frac{2}{3} \pi$	$\frac{\pi}{2}$
+6	S _{ACA}	S ₁₁ S ₂₃ S ₃₁	$\frac{2}{3} V_{AC}$	$\frac{2}{\sqrt{3}} i_b$	$\frac{2}{3} \pi$	$\frac{7\pi}{6}$
-6	S _{CAC}	S ₁₃ S ₂₁ S ₃₃	$-\frac{2}{3} V_{CA}$	$-\frac{2}{\sqrt{3}} i_b$	$\frac{2}{3} \pi$	$\frac{7\pi}{6}$
+7	S _{BBA}	S ₁₂ S ₂₂ S ₃₁	$\frac{2}{3} V_{BA}$	$\frac{2}{\sqrt{3}} i_c$	$\frac{4}{3} \pi$	$-\frac{1}{6} \pi$
-7	S _{AAB}	S ₁₁ S ₂₁ S ₃₂	$-\frac{2}{3} V_{AB}$	$-\frac{2}{\sqrt{3}} i_c$	$\frac{4}{3} \pi$	$-\frac{1}{6} \pi$
+8	S _{CCB}	S ₁₃ S ₂₂ S ₃₂	$\frac{2}{3} V_{CB}$	$\frac{2}{\sqrt{3}} i_c$	$\frac{4}{3} \pi$	$\frac{\pi}{2}$
-8	S _{BBC}	S ₁₂ S ₂₂ S ₃₃	$-\frac{2}{3} V_{BC}$	$-\frac{2}{\sqrt{3}} i_c$	$\frac{4}{3} \pi$	$\frac{\pi}{2}$
+9	S _{AAC}	S ₁₁ S ₂₁ S ₃₃	$\frac{2}{3} V_{AC}$	$\frac{2}{\sqrt{3}} i_c$	$\frac{4}{3} \pi$	$\frac{7\pi}{6}$
-9	S _{CCA}	S ₁₃ S ₂₃ S ₃₁	$-\frac{2}{3} V_{ca}$	$-\frac{2}{\sqrt{3}} i_c$	$\frac{4}{3} \pi$	$\frac{7\pi}{6}$
0 ₁	S _{AAA}	S ₁₁ S ₂₁ S ₃₁	0	0	0	0
0 ₂	S _{BBB}	S ₁₂ S ₂₂ S ₃₂	0	0	0	0
0 ₃	S _{CCC}	S ₁₃ S ₂₃ S ₂₃	0	0	0	0
-	S _{ABC}	S ₁₁ S ₂₂ S ₃₃	var	var	var	var
-	S _{BCA}	S ₂₂ S ₃₃ S ₁₁	var	var	var	var
-	S _{CAB}	S ₁₁ S ₃₃ S ₂₂	var	var	var	var
-	S _{ACB}	S ₁₁ S ₃₃ S ₂₂	var	var	var	var
-	S _{BAC}	S ₂₂ S ₁₁ S ₃₃	Var	var	var	var
-	S _{CBA}	S ₃₃ S ₂₂ S ₁₁	Var	var	var	var

3.3.1.3.1 Duty Cycle of the Matrix Converter

The duty cycle of the active vectors is calculated and shown in Equation (3.74) – (3.78).

$$d_{14} = d_1 \cdot d_4 = m_v \cdot \sin\left(\frac{\pi}{3} - \theta_0\right) \cdot m_c \cdot \sin(\theta_i) = \frac{T_{14}}{T_s} \quad (3.74)$$

$$d_{23} = m_v \cdot \sin(\theta_0) \cdot m_c \cdot \sin\left(\frac{\pi}{3} - \theta_i\right) = \frac{T_{23}}{T_s} \quad (3.75)$$

$$d_{24} = m_v \cdot \sin(\theta_0) \cdot m_c \cdot \sin(\theta_i) = \frac{T_{24}}{T_s} \quad (3.76)$$

$$d_{13} = m_v \cdot \sin\left(\frac{\pi}{3} - \theta_o\right) \cdot m_c \cdot \sin\left(\frac{\pi}{3} - \theta_i\right) = \frac{T_{13}}{T_s} \quad (3.77)$$

During the remaining part of T_s , the zero vector is applied

$$d_0 = 1 - d_{13} - d_{14} - d_{23} - d_{24} = \frac{T_0}{T_s} \quad (3.78)$$

In both, the rectifier and inverter hexagons contain six sectors. Hence, there are $6 \times 6 = 36$ active operating modes. For any instance, input current I_i^* and the reference output voltage V_o^* are both in the sector. Then get output voltage directly by combining Equation (3.44) and Equation (3.64) such as

$$\begin{bmatrix} V_A \\ V_B \\ V_C \end{bmatrix} = \left(d_1 \cdot \begin{bmatrix} 1 & 0 \\ 0 & 1 \\ 0 & 1 \end{bmatrix} + d_2 \cdot \begin{bmatrix} 1 & 0 \\ 1 & 0 \\ 0 & 1 \end{bmatrix} \right) \cdot \left(d_3 \cdot \begin{bmatrix} 1 & 0 & 0 \\ 0 & 1 & 0 \end{bmatrix} + d_4 \cdot \begin{bmatrix} 1 & 0 & 0 \\ 0 & 0 & 1 \end{bmatrix} \right) \cdot \begin{bmatrix} V_a \\ V_b \\ V_c \end{bmatrix} \quad (3.79)$$

$$= \left(d_1 \cdot d_3 \begin{bmatrix} 1 & 0 & 0 \\ 0 & 1 & 0 \\ 0 & 1 & 0 \end{bmatrix} + d_1 \cdot d_4 \begin{bmatrix} 1 & 0 & 0 \\ 0 & 0 & 1 \\ 0 & 0 & 1 \end{bmatrix} + d_2 \cdot d_3 \begin{bmatrix} 1 & 0 & 0 \\ 1 & 0 & 0 \\ 0 & 1 & 0 \end{bmatrix} + d_2 \cdot d_4 \begin{bmatrix} 1 & 0 & 0 \\ 1 & 0 & 0 \\ 0 & 0 & 1 \end{bmatrix} \right) \cdot \begin{bmatrix} V_a \\ V_b \\ V_c \end{bmatrix} \quad (3.80)$$

$$= \left(d_1 \cdot d_3 \begin{bmatrix} V_a \\ V_b \\ V_b \end{bmatrix} + d_1 \cdot d_4 \begin{bmatrix} V_a \\ V_c \\ V_c \end{bmatrix} + d_2 \cdot d_3 \begin{bmatrix} V_a \\ V_a \\ V_b \end{bmatrix} + d_2 \cdot d_4 \begin{bmatrix} V_a \\ V_a \\ V_c \end{bmatrix} \right) \quad (3.81)$$

Considered the S_i be Inverter stage sector and S_r be Rectifier stage, consider that S_i and S_r both is in Sector 1 as shown in Figure 3.34, In these sectors, the active voltage vectors are $V_1[100]$, $V_2[110]$ and the active current vectors are $I_1[AB]$, $I_2[AC]$, that will show the voltage vector and current vector pair and for the duty cycle d_{13} their switching combination. During d_{13} interval, $I_1[AB]$ current vector has been applied on the Rectifier stage and at the same time the $V_1[100]$ voltage vector is applied to the Inverter stage, by the Rectifier stage we get in out voltage V_{DC+} and V_{DC-} which then has become the input of Inverter stage, so the values of $V_A = V_{DC+}$ and $V_B = V_{DC-}$, this voltage is the input of Inverter side, Therefore the output voltage has become $V_a = V_{DC+}$, $V_b = V_{DC-}$ and $V_c = V_{DC-}$. Hence the switching sequence in the V_1 - I_1 pair is as follows $V_a = V_A$, $V_b = V_B$ and $V_c = V_B$ and it is termed to be as $[ABB]$. Similarly shown in Figure 3.35 - 3.38.

In the Figure 3.39 they employed a zero vector [ccc] having V_1 - I_1 Pair helps in the reduction of number switching transients of MC.

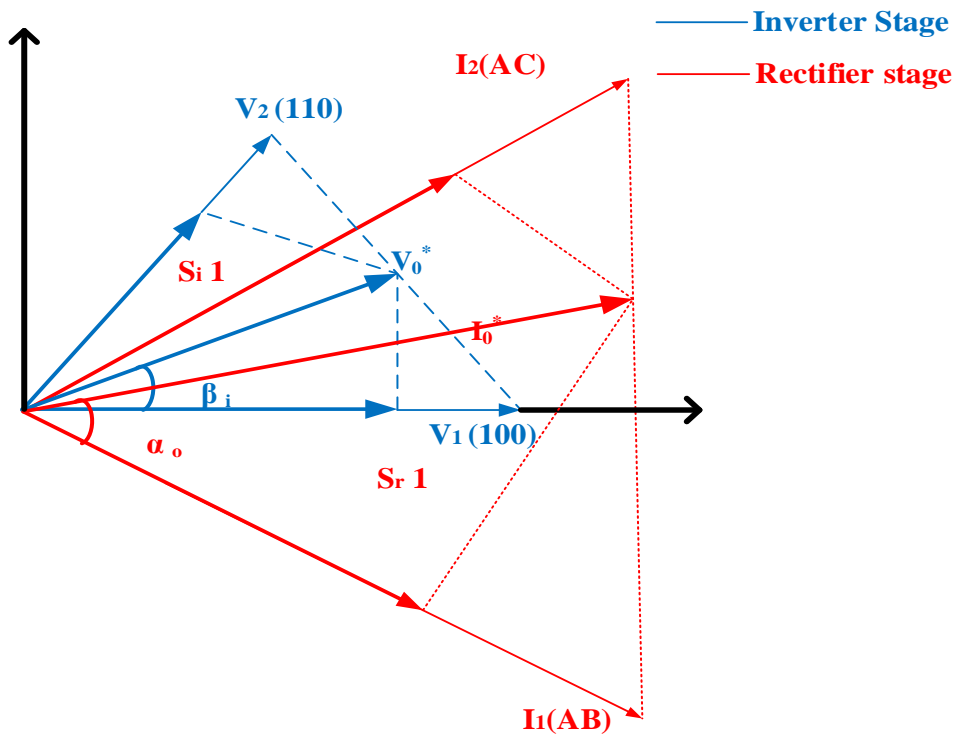


Figure 3.34 Sector 1 of rectifier and Inverter stage of MC

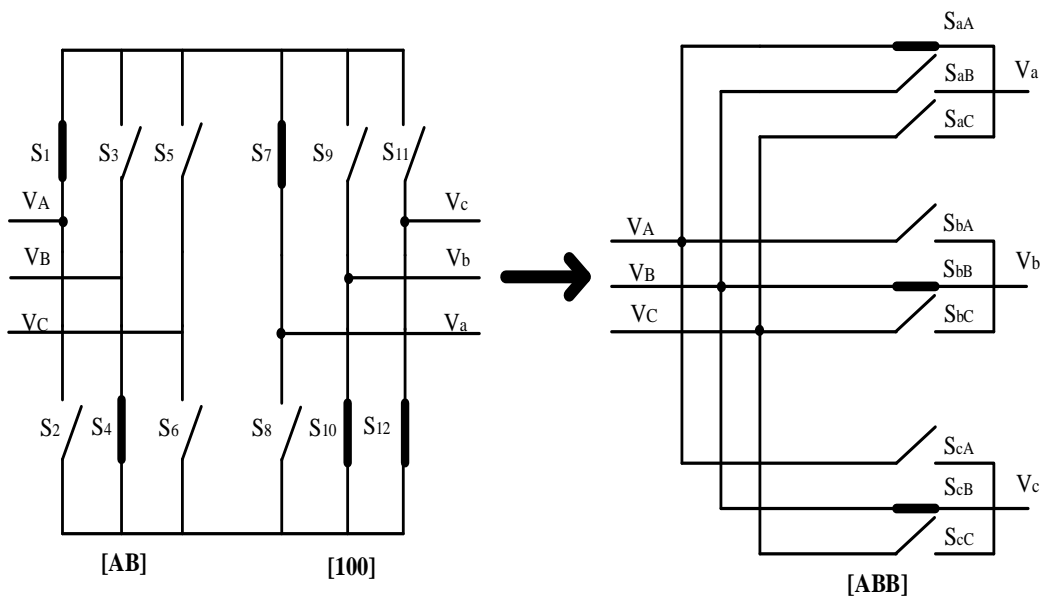


Figure 3.35 $V_1 - I_1$ pair during d_{13}

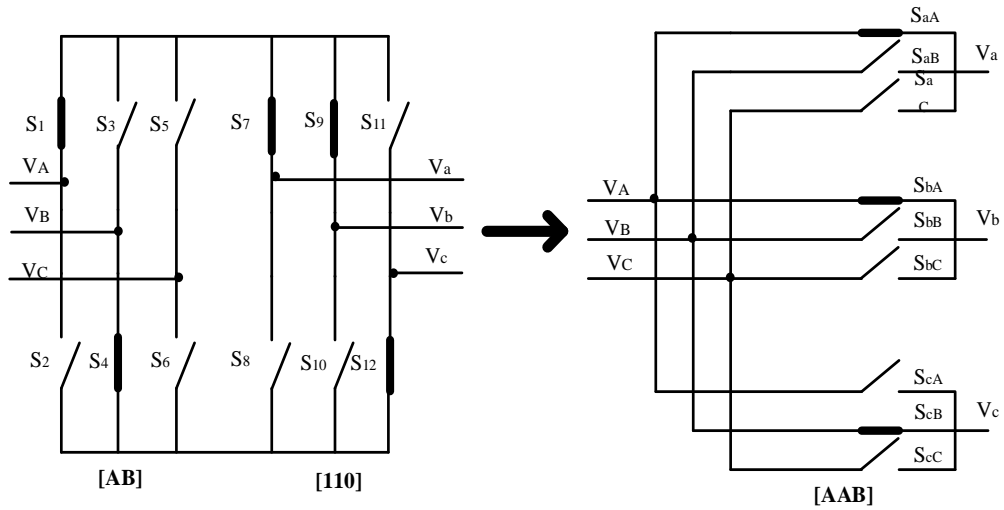


Figure 3.36 $V_2 - I_1$ pair during d_{24}

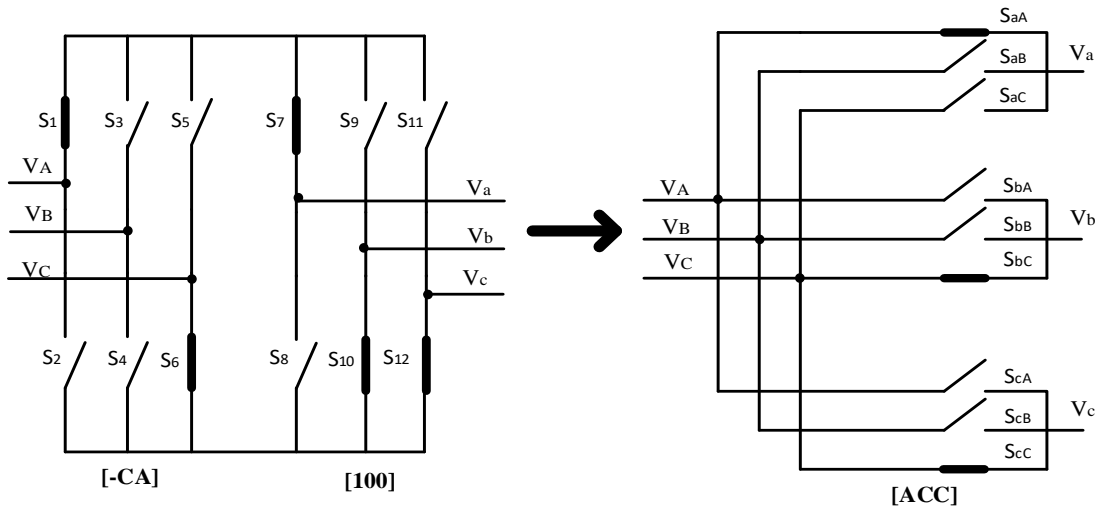


Figure 3.37 $V_2 - I_2$ pair during d_{14}

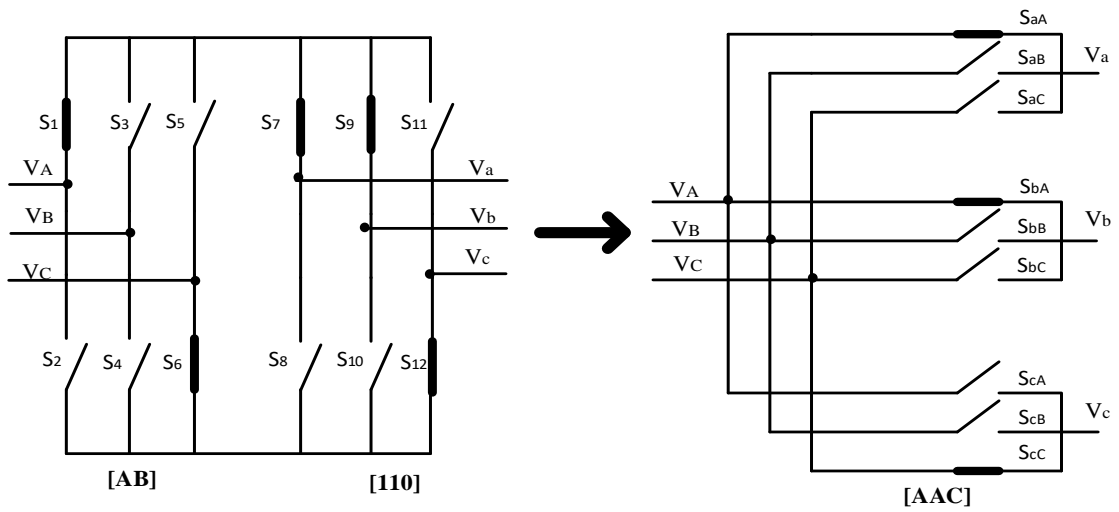


Figure 3.38 $V_1 - I_1$ pair during d_{13}

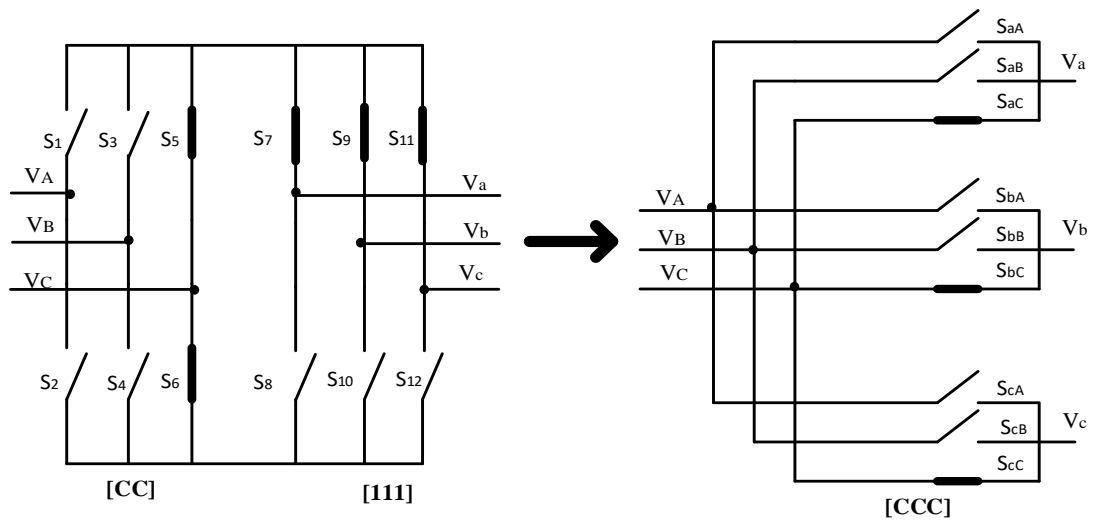


Figure 3.39 $V_0 - I_0$ pair during d_0

Table 3 15 Switching sequence of MC in current and voltage both are in sector 1

Switching State	ACC	AAC	AAB	ABB	BBB	ABB	AAB	AAC	ACC
Timing	$\frac{T_{14}}{2}$	$\frac{T_{24}}{2}$	$\frac{T_{23}}{2}$	$\frac{T_{13}}{2}$	T_0	$\frac{T_{24}}{2}$	$\frac{T_{14}}{2}$	$\frac{T_{13}}{2}$	$\frac{T_{23}}{2}$
VI vector pair	V_1-I_2	V_2-I_2	V_2-I_1	V_1-I_1	V_0-I_0	V_1-I_1	V_2-I_1	V_2-I_2	V_1-I_2

In the Table 3.15, it explains the switching sequence of above five vectors sequence has been applied to MC bidirectional switches. When all the current and voltage are in sector 1.

3.3.1.3.3 Matrix Converter Switching States Selection

After getting the result in the Table 3.14 and also from the Table 3.15, on the comparison with that shows the results that which switch are on during that interval. Table 3.16 and Table 3.17 explains the which switches are switches on during each 36 sectors.

Table 3.16 Selection of Combination of Switching state configuration of Inverter and Rectifier stages-1

S_r	S_i												
	Sector	1				2				3			
	1	+1	-3	-7	+9	-7	+9	+4	-6	+4	-6	-1	+3
2	-3	+2	+9	-8	+9	-8	-6	+5	-6	+5	+3	-2	
3	+2	-1	-8	+7	-8	+7	+5	-4	+5	-4	-2	+1	

	4	-1	+3	+7	-9	+7	-9	-4	+6	-4	+6	+1	-3
	5	+3	-2	-9	+8	-9	+8	+6	-5	+6	-5	-3	+2
	6	-2	+1	+8	-7	+8	-7	-5	+4	-5	+4	+2	-1
		I	II	III	IV	I	II	III	IV	I	II	III	IV

Table 3.17 Selection of Combination of Switching state configuration of Inverter and Rectifier stages-2

S _r		S _i											
	Sector	4				5				6			
	1	-1	+3	+7	-9	+7	-9	-4	+6	-4	+6	+1	-3
	2	+3	-2	-9	+8	-9	+8	+6	-5	+6	-5	-3	+2
	3	-2	+1	+8	-7	+8	-7	-5	+4	-5	+4	+2	-1
	4	+1	-3	-7	+9	-7	+9	+4	-6	+4	-6	-1	+3
	5	-3	+2	+9	-8	+9	-8	-6	+5	-6	+5	+3	-2
	6	+2	-1	-8	+7	-8	+7	+5	-4	+5	-4	-2	+1
		I	II	III	IV	I	II	III	IV	I	II	III	IV

3.2.2 Simulation of the Three Phase Matrix Converter:

Resistive Inductive with filters. Similarly, same procedure has been followed for the 50 and 25 Hz output synthesized frequency.

Figure 3.40 shows the output current and voltage of the phase a for resistive inductive load of 50 W and 10 mH without filters through Simulation model in MATLAB.

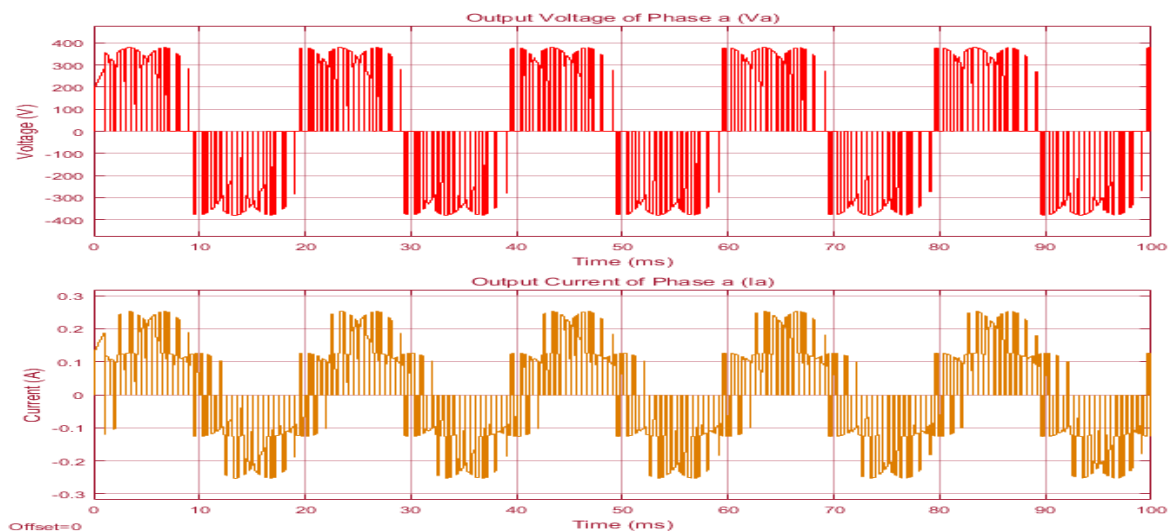


Figure 3.40 TPMC output voltage and current of phase a of 50 W and 10 mH without Filter

Figure 3.41 shows the output current and voltage for three phase for resistive inductive load of 50 W and 10 mH without filters through Simulation model in MATLAB.

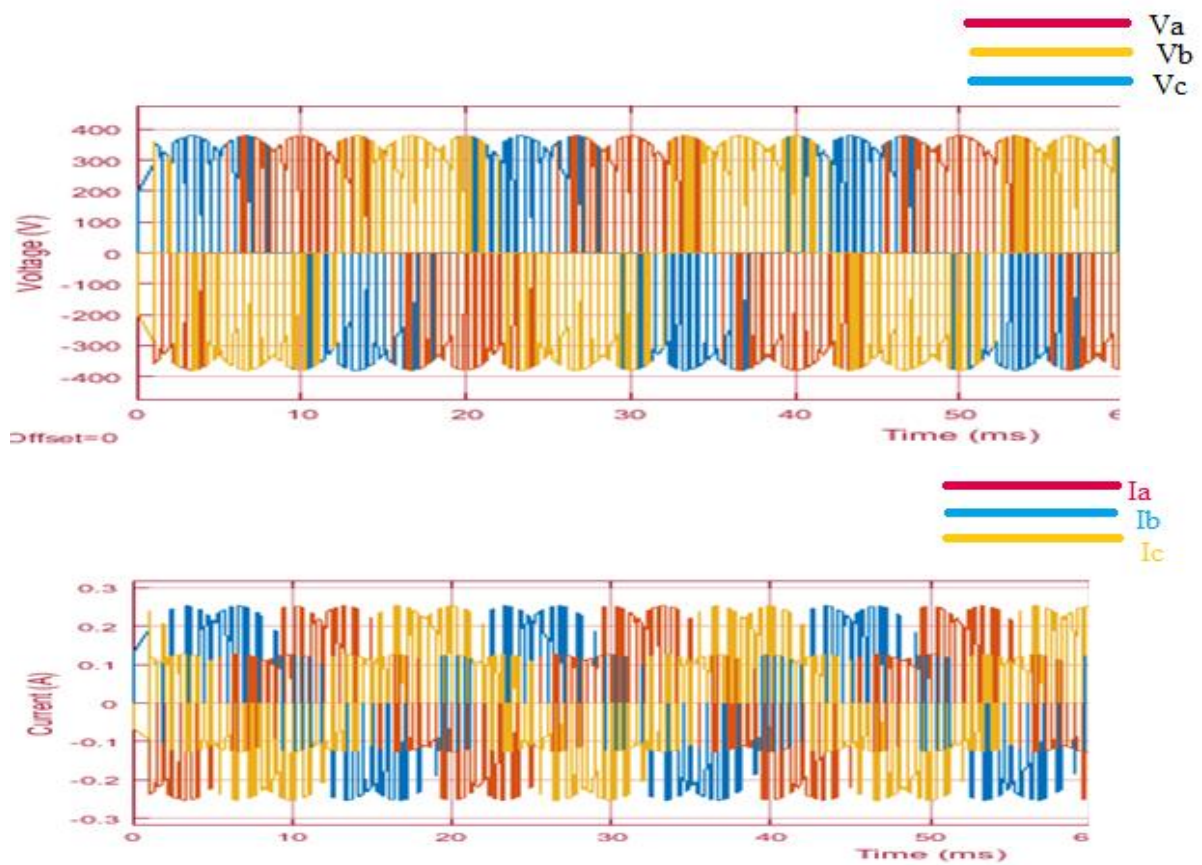


Figure 3.41 MC Output Voltage and current of 50 W and 10 mH without Filters

Figure 3.42 shows the output current and voltage of the phase a for resistive inductive load of 50 W and 10 mH with filter through Simulation model in MATLAB.

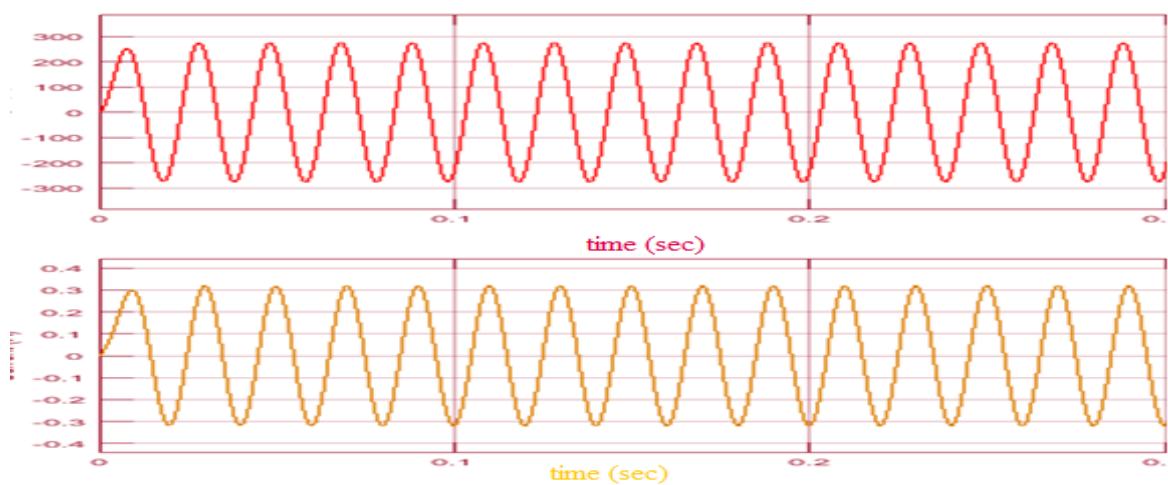


Figure 3.42TPMC output voltage and current of Ia phase without Filter

Figure 3.43 shows the output current and voltage for three phase for resistive inductive load with filter through Simulation model in MATLAB.

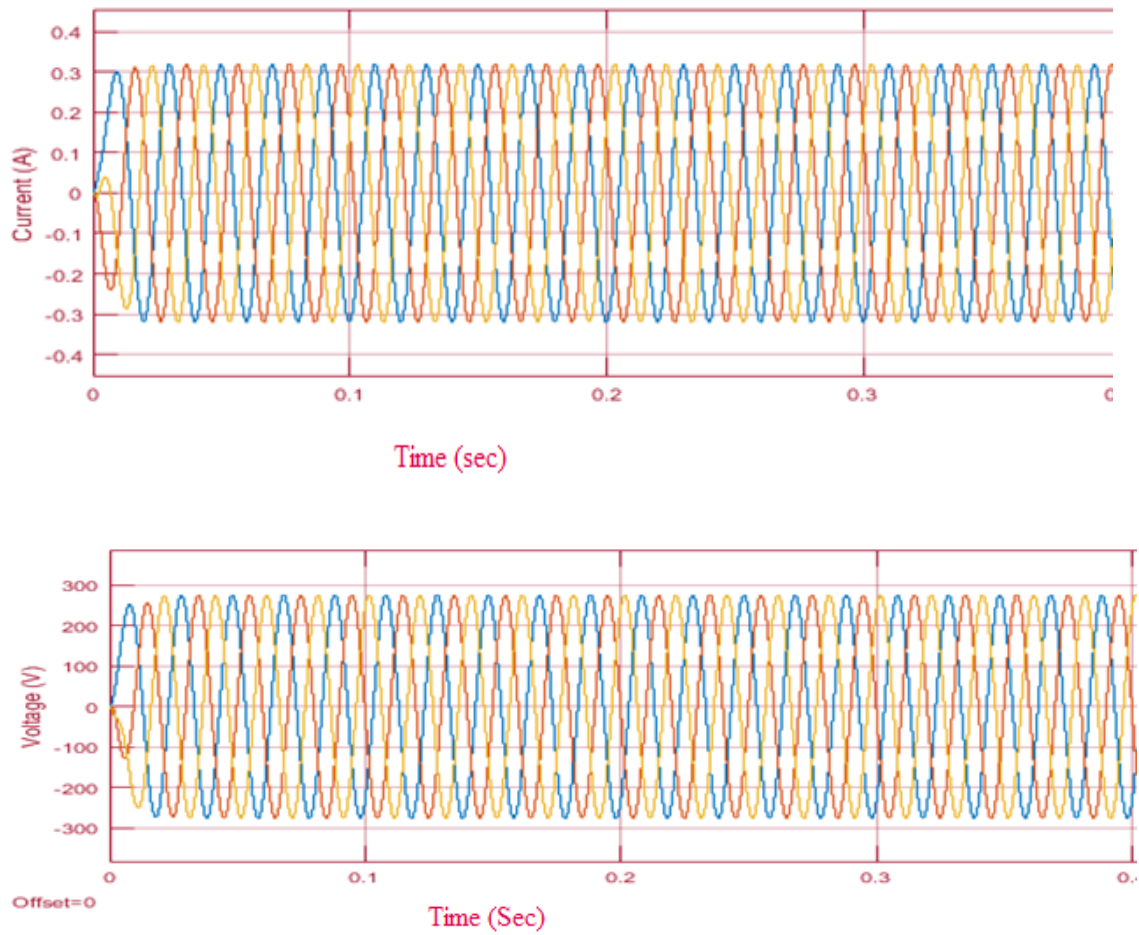


Figure 3.43 TPMC Output Voltage and current of 50 W and 10 mH with Filters

CONCLUSION AND FUTURE SCOPE

4.1 Conclusion

Mathematical analysis of single phase and three phase Matrix Converters is presented. Two different models have been proposed both having different topologies. Several conclusion has been concluded from this work: Switches of the MC is in the array of $m \times n$, where m is number of input lines and n is number of output lines. In MC the input mains fed up with the constant frequency and supply. The amplitude of this MC can step up or down the frequency by synthesized output voltage equals to the multipliers of the input fundamentals. For the safe commutation technique, by providing carefully arrangements of the switching sequence, the bi-directional switches used in this can be used for free-wheeling path itself and provides the path that allows the current to its dead time resulting in avoided generation of voltage spikes. The TPMC SVM is the combination of the Product of the Sum of the modulation of Inverter and Rectifier stage. There is an impact on the change of the MI in the modulation of the MC. The maximum input output voltage transfer ratio is just 0.866. The filter used in the MC has influence on the output result of the simulation.

4.2 Future Work

Continuation of this work there are many topics where research has yet to be carried in order just in the improvement of the MC in Frequency Changing applications.

- In this thesis, the losses of the converter have not been compared and evaluate with the traditional RFIS system. For the research point of view this is the most important step.
- This work does not analyze Electro Magnetic Interference (EMI). In order to pursue this application in industries, there is requirement of design and measurement of proper EMI filter.
- The work in this thesis only done in the open loop system, but according to the industrial application closed loop work also has to be done to get more precise and accurate results.
- The work in the thesis lead towards better transmission system by decreasing the losses during transmission by simply step down the frequency and increase its voltage. As frequency is directly proportional to reluctance. Decrease in the reluctance results in better transmission with low losses.

REFERENCES

- [1] A. Alesina and M. Venturini, "Solid-state power conversion: A Fourier analysis approach to generalized transformer synthesis," *IEEE Trans. Circuits Syst.*, vol. 28, no. 4, pp. 319–330, 1981.
- [2] P. D. Ziogas, Y.-G. Kang, and V. R. Stefanovic, "Rectifier-Inverter Frequency Changers with Suppressed DC Link Components," *IEEE Trans. Ind. Appl.*, vol. IA-22, no. 6, pp. 1027–1036, 1986.
- [3] L. Huber and D. Borojevic, "Space Vector Modulator for Forced Commutated Cycloconverters," *IEEE Ind. Appl. Soc. Annu. Meet.*, pp. 871–876, 1989.
- [4] L. Huber, "Voltage space vector based PWM Control of Forced Commutated Cycloconverters," *Ieee Ias*, pp. 871–876, 1989.
- [5] N. Burany, "Safe control of four-quadrant switches," *Conference Record of the IEEE Industry Applications Society Annual Meeting*, San Diego, CA, USA, 1989, pp. 1190-1194 vol.1.
- [6] R. R. Beasant, W. C. Beattie, and A. Refsum, "An approach to the realization of a high-power Venturini converter," *Proc. IEEE PESC '90*, pp. 291–297, 1990.
- [7] T. G. Habetler, "A Space Vector-Based Rectifier Regulator for AC/DC/AC Converters," *IEEE Trans. Power Electron.*, vol. 8, no. 1, pp. 30–36, 1993.
- [8] P. Wheeler, H. Zhang, and D. A. Grant, "A theoretical and practical consideration of optimised input filter design for a low loss matrix converter," *Electromagn. Compat. 1994.*, Ninth Int. Conf., no. 396, pp. 138–142, 1994.
- [9] A. Zuckerberger, D. Weinstock, and A. Alexandrovitz, "Single-phase matrix converter," *IEE Proc. - Electr. Power Appl.*, vol. 144, no. 4, pp. 235–240, 1997.
- [10] P W Wheeler, L Empringham " Matrix Converter Bi-Directional Intelligent Gate Drives" no. 456, pp. 21–23, 1998.
- [11] B. K. Lee and M. Ehsani, "A simplified functional simulation model for three-phase voltage-source inverter using switching function concept," *IEEE Trans. Ind. Electron.*, vol. 48, no. 2, pp. 309–321, 2001.
- [12] P. W. Wheeler, J. Rodriguez, J. C. Clare, L. Empringham and A. Weinstein, "Matrix converters: a technology review," in *IEEE Transactions on Industrial Electronics*, vol. 49, no. 2, pp. 276-288, Apr 2002.

- [13] U. T. Mara, U. T. Mara, and U. T. Mara, "Safe Commutation Strategy in Single Phase Matrix Converter," pp. 886–891, 2005.
- [14] R. Anusuya and R. Saravanakumar, "Realization of a Single Phase Matrix Converter with Reduce switch count as a buck/boost rectifier with close loop control," *2012 International Conference on Computing, Electronics and Electrical Technologies (ICCEET)*, Kumaracoil, 2012, pp. 218-223.
- [15] C. Wang, "A Novel Soft-Switching Single-Phase AC – DC – AC Converter Using New ZVS – PWM Strategy," vol. 22, no. 5, pp. 1941–1948, 2007.
- [16] F. A. Author, S. B. Author, and T. C. Author, "Improved Switching Strategy For Single Phase Matrix Converter." *Industrial Electronics and Applications*, 2008. ICIEA 2008.
- [17] H. Karaca, "Control of Venturini Method Based Matrix Converter in Input Voltage Variations," *Proc. Int. MultiConference Eng. Comput. Sci.* 2009, vol. II, no. 1, pp. 1412–1416, 2009.
- [18] S. Lopez Arevalo, "Matrix converter for frequency changing power supply applications," no. January, 2010.
- [19] J. Rodriguez, M. Rivera, J. W. Kolar, and P. W. Wheeler, "A Review of Control and Modulation Methods for Matrix Converters," vol. 59, no. 1, pp. 58–70, 2012.
- [20] "Realization of a Single Phase Matrix Converter with Reduce Switch Count as a Buck/Boost Rectifier with Close Loop Control," pp. 218–223, 2012.
- [21] M. Rivera, J. W. Kolar, J. Rodriguez, M. Rivera, J. W. Kolar, and P. W. Wheeler, "A Review of Control and Modulation Methods for Matrix Converters," vol. 59, no. 1, pp. 58–70, 2012.
- [22] Szcześniak, Paweł, "Review of AC–AC Frequency Converters," vol. 59, no. 1, pp. 58–70, 2013.
- [23] T. Nottingham and N. E. User, "Design control and implementation of a four - leg Matrix Converter for ground power supply application," 2013.

PLAGRISM CERTIFICATE

Sidharth_Pandit_ME_PED_Matrix_Converter			
ORIGINALITY REPORT			
% 14	% 9	% 10	% 0
SIMILARITY INDEX	INTERNET SOURCES	PUBLICATIONS	STUDENT PAPERS
PRIMARY SOURCES			
1	dspace.thapar.edu:8080 Internet Source		% 1
2	www.labplan.ufsc.br Internet Source		% 1
3	eprints.nottingham.ac.uk Internet Source		% 1
4	www.ijaet.org Internet Source		% 1
5	www.die.ing.unibo.it Internet Source		% 1
6	Chai, Merlin, Rukmi Dutta, and John Fletcher. "Space vector PWM for three-to-five phase indirect matrix converters with d2-q2 vector elimination", IECON 2013 - 39th Annual Conference of the IEEE Industrial Electronics Society, 2013. Publication		<% 1